CDKL5 AFFECTS NEURONAL POLARIZATION THROUGH ITS INTERACTION WITH SHOOTIN1

Thesis submitted to

University of Insubria

For the award of

Doctor of Philosophy (Ph.D.)

In Neurobiology

MOHAMMAD SARFARAZ NAWAZ

UNIVERSITY OF INSUBRIA

Department of Theoretical and Applied Sciences
Via Manara-7, 21052
Busto Arsizio, VA,
ITALY

OCTOBER 2013

Principal Investigator: ***Dr. Charlotte Kilstrup-Nielsen*** *No.* ***715987***

Prof. Nicoletta Landsberger *Cycle.* ***XXVI***

Coordinator: ***Prof. Daniela Parolaro***

"Every good act is a charity"
(Quran; 570 - 632)
Mohammad

DECLARATION BY THE CANDIDATE

I, **Mohammad Sarfaraz Nawaz**, hereby declare that the work presented in the form of this thesis was carried out by me under the supervision of **Dr. Charlotte Kilstrup-Nielsen** and **Prof. Nicoletta Landsberger** at the Laboratory of Genetic and Epigenetic Control of Gene Expression, Department of Theoretical and Applied Sciences, University of Insubria, Via Manara 7, Busto Arsizio (VA) 21052, Italy.

I also declare that no part of this thesis has been previously submitted for the award of any degree or diploma of the University of Insubria or any other university.

Place: Busto Arsizio (**Mohammad Sarfaraz Nawaz**)

Date: 31/10/2013

ACKNOWLEDGEMENT

If I look back at my stay in Italy, I am surprised at the way time has flown by and at the same time very grateful for all I have achieved throughout these years. At this moment, I take the opportunity to convey my heartiest gratitude to all the people who have been associated with this journey.

First and foremost, I would like to sincerely thank my lovely mentors, ***Dr. Charlotte Kilstrup-Nielsen*** *and* ***Prof. Nicoletta Landsberger****, for being patient and guiding me all through. Their enthusiasm and eagerness to see results of each experiment with the same zeal, inspires me a lot. They not only are a scientific thinker but very critical observer and most importantly very good human beings. Their deep scientific insights, critical suggestions and constructive criticism have always inspired me and enriched my growth as a student as well as a researcher. It was a great honor and a rewarding experience to work under their supervision. This thesis would have not come in present form without their ideas, support as well as expert assistance. I would like to show my heartfelt gratitude to* ***Dr. Charlotte Kilstrup-Nielsen*** *who went through my thesis several times with same enthusiasm, and her valuable suggestions made my thesis in a presentable form. Thank you, Charlotte and Nico…*

I would like to thank ***Prof. Daniela Parolaro****, Head of the PhD program in Neurobiology, DISTA, University of Insubria, Busto Arsizio, Italy, for providing a stimulating and conducive research environment.*

I am indebted to ***ITN7-Marie Curie Organization, Dischrom Group*** *to honor me 36 months scholarship. I am very thankful to* ***Prof. Maurizio D'Esposito****, IGB, CNR, Italy, and all the ITN7 and Dischrom group members who organized several conferences and workshops to enlighten us with latest research activities. I show my gratitude to* ***University of Insubria*** *for providing me 4 months fellowship to complete my PhD tenure.*

*I am very thankful to whole Laboratories of DISTA in Busto Arsizio, which functions as a family including my seniors and juniors who have made my stay a memorable one. On a personal note, I am grateful to all my present lab members (****Anna Bergo****,* ***Laura Rusconi****,* ***Paolo La Montanara****,* ***Chetan Chandola****,* ***Gilda Stefanelli****,* ***Isabella Barbiero****,* ***Marta Strollo****,* ***Martina Gri****,* ***Francesco Bedogni****,* ***Francesco Galli****,* ***Ana Gandaglia****,* ***Clementina Cobolli Gigli****,* ***Elisa Bellini****,* ***Korina****) and the past lab members (****Dionigio Prodi****,* ***Elisa Giarda****,* ***Dalila Ciceri****) for being great co-workers and friends. I must be thankful to* ***Francesco Bedogni****, who assisted me in getting a good hand in in utero electroporation techniques. Briefly, he could be a good mentor in the near future and I wish him for the same. His sense of humor will never be forgotten. The excellent assistance in the lab provided by all of them especially,* ***Paolo la Montanara****,* ***Laura Rusconi****,* ***Gilda Stefanelli****,* ***Dalila Ciceri****,* ***Isabella Barbiero****,* ***Francesco Galli****,* ***Clementina Cobolli Gigli****,* ***Marta Strollo****, is highly appreciated. We were like a family and interestingly, I got a new name "****Benedetto"*** *in this family. Cool enough… Indeed! I am thankful to all for constant encouragement, support and suggestions at various phases of this journey. I wish all of them a good fortune and stable professional careers.*

I would also like to show my gratitude to Dr. Shyamala Mani, Indian Institute of Science (IISc), Bangalore, India and Dr. Sayali Ranade, of National Brain Research Centre, Manesar, Haryana, India, for providing me an opportunity to work as a research assistant in their labs. The assistance and moral support from NBRC people made my stay at NBRC worth. It would be unfair if I do not acknowledge my previous lab members; Parthiv Haldipur, Upasna Bharti, Shailesh Kumar Gupta, Yunis Khan and ultimately, very good NBRC friends; Prakash Kumar Mishra, Priyanka Patel, Ranjan Maity, Saurav Roy Chaudhury, Partha Dey, Hena Khalique, Kashif Mahfooz, Chetan Chandola, Anupam Ghosh, Praseeda Venugopalan, Priti Yadav, Richa Tiwari, Chinmoyee Maharana Lenka, Kaushik Sharma, Arshed Nazmi, Kanchan Bisht, Shalini Sivarajan, Revathy Guruswamy, Shilpa Mishra, Vinay Shukla, Sabyasachi Maity, Durga Praveen Meka, Prakash Nidadavalu, Sourav Ghosh, Shahul Hameed, Shaily Mallick, Swetha Godawarthi, Himakshi Sidhar, Upasna Sahu, Swarupa Chakraborty and the list continues….The time spent with them is adorable and that place with beautiful memories will never fade away in my life.

I would like to appreciate my college friends (Hamdardians); Javed, Ahmad, Zeeshan, Satish, Nasreen, Nagisa, Shazia, Mehrnaz, Maaz, Fareed, Hashim, Hafeez, Ajitabh, Tabish and my seniors for sharing their views to be patient for anything. I was born and brought up in a small village in Darbhanga, Bihar, India, and it was my first exposure to meet individuals in metropolitan city, New Delhi, where I got admission in Jamia Hamdard, for Master of Science in Biotechnology. I was afraid and had a complex feeling about my region but these friends made my stay quite comfortable, smooth and easy going. I am indebted of their benevolent assistance and wish them good fortunes in their lives.

I show my heartfelt gratitude to my dear Mama, ***Md. Kabir Ansari*** *who encouraged me at every moment starting from the childhood. He is the person who helped my family in good and bad situations and only because of him, I am here. He owes me everything. I salute him for his dedication towards helping others with no expectation.*

Finally, I thank ***Him*** *for providing me an adorable family, who has always been there through thick and thin, and making this chapter of my life a complete and beautiful one. My* ***parents****, dear brothers (****Md. Shamim Ansari*** *and* ***Md. Waseem Ansari****) and sisters (****Saira Bano*** *and* ***Tabassum Ara****) played awesome role in my life and always encouraged me to be happy whatever the situations I go through. They have been and are my pillars of strength, and all I can say to them, inadequately, is a heartfelt thank you.*

At last but not the least, I would like to thank my beloved ***Aiman Kayenaat*** *who came to my life very recently and made me feeling worth being in this world. I would like to dedicate my PhD degree to her, my family members and indeed to my friends.*

Thank you……..

CONTENTS

ABBREVIATIONS

2D IEF	Two dimensional isoelectric focusing
AKO	Adult knock out
AMP	Adenosine monophosphate
AMPK	AMP activated protein kinase
AS	Angelman's syndrome
ASD	Autism spectrum disorder
ATP	Adenosine triphosphate
BDNF	Brain derived neurotrophic factor
BSA	Bovine serum albumin
CA3	Cornu ammonis 3 region
cAMP	Adenosine 3'5' cyclic monophosphate
CDC	Cell division cycle
CDK	Cyclin dependent kinase
CDKL5	Cyclin dependent kinase like 5
CGI	CpG Island
CGN	Cerebellar granule neurons
CHAPS	3-[(3-Cholamidopropyl) dimethylammonio]-1propanesulfonate
CNS	Central nervous system
CP	Cortical plate
CREB	cAMP responsive element binding
CRM1	Chromosomal maintenance 1
CTD	C-terminal domain
DAPI	4', 6-diamidino-2-phenylindole
DG	Dentate gyrus
DIV	Days in vitro
DNMT	DNA methyl transferase
DOCK7	Dedicator of cytokinesis 7
DPX	Distrene, Plasticiser, Xylene
EDTA	Ethylene diamine tetra acetic acid

EEG	Electroencephalogram
EGTA	Ethylene glycol tetra acetic acid
ERK	Extracellular signal related kinase
ESV	Early seizure variant
FOXG1	Forkhead box G1
GABA	Gamma amino butyric acid
GFP	Green fluorescent protein
GSK3-β	Glycogen synthase 3-β
HDAC	Histone deacetylases
HRP	Horse radish peroxidase
IC	Internal capsule
ICL	Inner cortical layer
ID	Intellectual disability
IF	Immunofluorescence
IgG	Immunoglobulin G
IHC	Immunohistochemistry
IP	Immunoprecipitation
IPG	Immobiline DryStrip gels
IRES	Internal ribosome entry site
ISH	In situ hybridization
IUE	*In utero* electroporation
IZ	Intermediate zone
L1 CAM	L1-cell adhesion molecule
LKB-1	Liver kinase B-1
LTP	Long term potentiation
MAP2	Microtubule associated protein 2
MAPK	Mitogen activated kinase
MBD	Methyl-CpG binding domain
MCL	Middle cortical layer
MECP2	Methyl CpG binding protein
MGE	Medial ganglionic eminence
mTOR	Mammalian target of rapamycin
NBT-BCIP	Nitro-blue tetrazolium chloride- 5-bromo-4-chloro-3'-indolyphosphate p-toluidine salt

NES	Nuclear export signal
NGL	Netrin-G1 ligand
NLS	Nucleus localization signal
OCL	Outer cortical layer
OCT	Optimal cutting temperature
OMIM	Online mendelian inheritance in man
PAT	Palmitoyl acetyl transferase
PBS	phosphate buffer saline
PBS	Predicted biological score
PCR	Polymerase chain reaction
PHB	Prehybrdization buffer
PI3K	Phosphatidylinositol 3-kinase
PKC	Protein kinase C
PLL	Poly L-lysine
pLL	plasmid lenti lox
PMP	Protein metallophosphatase
PN	Pyramidal neurons
PSD	Post synaptic domain
PTM	Post translational modification
Rac1	Ras-related C3 botulinum toxin substrate 1
RTT	Rett syndrome
SDS PAGE	Sodium dodecyl polyacryl amide gel electrophoresis
SEM	Standard error of mean
STK	Serine threonine kinase
SVZ	Sub ventricular zone
TAG1	Transient Axonal Glycoprotein-1
TBS	Tris buffer saline
TEY	Thr-Xaa-Tyr motif
TRD	Transcriptional repression domain
UTR	Untranslated region
UBE4A	U-box-type ubiquitin ligase
VGLUT1	Vescicular glutamate transporter 1
VZ	Ventricular zone
XCI	X-chromosome inactivation

aa	Amino acids
bp	Base pair
C	Celsius
H	Hour
Kda	Kilo Dalton
m	Milli
M	Molar
nt	Nucleotide
pH	Hydrogen ion concentration
α	Alpha
β	Beta
γ	Gama
g	Gram
µ	Micro
°	Degree
%	Percentage
#	Number
±	Plus/minus
≥	Greater than or equal to

INTRODUCTION

Rett Syndrome

Rett syndrome (RTT; MIM 312750) is named after Andreas Rett, the pediatric neurologist in Vienna who first recognized the characteristic features of the syndrome in 1954. Although his observation was published in the German medical literature in 1966 [1], it remained largely unnoticed until 1983 when Bengt Hagberg from Sweden revealed this unique syndrome to the international medical world [2].

In the late 1990s, researchers from Huda Zoghbi's laboratory suggested that the *MECP2* gene, located on the X chromosome, was a good candidate gene for RTT and, accordingly, identified mutations in this gene in a number of patients with Rett syndrome [3]. RTT was thus the first neurodevelopmental disorder related to epigenetics. Later, the *CDKL5* and *FOXG1* genes have been associated with variant forms of Rett syndrome.

A major challenge for understanding neurodevelopmental disorders, including Rett syndrome, is to advance the findings from gene discovery to an exposition of the neurobiological mechanisms that underlie these disorders and subsequently translate this knowledge into mechanism-based therapeutics.

Clinical features of Rett syndrome

Rett syndrome is a neurodevelopmental condition that affects approximately 1 in 10,000 females, which makes it the most common cause of severe female mental retardation. RTT is characterized by an apparently normal period of development lasting for 6-18 months, after which the loss of spoken language can be observed together with acquired microcephaly, intellectual disability, emergence of autistic features, loss of purposeful manipulation skills that are replaced by stereotyped hand movements, other motor abnormalities including abnormal muscle tone, ataxia and apraxia. RTT is considered as one of the most common causes of complex disability in girls as reviewed in Chahrour et al. 2007 [4].

For the diagnosis of classical Rett syndrome, which is based exclusively on a set of clinical criteria derived from expert consensus [5], the affected individuals must have had a period of relatively normal development after birth, followed by regression of skills as described below. Moreover, classic RTT has a characteristic disease progression, which has been subdivided into four distinct clinical stages.

The **stagnation stage** occurs between 6 months and 1.5 years of age after a period of normal development [2]. Sudden changes in interactive behavior of the girls can be noticed but since the overall developmental pattern of the child is still grossly normal, the behavioral declination is not always significant enough to warrant the concern of the physicians. In the period of **active regression,** occurring at 1 to 4 years of age, [2] acquired abilities, such as voluntary hand use and language, are completely or partially lost. In addition, some affected individuals show autistic traits and become socially withdrawn, disliking physical contact, avoiding eye gaze, and being indifferent to visual and aural stimulation. Without the development of more distinctive manifestations of RTT, such as the repetitive hand stereotypies, the diagnosis of autism may be entertained at this stage. In the third **pseudo-stationary phase,** the loss of skills stops and the typical repetitive hand stereotypies, which represent the hallmark of the disorder, become prominent. The hand stereotypies are classically described as hand wringing and washing but also hand tapping/clapping or clasping may be manifested. The visual contact somehow returns and the child may look more alert and joyful with typical eye-pointing behavior to express needs and wishes. Gait impairment, such as dyspraxic and ataxic gait, is typically noted at this time. In this stage that can last for decades, the girls and women might still be able to learn new things, situations, and persons. Finally, in the **late motor deterioration phase,** a deterioration of the skeleton-muscular apparatus is observed and RTT patients often become wheelchair dependent. Hand stereotypies become less intense and simpler with age. Lack of motor activity finally leads to a state of frozen rigidity. However, some patients never lose the ability to walk and remain in stage 3 throughout their lives.

Besides the above described clinical features, RTT patients may suffer from growth failure, acquired microcephaly, gastrointestinal problems, seizures and nonepileptic spells, breathing and cardiac abnormalities, autistic features, and other behavioral problems.

An impairment of the autonomic nervous system in RTT is suggested by an increased incidence of long Q-T intervals (measure of the time between the start of the Q wave and the end of the T wave in the heart's electrical cycle) during electrocardiographic recordings contributing to the higher incidence of sudden unexpected death in RTT patients. Even with the high risk of sudden death because of respiratory and cardiac dysfunctions, patients may survive till the 6^{th} or 7^{th} decade of life with limited mobility.

Along with symptoms described above, epilepsy is very common in Rett syndrome with a

frequency ranging from approximately 50-90% [6,7]. The onset of epilepsy generally correlates with clinical stages 2-3, meaning that the seizures appear between 2-5 years of age, with a very small percentage occurring after the age of 10 years [8,9,10]. The severity of epilepsy often tends to decline after adolescence, with decreased seizure frequency and overall less secondary generalized seizures even in those patients who were previously considered quite intractable [6,10].

The first group of proteins that were discovered with the potential of binding to methylated DNA were the methyl-CpG binding domain (MBD) proteins. The mammalian MBD family consists of 5 nuclear proteins, MBD 1–4 and Methyl-CpG binding protein 2 (MeCP2) [11]. *MECP2* is an X-linked gene, which was discovered as the prototype member of the DNA methyl binding proteins [12].
The *MECP2* gene is ubiquitously expressed in human and mouse tissues but is particularly abundant in the central nervous system, suggesting an important role of the protein in this organ. Accordingly, in 1999, mutations in the *MECP2* gene were unexpectedly identified in patients with Rett syndrome and surprisingly the gene turned out to be the epigenetic factor; in the following years mutations in *MECP2* have been found to account for more than 95% of patients with classical Rett syndrome [3,13].

Structure and function of *MECP2*

The *MECP2* gene maps between L1CAM and the RCP/GCP loci in Xq28 and is subject to X Chromosome Inactivation (XCI) in females [14,15]. The genomic locus of *MECP2* spans approximately 76 kb and consists of four exons encoding two different isoforms (MeCP2E1 and MeCP2E2) that are generated by alternative splicing of exon 2, as depicted in **figure 1**. Alternative 3'-UTR usage leads to a short 1.8 kb and a long 10 kb transcript that includes a highly conserved 8.5 kb long 3'-UTR, with a third additional low abundance transcript of approximately 5–7 kb [14].

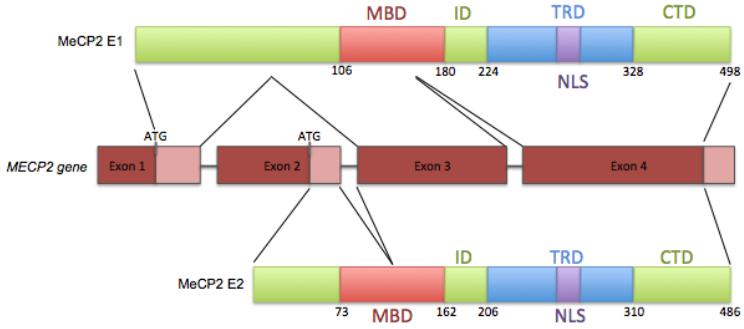

Figure 1: The *MECP2* gene and protein isoforms. Schematic illustration of the *MECP2* gene structure (middle part) and the different domains of the two protein isoforms, MeCP2E1 and MeCP2E2 (upper and lower bars, respectively). Adapted from Zachariah et al. (2012) [16].

Along with the methyl-CpG-binding domain (MBD), through which MeCP2 binds methylated DNA, the protein also contains a nuclear localization signal (NLS), a transcriptional repression domain (TRD), and a C-terminal domain (CTD). Whereas the NLS directs the protein to the nucleus, the TRD generates a physical association with transcriptional co-repressors such as Sin3a, which recruits the histone deacetylases HDAC1 and HDAC2 to methylated DNA resulting in a compact chromatin structure that represses local gene expression [17,18,19] as shown in **figure 2**. Recently, Baker and colleagues identified an AT-hook domain within the TRD of MeCP2 that plays an important role in chromatin organization. AT-hooks are regions of proteins that bind to AT-rich DNA and, accordingly, MeCP2 requires an A/T rich motif adjacent to the methylated CpG-dinucleotides for efficient binding [20]. The molecular function of the C-terminal domain is not entirely defined yet but it is supposed to be critically important for the proper functioning of the protein, facilitating DNA binding and protein-protein interactions [21,22].

Of the two isoforms, MeCP2E1 is 10 times more abundant than MeCP2E2 in brain. The two isoforms differ only in their N-terminal sequences, thus sharing the main functional domains, MBD and TRD, and it seems likely that their functional properties overlap considerably. A number of point mutations have been identified that are unique to the MeCP2E1, indicating that MeCP2E1-specific mutations are sufficient to cause RTT.

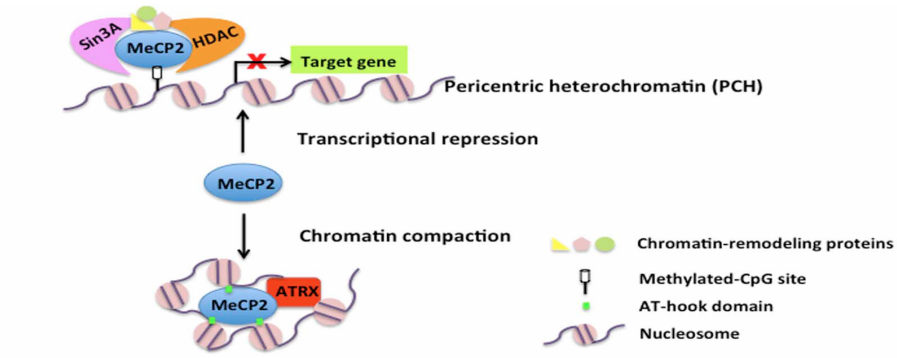

Figure 2: The function of MeCP2 in gene silencing and chromatin compaction. As a transcriptional repressor, MeCP2, when bound to methylated DNA, recruits Sin3A, HDACs and some chromatin remodeling proteins to silence target gene transcription. Adapted from Xin Xu and Lucas Pozzo-Miller (2013) [23].

While more than 90% of RTT cases are caused by sporadic mutations in *MECP2*, eight sites are the most common ones and account for more than 65% of all RTT causing mutations. The deamination of methylated cytosines generating C>T transitions are responsible for these so-called hotspot mutations that are depicted in **figure 3.** Although mutations are distributed throughout the gene, missense mutations tend to cluster in the MBD while, large multi-nucleotide deletions occur in the C-terminal domain (CTD) and the most nonsense mutations are distal to the MBD [24].

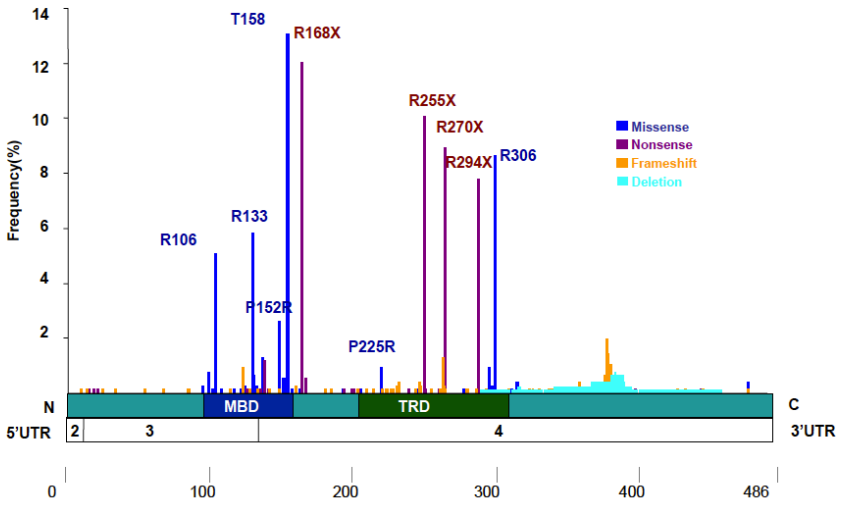

Figure 3: MeCP2 hotspot mutations. Adapted from the MeCP2 mutation database (http://www.mecp2.org.uk/).

MeCP2 functions

Based on a large body of evidence, MeCP2 was depicted as a transcriptional repressor and initially RTT was hypothesized to be caused by the deregulation of genes whose dysfunction was sufficient to cause the observed phenotypes. Transcription profiling experiments, however, failed to reveal gross changes in gene expression and only few genes such as Bdnf have been found consistently deregulated in the absence of MeCP2. Moreover, genome wide analysis of gene expression in MeCP2 mutant mice showed that MeCP2, contrary to expectation, could activate the expression of many genes directly or indirectly [25]. In support of this idea, a biochemical interaction between MeCP2 and the transcriptional activator CREB was reported [25]. In addition, MeCP2 has been proposed to regulate RNA splicing through its interaction with the splicing factor, YB1, and moreover, protein synthesis is reduced due to reduced mTOR activity. It is thus clear that further analyses are required to clarify whether MeCP2 is simply a methyl-DNA binding protein involved primarily in transcriptional repression or a multi-functional protein with global or local effects on chromatin. For instance, recent work demonstrates that MeCP2 in neurons, where it is particularly abundant, binds broadly throughout the genome, suggesting that it might function more as a global regulator of transcription and chromatin remodeling rather than as a sequence-specific transcription factor [26,27]. The current state of our knowledge therefore suggests that RTT might be caused by the misregulation of both transcription and other MeCP2 dependent processes.

Expression pattern and neuronal functions

Though MeCP2 protein expression is found through out the body, its expression is highly abundant in the central nervous system. The onset of *Mecp2* expression occurs in a defined pattern during perinatal development, where it becomes apparent in the most ontogenetically ancient part of the brain, such as the brainstem and thalamic regions, where after it gets expressed in progressively more rostral structures during development [28,29,30]. The transcript levels are high during embryogenesis with a post-natal decrease, but increase again towards adulthood. On the other hand, the protein levels are low during embryogenesis and increase post-natally upon neuronal maturation [29].

The loss of MeCP2 does not affect overall brain structure but neurons are smaller and more

densely packed resulting in a reduced brain volume. Moreover, decreased axonal and dendritic arborization and dendritic spine density are observed in hippocampal pyramidal neurons from *Mecp2*-null mice, demonstrating that the protein plays a significant role in regulating neuronal morphology. The levels of microtubule-associated protein 2 (MAP2) were also found reduced upon loss and gain of MeCP2 expression [31,32,33,34,35] in accordance with the involvement of MeCP2 in shaping dendritic morphology.

The imbalanced level of MeCP2 also affects synaptic connectivity since its loss tends to decrease the excitatory synapse number [32,35]. Accordingly, loss of MeCP2 causes reduced excitatory input while the inhibitory input was enhanced indicating that the homeostatic balance between excitation and inhibition depends on MeCP2 [36].

The change in MeCP2 expression also affects LTP (long term potentiation) as evidenced by the fact that the loss of MeCP2 produces significant deficits in hippocampal LTP [37,38], while enhanced synaptic plasticity can be observed in mice with increased MeCP2 protein levels. This suggests that MePC2 dysfunctions might cause deficits in learning and memory that are actually a hallmark of *MECP2* related disorders.

Despite the low abundance of MeCP2 in glial cells, recent evidence suggests that the methyl-binding protein may also play an important role in astrocytes and microglia [36,39,40,41]. An *in vitro* co-culture system showed that the microglia or astrocytes lacking MeCP2 inhibit dendritic arborization of wild-type neurons by producing a toxic factor, later proposed to be glutamate. *In vitro* evidence also confirmed that loss of MeCP2 within astrocytes leads to a gap junction dependent failure of affected astrocytes to properly support dendritic development as well.

Phosphorylation status of MeCP2 and its influence on pathogenicity of RTT

The post-translational modification (PTM), such as phosphorylation, has emerged as a potential mechanism to provide localized functional specificity to the widely distributed MeCP2. In the last years, MeCP2 has been found phosphorylated on a number of residues in neuronal cultures and in brain [42]; however, so far, the functional role and the upstream signaling of only few sites have been studied. Importantly, the phosphorylation of these sites is differentially induced by neuronal activity, brain-derived neurotrophic factor, or agents that elevate the intracellular level of 3′, 5′-cyclic AMP (cAMP), indicating that MeCP2 may function as an epigenetic regulator of gene expression that integrates diverse signals from the

environment.

In neuronal cultures, the phosphorylation of S421, which is induced by neuronal activity, was found to cause the release of MeCP2 from the Bdnf promoter, suggesting a mechanism involved in the activity dependent induction of this gene [43]. However, genome wide *in vivo* studies showed that upon S421 phosphorylation, MeCP2 remains associated with the genome [27]. A further understanding of how this PTM regulates gene expression is thus still awaiting but its role for neuronal functions is evident since dendritic growth and spine maturation are dependent on the activity dependent S421 phosphorylation of MeCP2 [43,27]. Moreover, knock-in mice carrying a phosphor-defective mutation (S421A) developed by Cohen and colleagues demonstrated that neuronal activity-dependent phosphorylation of S421 is necessary for animals to process novel experience and respond appropriately to previously encountered objects or animals. Whereas S421 phosphorylation is induced by neuronal activity, S80 and S399 are phosphorylated in resting neurons and get dephosphorylated with neuronal activity [42] reinforcing the idea that MeCP2 PTMs are highly dynamic. Lately, activity dependent phosphorylation of T308, was found to abolish the interaction of MeCP2 with the co-repressor NCoR and suppresses the repressive action of MeCP2 on transcription [44]. Interestingly, T308 phosphorylation is impaired by the RTT causing mutation R306C implicating that RTT in humans might be caused by disruption of important phosphorylation events of MeCP2. None of the phospho-defective mice models generated either by Cohen et al. (S421A), Tao et al. (S80A and S424A/S421A), or Ebert el al. (T308A) fully recapitulates the phenotypes that are observed with total MeCP2 disruption or overexpression, indicating the complexities in understanding the relevance of these modifications to RTT. Conclusively, these observations indicate that phosphorylation of MeCP2 determines its functional activity and that disruption of any of these phosphorylation events or its interacting partners may lead to neurological abnormalities in RTT. Accordingly, CDKL5, which is associated with the Hanefeld variant of Rett syndrome, has been proposed to act upstream MeCP2 in a common molecular pathway even if *in vivo* evidence for the capacity of CDKL5 to phosphorylate MeCP2 is still missing [45].

The mouse models: an insight into the RTT pathogenesis

To understand the molecular and cellular bases of RTT pathophysiology as well as to improve the basic knowledge of the role of MeCP2 for brain development and function, several mouse models have been generated that recapitulate a broad spectrum of RTT phenotypes.

The Jaenisch model was generated through cre-lox recombination causing the deletion of exon 3 of the *Mecp2* gene [46]. Male mice show normal development until 5 weeks of age when they start developing nervousness, body trembling, piloerection, and occasional breathing abnormalities. They typically experience weight loss at the age of 8 weeks and most of them die by the age of 10 weeks. They normally have smaller cortical neurons packed at a higher density and show reduced dendritic complexity in pyramidal neurons in the cortex [47] as well as in the hippocampal CA3 region and granule cells of the dentate gyrus [39]. The Bird model was obtained by deletion of exon 3 and exon 4 of *Mecp2* in embryonic stem cells to produce a complete null in terms of the production of MeCP2 protein [48]. Hemizygous males start developing symptoms such as stiff uncoordinated gait, hindlimb clasping, irregular breathing, and uneven teeth wear only after 10 weeks. Furthermore, they start showing weight loss and die at around 12-16 weeks. Conversely, heterozygous females survive longer and are fertile. The symptoms such as inertia and hindlimb clasping start at around 3 months and later on breathing abnormalities and decreased mobility occur. The $MeCP2^{308/y}$ model was developed by insertion of a stop codon at amino acid 308 resulting in the expression of a truncated protein retaining the MBD, TRD and NLS [29]. The mice show comparatively milder phenotypes and survive much longer than MeCP2 null models. $MeCP2^{308/y}$ mice have impairments in hippocampal-dependent spatial memory as well as social memory.

Additionally, Collins and colleagues developed a mouse model ($Mecp2^{Tg1}$) expressing MeCP2 at approximately 2 fold levels [49]. At the same time Luikenhuis et al. developed another mouse line overexpressing a Tau-MeCP2 fusion protein selectively in post-mitotic neurons from the *Tau* locus in homozygous *Tau* knockout mice [50]. Both transgenic models overexpressing MeCP2 show neurological phenotypes that are largely overlapping. The $Mecp2^{Tg1}$ mice appear clinically normal until 10–12 weeks of age when they start exhibiting symptoms such as enhanced motor and contextual learning and enhanced synaptic plasticity in the hippocampus. However, later on, these mice develop seizures and become hypoactive and approximately 30% die by the age of 1 year [49]. The phenotype associated with increased MeCP2 levels implies that *MECP2* is a dosage sensitive gene and that slight

perturbations in its levels are deleterious for brain functioning in mice. Accordingly, in humans the *MECP2* duplication syndrome has in the last years been recognized as a distinct clinical phenotype in males [51].

Since the viability of neurons is not affected by MeCP2 mutations and, therefore, rather than being a neurodegenerative disorder, RTT is considered a neurodevelopmental disorder. This led Guy and colleagues to test whether re-expression of Mecp2 in symptomatic mice lacking *Mecp2* might be sufficient to rescue the RTT-like symptoms. Intriguingly, several features of the disease such as general health condition, LTP defects, and viability were restored [52] raising the possibility of a beneficial effect of gene therapy to increase MeCP2 levels in RTT individuals. Two other studies demonstrated that restoring Mecp2 in postmitotic neurons rescues the RTT-like phenotypes observed in *Mecp2*-deficient mice [53,50]. Even if these studies have provided evidence that RTT is a reversible condition, at least in mice, it is important to recall that neuronal functions are highly sensitive to MeCP2 levels and a gene therapy approach in humans must be well controlled to express MeCP2 at physiological levels.

To understand whether the loss of MeCP2 in fully mature mice generate the same symptoms as the loss of the protein in early post-natal life, McGraw and colleagues developed an adult onset model of RTT by crossing mice harboring a floxed MeCP2 allele with mice carrying a tamoxifen-inducible CreER allele [54]. These adult knockout (AKO) mice displayed hypo-activity, abnormal gait and hind-limb clasping after tamoxifen administration and, later on, the AKO mice developed motor abnormalities and impaired nesting ability as well as impairment in learning and memory and finally they die. These studies suggest that the MeCP2 functions must be continuously maintained throughout the life for proper functioning of the brain [54].

It has already been discussed in previous section that MeCP2 plays an important role in glia. Microglia, the brain-resident macrophages, are of hematopoietic origin and have received increasing attention in the pathophysiology of several neurodegenerative and neuropsychiatric diseases. Derecki and colleagues analyzed the role of the microglia in RTT by transplantating wild type bone marrow into irradiation conditioned *Mecp2*-null mice resulting in the engraftment of brain parenchyma by bone marrow derived myeloid cells of microglial phenotype. Interestingly, the transplantation of wild-type MeCP2-expressing microglia attenuates numerous facets of disease pathology in *Mecp2*-null male and heterozygous female mice. Indeed, the targeted expression of MeCP2 in myeloid cells in an otherwise *Mecp2*-null background increased the lifespan, normalized the breathing patterns and improved locomotor

activity, restoring the normal body weight whereas neurological symptoms remained unaltered [55]. This effect was found to depend on the phagocytic capacity of the microglia. Based on these results it has been proposed that apoptotic debris accumulates over time in the *Mecp2*-null brain, contributing to neuronal malfunction and accelerating disease progression. Therefore, these observations suggest the importance of microglial phagocytic activity in Rett syndrome and finally it can be speculated that bone marrow transplantation might offer a feasible therapeutic approach for this devastating disorder.

Atypical forms of RTT

A variety of specifically defined variant forms of RTT have been recognized that have distinct clinical features. Some of these forms have been recognized in only a small number of cases, making it difficult to make any clear statement concerning the defining clinical features. However, multiple cases have been described for three distinct variant forms of RTT, including the preserved speech variant [56], the congenital variant [57], and the early-onset seizure variant [58]. In contrast to the preserved speech variant that is the most frequent one and has well-defined clinical features, mutations in *MECP2* have only rarely been identified in the congenital and the early seizure variants [59,60,61]. A varied range of mutations has been found in different loci associated with these variant forms such as mutations in CDKL5 in the early seizure variant [62] and mutations in FOXG1 in patients with the congenital variant [63].

Early-onset seizure variant (Hanefeld variant) of Rett syndrome

The apparent lack of *MECP2* mutations in a small proportion of clinically well-defined Rett syndrome cases suggested the existence of at least one other RTT locus. In 2005 genetic analyses [64,65,66] revealed mutations in the gene encoding cyclin dependent kinase-like 5 (CDKL5) in patients who had been diagnosed with atypical Rett syndrome but without mutations in *MECP2*, supporting the existence of genetic heterogeneity in RTT.

History

In 1985, Folker Hanefeld reported of a girl with infantile spasms and hypsarrhythmia in early life [58] who later developed many characteristics of Rett syndrome; he thus firstly described the "early-onset seizure variant of RTT syndrome" that was later named the Hanefeld variant of RTT. Goutieres and Aicardi described two additional cases with early and intense seizure activity followed by rapid and profound behavioral deterioration [67]. In one of those patients, the seizures were reminiscent of infantile spasms. The RTT Hanefeld variant presents a phenotypic overlap with West syndrome, also known as X-linked infantile spasm syndrome (ISSX; OMIM 3083350), which is characterized by the triad of infantile spasms, hypsarrhythmia, and severe to profound mental retardation. In 2003, Vera Kalscheuer et al. characterized 2 unrelated female patients with a similar phenotype, comprised of severe early-onset infantile spasms with hypsarrhythmia and profound global developmental arrest. The two patients showed an apparently balanced translocation where the X-chromosomal break-points disrupted *CDKL5* in both patients. Subsequently, several groups screened for *CDKL5* mutations in patients with both classic and atypical variants of RTT, but mutations were identified only in patients with seizure onset before 6 months of age [68,66,61].
The *CDKL5* gene was initially identified through a positional cloning study aimed at isolating disease genes mapping to Xp22. Sequence analysis revealed homologies to several serine-threonine kinase genes and identified one protein signature specific for this subgroup of kinases, hence the gene was named STK9 [69]. Moreover, since the kinase has a strong similarity to some cell division protein kinases [70], the STK9 gene subsequently appeared as CDKL5/STK9 and, eventually, got renamed CDKL5.

Clinical Features

The central features of the *CDKL5* related phenotype include the early onset epileptic encephalopathy with seizures starting within the fifth month of life, severe developmental delay, deceleration of head growth, impaired communication and, often, hand stereotypies resembling those observed in RTT. Several dozens of girls and a few boys with *CDKL5* gene mutations, or genomic deletions, have been reported, who were all having early-onset seizures

that in many cases were drug resistant.

Reports suggested that several of the distinctive clinical features of Rett syndrome are lacking in *CDKL5* related disorders; for instance, girls with *CDKL5* mutations do not exhibit a clear period of regression, neither do they present the intense eye gaze and impaired neurovegetative function such as breathing disturbances, cold extremities and gastrointestinal disturbances, typically seen in girls with classic RTT. Patients with *CDKL5* gene abnormalities are reported to be normal in the first days of life and subsequently exhibit early signs of poor developmental skills, including poor sucking and eye contact, even before seizure onset. Subsequently, absence of purposeful hand use, severe developmental delay, and lack of language skills become apparent [61,71,72,73,74,5,75]. About one third of patients will eventually be able to walk [71]. The typical neurological involvement in the Hanefeld variant of RTT is an epileptic encephalopathy with infantile spasms starting between the first days and fourth month of life [71]. Patients show a peculiar seizure pattern with ‘‘prolonged’’ generalized tonic-clonic events, lasting 2–4 min, consisting of a tonic-vibratory contraction followed by a clonic phase with series of spasms, gradually translating into repetitive distal myoclonic jerks [75]. Further studies of children older than 3 years showed that about half of them can experience seizure remission, whereas the remaining continue to have intractable spasms, often associated with multifocal and myoclonic seizures [71,74]. Early EEG findings vary from normal background to moderate slowing, with superimposed focal or multifocal interictal discharges and, in some cases, suppression burst pattern [75]. Although no specific seizure semiology has been described, two individual reports have noted a seizure pattern that may be unique to this disorder [75,76]. In one report a seizure pattern of tonic-tonic/vibratory contraction was observed, followed by a clonic phase with spasms and finishing with distal myoclonus [76]. In another report an initial hypermotor phase was seen, followed by tonic extension and then spasms.

Whereas *MECP2* mutations are rarely found in males, Liang et al. estimated that, in cohort of patients affected by epileptic encephalopathy, *CDKL5* mutations have a frequency of 5% in males and 14% in females [77]. Males with CDKL5 mutations have in some cases been described as being more severely affected than girls; in fact, it has been reported that few of them learned to walk and few acquired spoken communication and hand function. Moreover, seizure onset was slightly earlier than in females, and all males were having either daily or monthly seizures [78]. Altogether, this suggests that an amelioration of the phenotype in females might be explained by X-inactivation in females resulting in a mosaic expression of normal, and mutant CDKL5 protein. However, a study describing a male with Klinefelter

syndrome (47,XXY) and a large CDKL5 COOH-truncation presenting a phenotype comparable to those of other CDKL5-positive boys suggests that the presence of a wild-type CDKL5 allele and a balanced pattern of X inactivation does not reduce the severity of the disease [79]. In RTT, males with mutations that cause classic RTT in females tend to be extremely affected, often dying at an early age due to severe infantile encephalopathy; in some cases males are mildly affected and have been found to have hypomorphic *MECP2* mutations that are not found in females [80]. It would be of interest to further investigate the genetic variability between males and females with *CDKL5* disorders to determine whether a similar phenomenon exists.

Together with the aforementioned phenotypes in CDKL5 patients, it has been proposed that, contrary to classic RTT, the CDKL5 disorder can be associated with distinct subtle facial, limb and hand phenotype that may assist in its differentiation from other early-onset encephalopathies. Although mutations in *CDKL5* have been described in association with the early-onset variant of RTT, the majority of the patients do not fulfill the criteria for RTT [78]. According to the criteria established by Neul et al. for atypical RTT, five specific items (early-onset seizures before 5 months of age, infantile spasms, refractory myoclonic epilepsy, seizure onset before regression and decreased frequency of typical RTT features) were included that differentiate the ESV (early-onset seizure variant) from other atypical forms [5]. In particular, the period of regression, which is a necessary criterion for RTT, is often absent in patients with CDKL5 mutations. Altogether, the CDKL5 disorder is now started being considered separate to RTT, rather than another variant of this syndrome.

Structure of the *CDKL5* gene and its protein isoforms

The human *CDKL5* (Gene bank accession number Y15057) gene occupies approximately 240 kb of the Xp22 region and is composed of 24 exons. The first three exons (1, 1a, 1b) are untranslated and probably represent 2 transcription start sites, whereas the coding sequences are contained within exons 2-21. Two splice variants with distinct 5'UTRs have been found: isoform I, containing exon 1, is transcribed in a wide range of tissues, whereas the expression of isoform II, including exons 1a and 1b, is limited to testis and fetal brain [70,81]. An altered C-terminal region characterizes these two isoforms as depicted in **figure 4**. Importantly, one of these (CDKL5$_{107}$) is common in a number of species, including mouse. Interestingly, an alternative splice variant, containing yet another distinct C-terminus, has been predicted

through a bioinformatics simulation but its existence still needs to be revealed [82].

Moreover, in rats, 2 splice isoforms named *CDKL5a* and *CDKL5b* (GenBank accession numbers: FJ807484 and GU351881) corresponding to predicted proteins of 934 and 877 amino acids, respectively, have also been identified [83]. While *CDKL5a* appears to be the major isoform in pure neuronal cultures, *CDKL5b* is the only form present in pure glial cultures suggesting a function in gliogenesis. Recently, a novel and highly conserved 123-bp exon was identified between exons 16 and 17, referred as *CDKL5* exon 16b [84] or *CDKL5* exon 16a [85]; the inclusion of the encoded 41 amino acids seems to occur specifically in the brain [84].

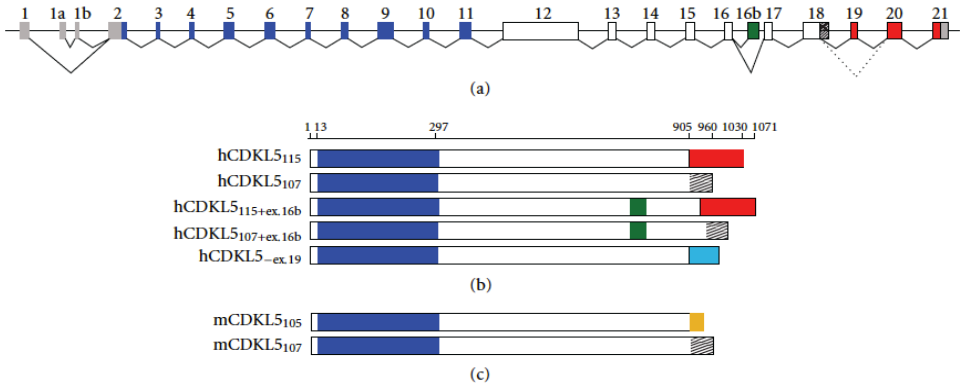

Figure 4: Genomic structure of *CDKL5* and its splice variants. (a) The human *CDKL5* gene with non-translated sequences in grey and exons encoding the catalytic domain in blue. Exons encoding the common C-terminal region appear in white, whereas isoform-specific sequences are shown in red, green, and as hatched. (b) hCDKL5 protein isoforms differing in the C-terminal region. CDKL5$_{115}$ [45] contains the primate-specific exons 19–21. In CDKL5$_{107}$ [81], intron 18 is retained. The inclusion of exon 16b would generate CDKL5$_{115+ex.16b}$ and/or CDKL5$_{107+ex.16b}$ [84,85]. hCDKL5$_{–ex19}$ is a hypothetical splice variant in which exon 19 is excluded generating an alternative C-terminus (light blue) (c) The murine CDKL5 isoforms. mCDKL5$_{105}$ harbors a distinct C-terminal region encoded by a mouse-specific exon 19 (orange). As in humans, the retention of intron 18 generates the common CDKL5$_{107}$ isoform [81]. Adapted from Kilstrup et al. 2012 [82].

The originally identified human CDKL5 is a large protein of 1030 amino acids with an estimated molecular mass of 115 kDa [86]. Initially, Montini et al. suggested that CDKL5 is a

putative proline-directed serine/threonine kinase (due to the presence of a critical arginine-residue in the kinase subdomain VIII), which is closely related to p56 KKIAMRE and p42 KKIALRE (encoded by CDKL2 and CDKL1, respectively) that share homology with members of the mitogen-activated protein (MAP) kinase and cyclin dependent kinase (CDK) families [69]. The sequence analysis of the CDKL5 protein showed 2 kinase signatures in the catalytic domain: an ATP-binding region (amino acids 13-43) and a serine-threonine protein kinase active site (amino acids 131-143). Moreover, CDKL5 is characterized by a Thr-Xaa-Tyr motif (TEY) at amino acids 169-171, whose dual phosphorylation is normally involved in activating, among others, kinases of the MAP kinase family. CDKL5 appears to be capable of auto-phosphorylating its TEY motif like some other MAPKs [86]. Additionally, CDKL5 is unique in this family of kinases as it displays an unusual long tail of more than 600 amino acids without obvious similarity to other protein domains but with a high degree of conservation between different CDKL5 orthologs that differ in the most extreme C-terminus. Moreover, putative signals for nuclear import (NLS) and export (NES) are present in the C-terminus of the protein as depicted in **figure 5**.

As mentioned above, recently, a new 107-kDa isoform with an alternative C-terminus that terminates in intron 18 was identified [81] and appeared to be the major isoform in human brain and all other tissues investigated except testis [81].

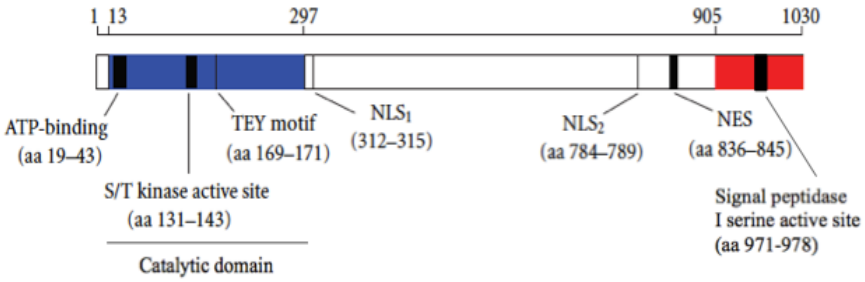

Figure 5: Schematic illustration of full-length human CDKL5 of 1030 amino acids containing the ATP binding site, the serine/threonine (S/T) kinase active site and the conserved Thr-Xaa-Tyr (TEY) motif within the catalytic domain. A putative signal peptidase I serine active site, 2 supposed nuclear localization signals (NLS) and one supposed nuclear export signal (NES) are indicated. The number on the top refers to the amino acids positions. Adapted from Kilstrup et al., 2012 [82]

Mutations in the *CDKL5* gene and their influence on the phenotypic outcome

The *CDKL5*-related disorder is an X-linked dominant disorder. Almost all the described cases are simplex cases (i.e., a single occurrence in a family), resulting from a *de novo* mutation except 1 familial case with 3 affected individuals [65]. The diagnosis of the *CDKL5*-related disorders relies on molecular genetic and cytogenetic testing. Though, the overall frequency of *CDKL5* mutations in females with early-onset seizure is around 8-16% [62,73,74], the *CDKL5* mutation rate is higher (28%) in female patients with early-onset seizures combined with infantile spasms [62].

Approximately 100 different CDKL5 patients, harboring a wide range of pathogenic mutations have been described so far, including missense and nonsense mutations, frameshifts, deletions (small and large), and aberrant splicing as described in **figure 6.** Albeit the small number of cases does not allow to draw any conclusive data, hot-spots have been suggested so far only for few mutations such as A40V, 172N/T, R178P/W/Q (**Figure 6**). The mutations are spread all over the coding sequence of *CDKL5* with missense mutations found almost exclusively in the catalytic domain, thus confirming the relevance of the kinase activity of CDKL5 for proper brain functions. The missense mutations seem to reduce the kinase activity of CDKL5 [86]. Indeed, observations suggest that mutations in the catalytic domain of CDKL5 cause impairment in auto-phosphorylation and phosphorylation of target proteins such as MeCP2 [64,86]. On the contrary, truncating mutations can be located anywhere in the gene, leading to CDKL5 derivatives of various lengths. Again, the relevance of the rather uncharacterized C-terminal part of CDKL5 is suggested by the fact that many pathogenic alterations involve the C-terminus. Even though, so far, no reports have demonstrated the existence of the truncated CDKL5 proteins in human cells, the molecular effects of some pathogenic CDKL5 mutations (missense and truncating derivatives in the background of the CDKL5$_{115}$ isoform) have been addressed through the overexpression of mutated derivatives in non-neuronal cell lines [87,86,88]. A regulatory role of the tail of CDKL5 has emerged from the characterization of few C-terminal truncating derivatives that have enhanced kinase activity and a constitutive nuclear accumulation [89]. It thus seems to act as a negative regulator of the catalytic activity of CDKL5 and to modulate the subcellular localization. In particular, since both the pathogenic derivatives L879X and R781X confine

CDKL5 to the cell nucleus, it can be assumed that the very last portion of CDKL5 contains a signal localizing the protein to the cytoplasm. However, since the leucine-rich NES-like motif indicated in **Figure 6** is preserved in the L879X derivative, such motif seems insufficient for driving CDKL5 to the cytoplasm. Further studies have to be carried out to evaluate whether, a significant reduction of the catalytic activity of CDKL5 influences its subcellular distribution and the truncated CDKL5 mutants act as a loss or gain of function as well.

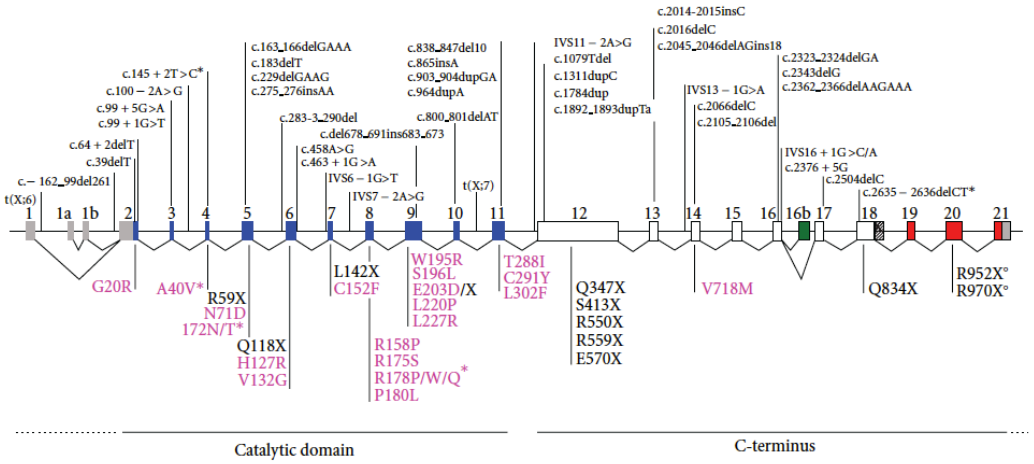

Figure 6: Pathogenic *CDKL5* mutations. All mutations in *CDKL5* reported to date are indicated corresponding to their location within the gene. Mutations shown above the *CDKL5* gene are deletion and frame shift mutations as well as splice variants indicated with cDNA nomenclature. Missense and nonsense mutations (fuchsia and black, resp.) are represented with amino acid nomenclature below the *CDKL5* gene. *: Recurrent mutations; ◦: Uncertain pathogenicity. Modified from Kilstrup et al., 2012 [82].

Interestingly, also duplications of larger genomic regions including, among other genes, CDKL5 have been identified [90,91,92], suggesting that a tight regulation of CDKL5 levels and/or activity is essential for the proper function of the nervous system. This hypothesis, if confirmed by further studies, will also have implications for gene therapy approaches.

CDKL5-Genotype-phenotype correlation

There is a versatile range of phenotypes associated with *CDKL5* mutations, including a milder form, where the epilepsy is controlled and independent ambulation is achieved, to a severe form with microcephaly, virtually no motor development and refractory epilepsy. The severity is determined by the protein product of the mutated allele of *CDKL5* along with the variability of X-chromosome inactivation. The limited number of patients does not permit drawing any genotype-phenotype correlation yet; however, some reports suggested that mutations in the COOH-terminus contribute to a milder clinical picture compared to mutations in the catalytic domain. Additionally, it was also reported that patients with stop codon mutations have a milder phenotype than those with missense or splicing mutations [93], whereas others state that the nature of the mutation does not correlate with the clinical heterogeneity. It is well known that the *CDKL5* gene is subject to X-chromosome inactivation (XCI). Therefore, skewed patterns of inactivation could explain phenotypic variability in females heterozygous for a mutated allele. For instance, Kalscheuer and colleagues reported some females with very severe phenotypes who carried X; autosome translocations, where the normal X chromosome was completely inactivated [70]. Conversely, Weaving et al. described two twin sisters exhibiting significant discordant phenotypes but with similar XCI pattern [65]. One proband showed a clinical phenotype overlapping with RTT while her twin sister showed autistic disorder and mild to moderate intellectual disability. The phenotypic differences in these two girls thus cannot be attributed to different degrees of XCI and an alternative explanation proposed that modifier genes might have influenced the disease severity.

Expression pattern, localization and functional consequences of CDKL5

Expression studies in human and mouse tissues have shown that *CDKL5* mRNAs can easily be detected in tissues such as testis, lung, spleen, prostate, uterus, and placenta but the levels are highest in brain, whereas they are hardly present, or under detection levels in heart, kidney, liver, and skeletal muscles. In the brain, CDKL5 levels reach a plateau in conjunction with the development and differentiation of this organ. *In situ* hybridization analysis of adult mouse brain revealed that the mRNA levels are particularly high in the adult forebrain, especially in the most superficial cortical layers particularly involved in the connection of the

two hemispheres through the corpus callosum. The higher abundance of *Cdkl5* mRNA in frontal cortical areas might suggest a role of the kinase in the physiology of such brain districts. The other brain areas such as motor cortex, the cingulate cortex, and pyriform cortex, possibly, in entorhinal cortex, also show significantly high levels of *Cdkl5* mRNA. Additionally, very high levels of *CDKL5* mRNA are detected in all the cornu ammonis (CA) regions of hippocampus compared to dentate gyrus (DG). Since the striatum also shows fair expression levels of *CDKL5,* it is assumed that the glutamatergic and gabaergic neurons are by far the two cellular types expressing most of the brain *CDKL5*. Comparatively, very low levels of *CDKL5* are found in the dopaminergic areas such as substantia nigra or the ventral tagmental area, and the noradrenergic areas such as the locus coeruleus. Interestingly, in several thalamic nuclei, including the geniculate nuclei, the *CDKL5* level is quite high. In the cerebellum, *CDKL5* mRNA is found in all the lobules and, possibly, in the Purkinje cells; its levels, however, appear significantly lower than the other brain areas.

Protein expression analyses have shown that the levels of the kinase more or less coincide with its transcripts in the developing and adult brains. During brain development, CDKL5 expression is very low in abundance in the embryonic cortex and is strongly induced in early postnatal stages where it reaches maximum levels at P14 and then declines slowly up to adult stages. Additionally, in the cerebellum, the expression of CDKL5 appears to be induced slightly later and continues to increase until adult stages [89]. Immunohistochemistry experiments in human adult brains revealed numerous and diffusely CDKL5-positive cells in both cerebral cortex and corpus callosum with a general pattern very similar to that observed in the adult mouse brain. Rusconi and colleagues showed that CDKL5 is easily detectable in virtually all NeuN-positive neurons while it is expressed at very low levels in the glia [89]. It was also observed that CDKL5 is found in the majority of the neuronal fraction regardless the neural origin; however, some neurons display increased levels of CDKL5, particularly in the dentate gyrus (DG). GABAergic cortical interneurons within the hilus express CDKL5 much stronger than the dentate granular neurons. Additionally, CDKL5 levels were observed comparatively higher in GABAergic neurons than glutamatergic neurons [89]. Furthermore, in the human cerebellum, CDKL5 is present in the majority of the cells corresponding to granular, molecular, and Purkinje cell layers, although increased levels were present in Purkinje neurons [89]. Therefore, the different CDKL5 expression patterns in different neuronal populations suggest that a strict control of CDKL5 levels is required to regulate specific neuronal activities.

Regulation of CDKL5 expression

As mentioned, the levels of *Cdkl5* transcripts vary during development and in the different brain regions. Presently, little is known regarding the regulation of Cdkl5 at the transcription level but 2 CpG islands (CGI) have been found upstream and downstream of the transcriptional start site that are conserved among mouse and human counterparts. The conservation and position of these CGIs suggest their possible involvement in the epigenetic regulation of CDKL5 expression based on DNA methylation. Accordingly, Cdkl5 expression was found to be silenced by DNA methylation, involving this area, and by the action of MeCP2 [94]; earlier reports, however, showed that *CDKL5* mRNA levels are unaltered in RTT patients' lymphocytes or brains of *Mecp2*-null mice [65,45]. Therefore, more studies are required to confirm a role of MeCP2 in inhibiting CDKL5 expression. Notably, Carouge et al. demonstrated that *Cdkl5* transcription appears to be regulated by different stimuli and depending on the specific brain areas; in the striatum of rats treated with cocaine (a pro-methylation agent), *Cdkl5* mRNA levels were found significantly reduced (probably as a consequence of methylation at the 5' of the *Cdkl5* gene), whereas this reduction was not noticed in frontal cortices of the same animals [94].

Several mechanisms seem to regulate CDKL5 functions and levels. The presence of various CDKL5 splice variants in the brain indicates that alternative splicing is involved in regulating CDKL5 functions; however, the distinct functions of different splice variants are still under consideration. The difference that has been observed so far is that CDKL5$_{107}$ appears to be more stable than the longer human CDKL5$_{115}$ isoform [81], whereas the subcellular localization of exogenous CDKL5 derivatives (CDKL5$_{115}$, CDKL5$_{107}$, and CDKL5$_{115+16b}$) is grossly identical [81,84]. CDKL5 functions seem to be regulated both through its subcellular localization and through its synthesis and degradation. The kinase is present in both nucleus and cytoplasm of cultured cortical neurons and in different neurons throughout the brain. In some regions of the brain such as hippocampus, cortex, hypothalamus, and thalamus, CDKL5 is almost equally distributed in cytoplasm and nucleus (around 40% of the protein is nuclear), whereas in the striatum and cerebellum, the cytoplasmic fraction accounts for almost 80% of CDKL5, suggesting that the difference in specific distribution of the protein between the two main cellular compartments must play a pivotal role in brain development. In late embryonic and early postnatal stages, CDKL5 is predominantly present in the cytoplasm with less than 20% of the protein being present in the nucleus. It gets progressively accumulated in the nucleus starting from roughly P14, indicating that there are some regulatory mechanisms

modulating the subcellular localization of CDKL5 in murine brain development [89]. In the nucleus, endogenous CDKL5 can be observed in nuclear clusters that have recently been demonstrated to correspond to the small nuclear ribonuclear protein complexes [95], linking the kinase to the complex machinery of RNA processing. Exogenous CDKL5 shuttles constitutively between the two main compartments in cultured non-neuronal cells through an active nuclear export-dependent mechanism involving the C-terminus of the protein and the CRM1 nuclear export receptor. Interestingly, however, in resting hippocampal neurons, the endogenous protein is not dynamically shuttling and its nuclear exit appears to be regulated by specific stimuli. In fact, glutamate treatment induces nuclear export of CDKL5 leading to its accumulation in the cytoplasm, suggesting that specific stimuli determine the shuttling of the kinase between the cellular compartments. It would be quite interesting to understand whether (a) posttranslational modifications or interactions with other proteins are involved in regulating the nuclear export/import of CDKL5, (b) the enzymatic activity of the protein is modulated by its localization and interaction with other factors, and eventually (c) with other stimuli influence the localization and activity of CDKL5.

CDKL5 functions seem to be regulated through its degradation under certain stimuli such as sustained glutamate treatment or other cell death signals but how the regulation of this degradation occurs and its significance for cell death/survival are still unknown. Williamson and colleagues demonstrated that the $CDKL5_{107}$ isoform is more stable, while $CDKL5_{115}$ is rapidly degraded in a proteasome-dependent manner in transfected cells, indicating that the very C-terminal region, from amino acid 905, contains signals responsible for this degradation [89].

CDKL5 involvement in neuronal morphogenesis, synaptic function, structure and plasticity

Although little is still known about the neuronal functions of CDKL5, an accumulating body of evidence suggests that the kinase is involved in the processes related to the regulation of gene expression and neuronal morphogenesis [83]. As mentioned, in neurons CDKL5 is present both in the nucleus and in the cytosol [89] where it interacts with several specific proteins and, therefore, the study of these interactions would provide information regarding the functions of CDKL5, the signaling pathways in which it might be involved and, finally, the relationship between CDKL5 mutations and the pathogenesis of the neurological disorders

caused by mutations in this gene.

As mentioned in the previous section, endogenous CDKL5 shows a diffuse staining with brilliant nuclear dots that do not overlap with heterochromatic DAPI-positive DNA in the nuclear compartment of cycling cells and primary hippocampal neurons [86,96], while the cytosolic CDKL5 immunostaining is finely dotted in both the soma and along the dendrites. Likewise, in adult mouse brain the punctate pattern of CDKL5 immunoreactivity is evident in cell bodies, along dendrites and in synaptic spines [97].

In the nucleus, CDKL5 has been found to interact with various proteins/factors and, in particular, several pieces of evidence suggest that CDKL5 belongs to the same molecular pathway as MeCP2. Mari and colleagues revealed that CDKL5 interacts with MeCP2 and is capable of phosphorylating the protein *in vitro* [45]. Moreover, the two proteins share a common spatial and temporal expression profile and, therefore, it can be speculated that CDKL5 may regulate MeCP2 functions through its post-translational modification. The loss of this phosphorylation dependent activity of MeCP2 might explain the presence of a subset of RTT like symptoms in patients with CDKL5 mutations whereas the distinct symptoms characterizing CDKL5 disorders would be caused by MeCP2-independent functions of the kinase. However, the influence of CDKL5 in determining the phosphorylation state of MeCP2 *in vivo* is still unclear. Some reports revealed two more interactors of CDKL5 in the nucleus, both involved in the regulation of gene expression. One is DNA methyltransferase 1 (DNMT1), an enzyme that recognizes and methylates hemimethylated CpG after DNA replication. *In vitro*, a truncated CDKL5 derivative, containing only the catalytic domain, binds and phosphorylates DNMT1 in the N-terminal region in the presence of DNA; however, further studies are required to confirm whether also full length CDKL5 associates with DNMT1 *in vivo* [98]. Considering the interaction of CDKL5 with DNMT1 and MeCP2, it can thus be speculated that CDKL5 may regulate the functions of epigenetic factors and transcriptional regulators. Another proposed interacting protein, the SR-family splicing factor, SC35, was found to co-localize with CDKL5 in the neuronal nuclear speckles both *in vitro* and *in vivo* and to co-immunoprecipitate with the kinase [95]. Interestingly, *in vitro* splicing assays indicated that some splicing deficits might be caused by the loss of CDKL5.

As mentioned, the expression pattern of CDKL5 correlates both *in vitro* and *in vivo*, with neuronal maturation; in fact, the protein reaches the highest levels of expression when neurons acquire a mature phenotype, suggesting an involvement of the kinase in neuronal differentiation and arborization [83,89,96]. Some of the CDKL5 dendritic punctae were found to localize to dendritic spines where a significant co-localization with PSD95 (post-synaptic

density protein 95) could be determined [97]. Consistent with the postsynaptic localization, CDKL5 immunolabelling was closely juxtaposed with presynaptic VGLUT1. Conversely, CDKL5 was also found to co-localize marginally with inhibitory synaptic markers, indicating that the majority of CDKL5 is localized at excitatory synapses both *in vitro* and *in vivo* [97].

It is well established that PSD-95 plays an essential role in synapse development and function by acting as the major scaffolding protein in the post-synaptic densities [99]. In excitatory synapses, PSD-95 associates with neurotransmitter receptors, adhesion molecules, and signaling enzymes, and its synaptic clustering precedes any of these associated partners, suggesting that it functions as an organizer to initiate synapse maturation. Recently, it was found that the N-terminal region of PSD-95 interacts efficiently with CDKL5 [100]. Interestingly, the palmitoylation of N-terminal residues of PSD-95 is necessary for the association with CDKL5. PSD-95, as any palmitoylated proteins, undergoes consecutive cycles of palmitoylation and depalmitoylation. In particular, the depalmitoylation of PSD-95 is accelerated by glutamate receptor activation, whereas palmitoylation is increased by blocking synaptic activity or by BDNF stimulation [101]. Palmitate cycling on PSD-95 controls its polarized targeting to synapses, which is essential for its synaptic functions [102]. Mutations within PSD-95 that interfere with palmitoylation reduced the synaptic targeting of CDKL5, suggesting that PSD-95 recruits the kinase to the synapses. Furthermore, some truncating disease causing mutations of CDKL5 abolish the association with PSD-95 suggesting a mechanistic insight to some cases of CDKL5-related disorders [100].

In accordance with the localization of CDKL5 at the excitatory synapses it has been shown that CDKL5 participates in the regulation of excitatory dendritic spine development and dendritic morphogenesis. In the excitatory synapses, CDKL5 also interacts with NGL-1 (Netrin-G1 Ligand 1), a transmembrane protein localized in the post-synaptic densities (PSD) [97]. NGL-1 specifically interacts with Netrin-G1, a lipid-anchored protein related to the netrin family of axon guidance molecules, and promotes the early synapse formation and subsequent maturation [103]. Among PSD-enriched proteins, the three components of the NGL-family (NGL-1, NGL-2 and NGL-3) were identified as CDKL5-interacting partners. Interestingly, CDKL5 was found to phosphorylate NGL-1 *in vitro* on Ser 631 and this phosphorylation event seems to strengthen the interaction between NGL-1 and PSD95 [97]. In line with a role of CDKL5 for synapse functions, dendritic spine morphogenesis and synaptic activity has been found altered in neurons devoid of CDKL5. Neurons depleted for CDKL5 showed a significant increase in protrusion density with dendritic protrusions being significantly thinner when compared with controls and showing a filopodia-like morphology.

Some of these thin filopodia-like spines were particularly branched and exhibited an aberrant morphology. Furthermore, the percentage of filopodia-like spines and thin-headed spines increased, whereas the percentage of stubby and mushroom-shaped spines decreased. These observations indicate that CDKL5 is required for ensuring a correct number of well-shaped spines, correct dendritic spine structure and synapse activity. In agreement with the *in vitro* studies, also the depletion of Cdkl5 in cortical pyramidal neurons *in vivo* by *in utero* electroporation (IUE) of mouse embryonic cortices generated a significant decreased density of VGLUT1 puncta in excitatory presynaptic buttons, confirming that CDKL5 is crucial for dendritic spine morphogenesis and synaptic contact maintenance also *in vivo* [97]. Given that CDKL5 is a protein kinase, its phosphorylation activity is likely to play an important role for neuronal functions. Studies with a kinase-dead CDKL5 derivative, CDKL5-K42R that is unable to bind ATP, confirm this hypothesis: Primary neurons overexpressing CDKL5-K42R exhibited a significantly high number of thinner and longer dendritic protrusions and a corresponding loss of stubby and mushroom-shaped spines. As the phenotype discovered for the CDKL5-K42R mutant was similar to the phenotype of CDKL5 knock-down neurons, it is conceivable that CDKL5 promotes spine formation through a mechanism that is dependent on its kinase activity and that the kinase-dead derivative acts as a dominant negative.

In addition to a role in regulating dendritic spine formation, CDKL5 has also been found to regulate neuronal morphogenesis [83]. Indeed, shRNA mediated silencing of Cdkl5 in cortical neurons leads to a marked reduction in the total length of both dendrites and axons. The total dendrite length and the complexity of arborization were also reduced upon Cdkl5 depletion, indicating that the expression of the kinase in cortical neurons is required for dendritic arborization as well as dendrite growth. *In vivo* studies also confirmed that CDKL5 is required for dendritic arborization. Indeed, morphological analysis of layer II/III pyramidal neurons in cortices silenced for Cdkl5 by IUE showed that the silenced neurons were characterized by a marked reduction in both the total length of apical dendrites and number of apical dendrite branches. Moreover, the IUE studies revealed that the silencing of Cdkl5 in rat embryos at E15 causes migration defects that can be observed at P0. The migration was not altogether blocked but delayed, since at P14 the neurons had migrated into cortical layers and extended apical dendrites towards the pial surface. Neuronal migration disorders are characterized by abnormal neuronal positioning in the cerebral cortex, which have been implicated in infantile spasm and seizures. For example, mutations in the human doublecortin (*DCX*) and reelin (*RELN*) genes cause profound defects in cortical neuron migration, and patients with these mutations have severe mental retardation and epilepsy [104,105].

Therefore, the delay in neuronal migration [83], caused by the loss of CDKL5, might be involved in the presence of seizures characterizing patients with *CDKL5* mutations.

According to the observations by Chen and colleagues [83], CDKL5 co-localizes with F-actin in the peripheral domain of growth cones, suggesting that CDKL5 might be involved in regulating actin cytoskeleton. Rac1 (Ras-related C3 botulinum toxin substrate 1), a small signaling G protein, which is a member of the Rho family, plays a crucial role in the regulation of cell growth and cytoskeletal reorganization and was found to mediate the effect of CDKL5. In COS-7 cells, the constitutively active form of Rac1 (CA-Rac1) forms a protein complex with CDKL5 and recruits the kinase to the membrane while a dominant negative form of Rac1 (DN-Rac1) failed to do so even under stimulation. In cultured neurons, Rac1 is activated by BDNF, a critical regulator of neuronal development and function. Moreover, BDNF stimulation was found to enhance the CDKL5 and Rac1 interaction directly or indirectly by formation of protein complex, and to trigger a transient increase in CDKL5 phosphorylation, suggesting that CDKL5 is involved in BDNF-induced activation of Rac1 and providing a reasonable explanation of the correlation between *CDKL5* mutations and the observed defects in cognitive functions [83].

Importantly, a *Cdkl5* knock-out mouse model has recently been developed, mimicking a disease causing mutation that leads to a frame-shift and the premature truncation within the N-terminal kinase domain, thus generating a loss-of-function mutation. Male mice lacking Cdkl5 ($Cdkl5^{-/y}$) and heterozygous females ($Cdkl5^{-/+}$) were viable, fertile, and displayed normal appearance, growth, and overall brain morphology [106]. Interestingly, the mice exhibit hyperactivity, impaired motor control, decreased anxiety and some autistic-like behavioral abnormalities such as impairment in social interaction as well as impairment in learning and memory. Although this mouse model mimics well the autism spectrum features characterizing patients with *CDKL5* deficits, the *Cdkl5*-null mice did not develop seizures and therefore does not fully mirror all the key-characteristics of humans with *CDKL5* mutations. A possible explanation could be given by distinct functions or modifications of CDKL5 in humans that might be absent in lower organisms. Moreover, the C57BL/6 genetic background is known to confer increased seizure resistance [107], possibly explaining the absence of seizures in the knock-out mice. Interestingly, the male mice lacking Cdkl5 ($Cdkl5^{-/y}$) exhibited a decrease in the phosphorylation profiles of various kinases that are involved in synaptic plasticity as well as in cellular metabolism, indicating that CDKL5 may play a critical role in coordinating multiple signaling cascades. In spite of lacking some characteristics of CDKL5 related disorders in humans, this model has paved the way of future understanding of the loss

of CDKL5 for various neurological functions and represents a crucial tool for future studies of the involvement of CDKL5 for human pathologies.

Neuronal polarization

Neurons are among the most polarized cell types in our body and possess two types of morphologically and functionally distinct processes: a single, long, and slender axon and several dendrites that are shorter processes with a tapered morphology. During the transmission of neuronal information, dendrites integrate synaptic inputs triggering the generation of action potentials at the level of the soma and propagate along the axon making presynaptic contacts onto the dendrite of target neurons [108].

Mammalian neurons usually migrate over a long distance before reaching their final destination. *In vivo,* most neurons undergo axon-dendrite polarization during migration where post-mitotic neurons form a leading and a trailing processes, which determine the axon or the dendrite depending on the cell type. For instance, the retinal ganglionic cells and bipolar cells in the developing vertebrate retina can inherit their axon and dendrite polarity directly from the apico-basal polarity of their progenitors whereas cerebellar granule neurons (CGN) as well as cortical and hippocampal pyramidal neurons (PN) undergo extensive stereotypical changes in their morphology that lead to a polarized outgrowth of their axon and dendrite. Importantly, both CGN and PN acquire their axon dendrite polarity from the polarized emergence of the trailing-leading processes during migration.

So far, most studies on the establishment of neuronal polarity are performed on dissociated, embryonic cortical and hippocampal neurons or post-natal cerebellar granule neurons [108]. Cultured primary hippocampal neurons undergo several stages during polarization as described by Dotti and Banker [109] (**Figure 7**). When the dissociated hippocampal neurons are plated, neurons attach to their substrate as round spheres (stage1) surrounded by actin-rich structures, lamellipodia and filopodia. In stage 2, several minor immature neurites, emerge, thanks to the coalescing lamellipodia in some areas of the growth cone. One of these minor neurites starts growing rapidly to become an axon at stage 3, while other minor neurites remain short and develop into dendrites at stage 4. Ultimately, at stage 5, the cells undergo further maturations and establish a neuronal network through synaptic contacts between dendritic spines and axon terminals.

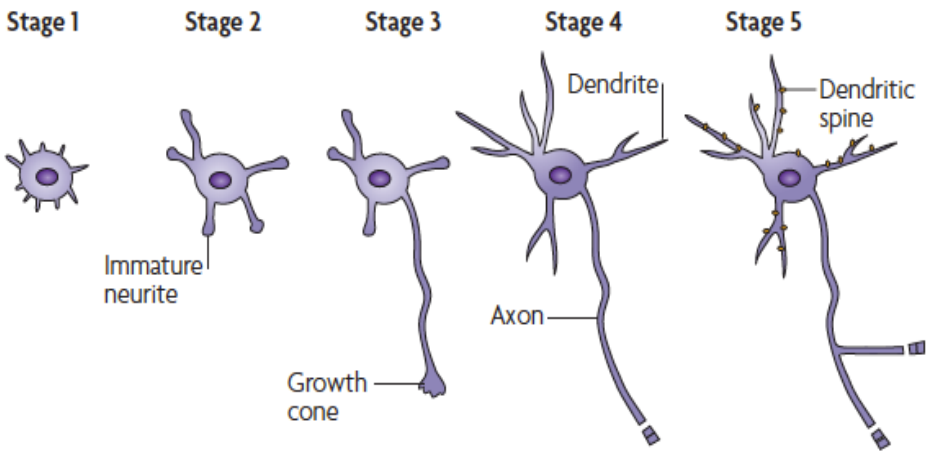

Figure 7: Schematic illustration showing the alteration of neuronal morphology during the process of polarization. Adapted from Arimura and Kaibuchi, 2007 [110].

The mechanisms underlying the specification of a single axon among equally potential neurites has been extensively studied in cultured hippocampal neurons. A large body of evidence suggests that neuronal polarization is largely specified by the stochastic, asymmetric activation of intracellular signaling pathways and that extracellular cues can play an instructive role during polarization *in vitro* and *in vivo*. A varied range of positive and negative signaling molecules control neurite extension and retraction. These molecules diffuse within neurites to regulate the behavior of cytoskeleton and or to influence cargo transport [111].

During polarization, positive and negative signals seem to be intricately balanced. When this balance is broken by a positive cue, a continuous self-activation system (positive feedback loop) [112] is activated, through which a single minor process becomes an axon. Simultaneously, this self-activation system creates strong negative feedback signals that prevent other neurites from forming a second axon [111]. This scenario might fulfill the query of a single axon formation among equally potential neurites.

During the accelerated outgrowth of the axon the differential organization of the cytoskeleton plays a fundamental role. In fact, before axonal outgrowth, the growth cone of the future axon increases in size and its actin cytoskeleton becomes more dynamic and less condensed, whereas the other growth cones remain rather static and retains a rigid actin cytoskeleton [113]. At the same time, the transient stabilization of microtubules occurs in the neurites of

the future axon. Altogether, the regulation of microtubule stability and actin dynamics plays a fundamental role in the process of neuronal polarization.

Shootin1 and axon outgrowth

Shootin1 (KIAA1598) has in the last years been described as a key factor for neuronal polarization by providing the asymmetric signal initiating this process. In 2006, Toriyama and colleagues identified a novel brain specific intracellular protein, shootin1 (KIAA1598) in a screen for proteins that get induced during neuronal polarization [114]. *Shootin1* encodes a protein of 456 amino acids and belongs to a novel class of proteins that contains three coiled-coil domains and a single proline-rich region. The expression of shootin1 gets upregulated during the period of axon formation and elongation, both in hippocampal neurons and in brain, suggesting its involvement in refining neuronal morphology.

In young non-polarized stage 2 neurons, shootin1 is diffused in the cell body but in the phase of stage 2 the relative concentration of shootin1 changes and the protein accumulates in a single neurite right before its accelerated outgrowth leading to axon formation. The active transport of shootin1 from the soma to the distal tip has been found dependent on KIF20B whereas its retrograde movement is by passive diffusion [115]. When the anterograde transport of shootin1 is inhibited, its asymmetric accumulation gets disturbed and axon formation is impaired. The involvement of shootin1 for axon formation has been further demonstrated by the fact that its overexpression causes the formation of multiple axons whereas its depletion causes a defect in neuronal polarization [114]. The aforementioned observations led to propose a model explaining the involvement of shootin1 in generating an asymmetric signal for neuronal polarization where its up-regulation triggers positive feedback and negative regulation (as depicted in **figure 8**) allowing the outgrowth of one axon only.

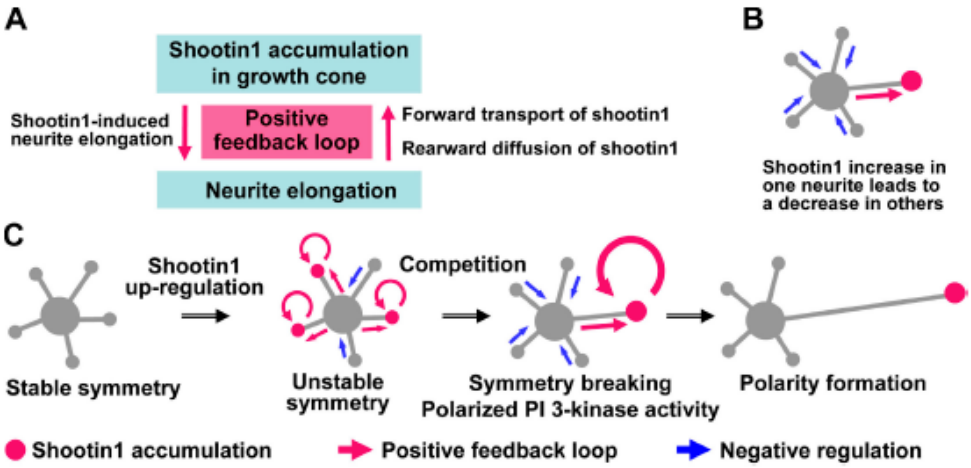

Figure 8: A proposed model for the involvement of shootin1 in generating an asymmetric signal for neuronal polarization. (**A**) A positive feedback loop between shootin1 accumulation in growth cone and shootin1-induced neurite elongation. (**B**) Competition among neurites for a limited amount of shootin1. (**C**) Shootin1 up-regulation triggers local positive feedback loops (red arrows) and negative regulations (blue arrows), shifting the symmetry of neurons from unpolarized to polarized state. Eventually, shootin1 gets asymmetrically accumulated in a single neurite and recruits PI3-kinase activity there, thereby leading to neuronal polarization. Adapted from Toriyama et al., 2006 [114].

Interestingly, shootin1 was found to interact with PI3-kinase regulating the spatial localization of the activity of this kinase in the axonal growth cone of hippocampal neurons [114]. PI-3 kinase is located at an upstream position in the signaling pathways for neuronal polarization involving many molecules, such as phosphatidylinositol (3,4,5) triphosphate, the mPar3-mPar6-aPKC complex, Cdc42, Rap1B, STEF/Tiam1, Rac, Akt, adenomatous polyposis coli, glycogen synthase kinase-3β, and collapsin response mediator protein-2 (CRMP2) [116,110]. By regulating the localization of PI3 kinase activity shootin1 thus seems to play a crucial role in axon formation [114].

Recently, Toriyama and colleagues demonstrated that shootin1 is located at a critical interface that transduces a chemical signal into traction forces for axon outgrowth. A chemoattractant, netrin-1, triggers a signaling pathway activating a Cdc42 and Rac1 dependent up-regulation of Pak1 (p21-activated kinase 1) leading to shootin1 phosphorylation. Pak1 was found to

phosphorylate two sites, Ser101 and Ser249, within shootin1, causing an enhancement of the association of shootin1 with F-actin retrograde flow at the growth cones [117]. It has been proposed that "clutch" molecules regulate the coupling efficiency between F-actin flow and the extracellular substrate (**figure 9**). The Pak1-mediated phosphorylation of shootin1 thus seems to promote this clutch engagement and the concomitant formation of traction forces at axonal growth cones that lead to filopodium extension and axon outgrowth.

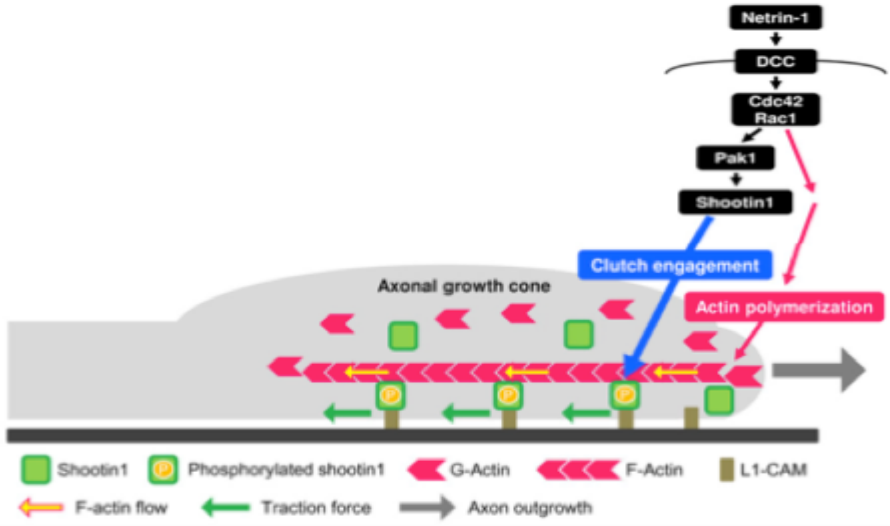

Figure 9: A model for signal-force conversion for axon outgrowth. Netrin-1, via activation of DCC (netrin-1 receptor), Cdc42, and Rac1, induces Pak1-mediated shootin1 phosphorylation (black arrows), thereby enhancing clutch engagement through shootin1-F-actin interaction (blue arrow). Clutch engagement converts the F-actin flow (yellow arrows) into traction forces exerted on the substrate (green arrows). This engagement also reduces the speed of the F-actin flow, converting actin polymerization into protrusion of the leading edge (gray arrow). Clutch engagement (blue arrow) and Cdc42 and Rac1-induced actin polymerization (red arrows) may work coordinately to effectively regulate mechanical forces for cell motility. (Adapted from Toriyama et al., 2013 [117])

MATERIALS AND METHODS

Yeast two-hybrid screening

The yeast two-hybrid screening was performed by Hybrigenics Services, S.A.S, Paris, France (http://www.hybrigenics-services.com). The coding sequence for amino acids 299-1030 of human CDKL5 (GenBank accession number gi: 83367068) was PCR-amplified and cloned into the inducible pB35 vector as a C-terminal fusion to Gal4 DNA-binding domain (N-Gal4-CDKL5-C). The construct was used as a bait to screen a random-primed Human Adult Brain cDNA library constructed into pP6.

Using the Gal4 inducible construct, 113 million clones (11-fold the complexity of the library) were screened using a mating approach with Y187 (MAT**α** Gal4**Δ** Gal80**Δ** ade2-101 his3 leu2-3,-112 trp1-901 ura3-52 URA3::UASGAL1-LacZ, (met-)) and CG1945 (MATa Gal4-452 Gal80-538 ade2-101 his3-D200 leu2-3,112 trp1-901 ura3-52 lys2-801 URA3::Gal4 17mers (X3)-CyC1TATA-LacZ lys2::GAL1UAS-GAL1TATA-HIS3 cyhR) yeast strains. A total of 171 His+ colonies were selected on a minimal medium lacking tryptophan, leucine, methionine and histidine. The prey fragments of the positive clones were amplified by PCR and sequenced at their 5' and 3' junctions. The resulting sequences were used to identify the corresponding interacting proteins in the GenBank database (NCBI) using a fully automated procedure. A confidence score (PBS, for Predicted Biological Score) was attributed to each interaction as previously described [118].

Plasmids and constructs

pCAGGS-Cdkl5-ires-GFP was cloned by inserting an EcoRI-EcoRV digested PCR product containing the murine Cdkl5 cDNA (NP_001019795) into pCAGGS-ires-GFP digested with EcoRI and SmaI. pCAGGS-shootin1-ires-GFP, encoding human shootin1 isoform 2 (ABK56022) was generated in a similar way. Cdkl5-A40V mutant was generated by a PCR based method and cloned into pCAGGS-IRES-EGFP as wild-type Cdkl5. Lentiviral vectors to silence endogenous CDKL5 and shootin1 were generated by cloning double stranded oligonucleotides into the HpaI and XhoI sites of pLentiLox 3.7 (pLL 3.7). The target sequences of the shRNAs are as follows: shCDKL5#1: CTATGGAGTTGTACTTAA; shCDKL5#2: GTGAGAGCGAAAGGCCTT; shShootin1#1: 5'CCACGGTGAATAAATAGAAAT (against the 3'UTR); shShootin1#2: GCAGAACCATCTTGAAATA; shShootin1#3: GCACAAGAGATGATCATTGAA, a shRNA against LacZ was used as control. All PCR derived constructs were sequence verified.

Virus preparation

HEK293T cells, grown in 150 mm dishes, were co-transfected with the packaging vectors pVSV-G, pMDL, pREV and either pLL3.7-shCDKL5#1, pLL3.7-shCDKL5#2, pLL3.7-shShootin1#1, pLL3.7-shShootin1#2, pLL 3.7-shShootin1#3 or pLL3.7-shLacZ using calcium phosphate. The viral particles were harvested 36 hours post-transfection and concentrated by ultracentrifugation with SW32 rotor (Beckman Instruments) at 20,000 rpm for 2 hours. The viruses were resuspended in PBS and stored at -80°C.

Reagents and antibodies

The following primary antibodies were used in immunofluorescence (cultured neurons), immunohistochemistry (brain sections), and in western blotting experiments: Anti-CDKL5 (HPA002847, Sigma-Aldrich), chicken anti-GFP (A10262, Life Technologies), anti-PERK (9101S, Cell Signaling), anti-shootin1 (PA5-17167 Thermo; 3279 Cell Signaling), anti-Tau1 (MAB3420, Millipore), anti-Tag1 (DHSB, University of Iowa), anti-Tuj1 (MMS-435P, Covance), anti-β-actin (A5441, Sigma-Aldrich), anti-MAP2 (ab24640, Abcam). A custom-made immunopurified rabbit polyclonal anti-CDKL5 antibody (Covance Research Products Inc.) was used for co-immunoprecipitation experiments, which was raised against CDKL5 amino acids 301-751 as described by Bertani et al. in 2006. DAPI and secondary Alexa Fluor anti-rabbit, anti-mouse and anti-chicken antibodies for immunofluorescence experiments were purchased from Life Technologies. HRP-conjugated secondary anti-mouse and anti-rabbit antibodies for Western blottings were obtained from Thermo Scientific.

Animal and Tissue preparation

Wild-type CD1 mice were purchased from Charles River Laboratories and maintained as a breeding colony. Animals were housed under standard conditions (12 h light/dark cycle). Successful mating of mice was identified by vaginal plugs, with noon on the day of plug appearance designated embryonic day (E) 0.5. Animals were killed by cervical dislocation under Avertin anesthesia (pregnant females) or cryo-anesthesia (neonatal mice). Embryos were rapidly removed and perfused with 4% paraformaldehyde diluted in PBS (phosphate buffer saline). Embryonic brains were post-fixed by immersion in cold (4 °C) 4% paraformaldehyde for 4–6 h (for immunofluorescence) or overnight for in-situ hybridization.

Brains were cryo-protected in cold-buffered sucrose (30% in 0.1 M sodium phosphate, pH 7.0), frozen in optimum cutting temperature compound (Sakura Finetek, Torrance, CA), cryo-sectioned at 12 μm, and mounted on Superfrost Plus slides (Thermo Fisher Scientific, Waltham, MA). Slides were stored at –20 °C until needed.

In utero Electroporation (IUE)

Wild type C57BL/6J pregnant mice were used for *in utero* electroporation experiments, which were purchased from Charles River, Italy. The day on which the vaginal plug was found, considered as embryonic day 0 (E0). Briefly the pregnant mice were anesthetized with Avertin (mixture of 2,2,2-tribromoetahnol and tertiary amyl alcohol). After cleaning the abdomen with 70% ethanol, a 3-4-cm midline lapratomy was performed and then the uterine horns were exposed. Plasmids such as pLL3.7 shShootin1#1, pLL.3.7 shShootin1#2, pLL3.7 shCdkl5#1 and pLL3.7 ShLacZ, were prepared by using Endofree Plasmid Kit (Qiagen, Hilden, Germany).

Approximately 1μl of plasmid (1μg) containing fast green dye (Sigma) was injected through the uterus wall into the lateral ventricle of telencephalon of E13 and E14 embryos with a glass micropipette. Thereafter, a pair of 4-5 mm at the tip of forceps electrode was placed outside the uterus at the head position. Electroporation was performed by using the Gene Pulser Xcell main unit #165-2666, set at four repeats of 50 ms pulses of 40 V with an interval of 900 ms. then the uterine horns were repositioned in the abdominal cavity, and the abdominal wall and skin were sewed up with surgical sutures. Embryos were allowed to develop *in utero* for certain time points, such as E17, E18, P0 and P8. Brains were dissected, fixed overnight in 4% paraformaldehyde (PFA) at 4°C and then placed in 30% sucrose prepared in 1XPBS for over night to settle down. Brains were frozen in OCT (Tissue-Tek) and sliced coronally at 12 μm by cryostat (Leica CM1850).

Brain extracts and Immunoprecipitation

Proteins were extracted by homogenizing P7 mouse brain in lysis buffer (50 mM Tris-HCl pH 7.5, 150 mM NaCl, 1 mM EDTA, 1 mM EGTA, 1% Triton X-100, 0.1% SDS, 2 mM sodium pyrophosphate, 1 mM sodium orthovanadate). The lysates were incubated on ice for 20 minutes and centrifuged at 100,000g for 30 minutes at 4°C. The supernatant were taken out and incubated overnight at 4°C with 20ul of purified *anti*-CDKL5 or 2ul of *anti*-shootin1 or

unrelated IgGs as a negative control. The equilibrated protein-G agarose beads (in lysis buffer) were incubated with 5%BSA at 4ºC on rotating wheel for 1 hour. The required amount of blocked beads was added to the incubated samples and the mixture was incubated again at 4ºC on rotating wheel for 2 hours. After washing with the lysis buffer, immunocmplexes were analyzed by SDS-PAGE.

In Situ Hybridization

12 µm slide-mounted cryostat sections were thawed and washed in PBS. Slides were fixed for 30 min at room temperature in 4% paraformaldehyde in PBS. Samples were processed as follows: washed in PBS, H2O and then incubated 5 min in Sodium Metaperiodate (2.3% in H2O), 5 min in 20% Acetic Acid, 3 min in TrisHCl (0.1M pH 7.5) and 5 min in Sodium Tetraborate (1% in Tris HCl 0.1M pH 7.5); washed in H2O and PBS; incubated 5 min in PBS with Proteinase K (30mg/ml, Promega), 5 min in 4% PFA in PBS, washed in H2O. Tissues were then incubated in Pre-Hybridization Buffer (PHB) (prepared in solution containing salt solution (NaCl 2M, TrisHCl 0.089 M, Tris base 0.011 M, NaH2PO4 0.05 M, Na2HPO4 0.05 M, EDTA 0.05 M), 50% formamide, H2O) for 4 minutes and hybridized with the diluted antisense riboprobes against mouse *Cdkl5* (full length) and *shootin1* (full length) in hybridization solution (50% Formamide, salt solution, 10% dextran sulfate, Denhards's 1X, tween20 0.05%, tRNA 1mg/ml) at 55°C overnight. Next day, slides were washed twice for 1 hour in pre-warmed PHB and twice for 1 hour in pre-warmed 0.5X Salt Solution at 55°C. After cooling to room temperature, tissues were washed twice in Buffer 1 (TrisHCl pH 7.5, NaCl pH 8 0.1M), incubated for 1 h in blocking solution (TrisHCl pH 7.5 0,1M, NaCl 0,1M, Roche blocking solution 1%, TritonX-100 10%) and overnight at 4°C with anti-digoxigenin (1:1000, Roche #11207750910) diluted in blocking solution.

The third day, slides were washed in Buffer1 (4 times for 10 min) and then twice in Buffer 3 (TrisHCl 0.1M pH 9.5, NaCl 0.1M) with Levamisole (1mM). To stain the samples, slides were incubated in BCIP-NBT (Millipore) that reacted with the Alkaline Phosphatase bound to the anti-digoxigenin antibody. Slices were eventually washed in 50%, 80%, 100% ethyl alcohol, 100% xylene and mounted with DPX (Leica). Tissues were kept at room temperature to dry and images were obtained under bright field microscope (Nikon Eclipse Ni-U) at different magnifications.

Primary neuronal cultures

Primary hippocampal cultures were prepared from embryonic day 16 CD1 mouse embryos (E16), considering the day of the vaginal plug as E0, as described previously [99] and plated on poly-L-lysine coated dishes at different densities: $2x10^3/cm^2$ for immunostainings and $10x10^4/cm^2$ for western blots. For overexpression studies, hippocampal neurons were isolated at E17 and transfected at DIV0 by nucleofection using the Amaxa Basic Neuron Small cell Number Nucleofector Kit following the manufacturer's instructions. Infection of hippocampal and cortical neurons was performed by adding lentiviral particles to the neurons before plating.

Immunohistochemistry (IHC)

12 μm slide-mounted cryostat sections were thawed and washed in PBS. Single- and double-label immunofluorescence were performed. Blocking solution, consisting of PBS with 0.2% Triton X-100 (PBS-T), 10% normal horse serum was applied to slides for 30 minutes. Slides were incubated overnight at 4 °C with primary antibodies [anti-shootin1 (1:100), anti-Tag1 (1:50), and anti-GFP (1:1000)] in blocking solution, rinsed 3 times in PBS for 30 min, and then incubated for 1 h at room temperature with fluorescent secondary antibodies (Alexa Fluor, Invitrogen) in the same blocking solution. Sections were rinsed 3 times in PBS for 10 min and counterstained with DAPI (0.01%, Invitrogen). Sections were then mounted in ProLong Gold Antifade reagent (Life Technologies), dried and the images were obtained under fluorescent microscope (Nikon Eclipse Ni-U) at different magnifications.

Immunofluorescence (IF)

E17 or E18 mouse hippocampal neurons were fixed with 4% para-formaldehyde, 4mM EDTA and 4% sucrose for 10 minutes at room temperature, washed twice with 1X PBS and kept at 4^oC with 0.02% sodium azide in PBS until needed. The coverslips containing neurons were washed thrice with TBS (Tris Buffer Saline), permeabilized and blocked with permeabilization cum blocking solution (5% horse serum, 0.2% Triton-X100 in TBS) for 1 hour at room temperature. The neurons were incubated in the same blocking solution with polyclonal *anti*-CDKL5 1:100, monoclonal *anti*-TAU1 1:5000, polyclonal *anti*-shootin1 1:100, overnight at 4°C.

The next day, neurons were washed three times with TBS 1X followed by incubation with secondary antibodies (Alexa Flour; Invitrogen) for 1 hour at room temperature. Cells were rinsed in TBS 1X three times followed by addition of DAPI (4',6-diamidino-2-phenylindole; IF 300 nM; Invitrogen) for 5 minutes at room temperature. The samples were rinsed three times with TBS1X and mounted in ProLong Gold antifade reagent. After drying up, slides were kept at 4°C/20°C depending upon the requirement of acquisition of images.

Two-dimensional isoelectric focussing (2D IEF)

$2.5x10^6$ cortical neurons isolated from E16 mouse embryos were infected at DIV0 to silence Cdkl5 expression. At DIV7, cells were washed and lysed in UTC buffer (7 M urea, 2 M thiourea, 4% CHAPS). Approximately 200 µg of extract were loaded on 7 cm IPG DryStrips with a linear 4-7 pH gradient and isoelectric focusing was performed with an IPGphor II apparatus (GE Healthcare) according to the manufacturer's instructions. Subsequent SDS-PAGE was performed using 8% gels and proteins detected by Western blotting. Phosphatase treatment was done by adding 100 units of Lambda Protein Phosphatase (Lambda PP; New England Biolabs) to the extract diluted in 2 ml 0.1% SDS, 0.1 mM $MnCl_2$, and 1x PMP-buffer. After an over night incubation at 30°C the samples were concentrated with Ultracel 10K centrifugal filters (Millipore) and subjected to isoelectric focusing.

Cells medium and solutions

DMEM: DMEM 1X (Invitrogen), Foetal bovine serum (FBS), 10% Euroclone), L-glutamine 200 mM (Euroclone), Penicillin/streptomycine 1X (Euroclone).

DMEM-HS: DMEM+Glutamax (Invitrogen), Horse serum (HS), 10%, L-glutamine 200mM (Euroclone), Sodium pyruvate (Gibco).

TRYPSIN-EDTA (Gibco)**,** **HBSS** (Gibco)

RESULTS

Analysis of the Yeast-Two Hybrid Assay results

To understand in more details the neuronal functions of CDKL5 we decided to perform a yeast two-hybrid screening that should allow the identification of interaction partners and possible substrates of the kinase.

Previous studies have shown that the C-terminal region of CDKL5, spanning amino acids 299-1030, regulates CDKL5 activities and harbours the surface of interaction with MeCP2 and DNMT1 [45,98]; altogether, this suggests that both upstream and downstream effectors might target the C-terminus to regulate CDKL5 functions. Therefore, we decided to use the unique C-terminus of CDKL5, comprised between amino acids 299 and 1030 (115 kDa CDKL5 isoform) as a bait to perform a yeast two-hybrid screening. Hybrigenics, a company located in S.A. Paris, France, which is highly specialized in performing high throughput yeast two hybrid screens and delivers the final list of interactors with a biological confidence score, was chosen to perform the screen.

In the initial tests, this bait, when constitutively expressed, was found to be highly toxic to the cells. Consequently, it was decided to use an inducible vector to express the $GAL4_{DBD}$ – CDKL5 fusion protein containing the bait, thus bypassing the toxicity. A human adult brain cDNA library, containing approximately 10 million independent clones, was screened. By testing more than 100 million clones, the complexity of the library was covered more than 10 times and 171 positive clones were isolated.

Although only little is known about the neuronal functions of some of the identified CDKL5 interactors, the yeast two hybrid screening gave a major insight into the putative interactors of CDKL5 and its possible involvement in several cellular activities. Different degrees of confidence score were assigned to the interactors and only one, KIAA1598, which is also named shootin1, obtained the highest confidence score. Given the role of shootin1 in neuronal polarization and its high confidence score, we decided to elucidate the role of CDKL5 in neuronal polarization through its interaction with shootin1.

Shootin1 is a novel interactor of Cdkl5 *in vivo*

As described previously, shootin1 is a brain specific protein that plays an important role in axon specification and neuronal polarization [114]. A total of seven clones containing different but overlapping regions of shootin1 enabled us to map the central region of shootin1,

spanning amino acids 53-290, as the surface that interacts with the C-terminal region of CDKL5 (**Fig 1 *A***). Previous studies determined that the level of shootin1 expression in rat brain is relatively low at embryonic day 15 (E15), gradually increases in early postnatal life, peaks at P4, starts decreasing at P14 [114] and is under detection level in the adult brain. Altogether this strongly indicates the involvement of shootin1 in early developmental stages of brain development. Conversely the expression of Cdkl5 correlates with neuronal maturation and the protein remains significantly expressed through adulthood [89]. To understand whether a common expression pattern of these two proteins exists in mouse brain, we decided to perform immunoblotting of mouse brain lysates at different developmental stages with antibodies against Cdkl5 and shootin1. Consistent with previous findings [89,83], Cdkl5 is lowly expressed at embryonic stage 18 (E18) and postnatal day 1 (P1), gets induced in the early post-natal days and gets stabilized at around P14, persisting through adulthood. Conversely, shootin1 is significantly expressed at E18, peaks in the first post-natal days and decreases to undetectable levels after P14 (**Fig 1 *B***).

The rather strong expression of both proteins in the early post-natal period allowed us to test whether Cdkl5 and shootin1 associate *in vivo*. Indeed, by co-immunoprecipitation assays with P7 brain lysates we were able to detect Shootin1 as co-precipitating with Cdkl5 but not with an unrelated anti-IgG. Moreover, in the reciprocal experiment, Cdkl5 co-precipitated with shootin1 (**Fig 1 *C***). The immunoprecipitation assay thus confirmed the interaction identified in yeast and established that Cdkl5 and shootin1 form a complex in mouse brain.

Since exogenously expressed shootin1 and CDKL5 in HEK293 cells did not co-immunoprecipitate (data not shown), it is possible that the interaction requires other mediator proteins.

Cdkl5 and shootin1 are co-localized in differentiating neurons and developing brain

For further clarification, we analyzed whether the two proteins are physically present in neurons during the first stages of neuronal differentiation. We therefore cultured hippocampal neurons prepared from E16 mouse embryos and collected them at different time points (18, 24, 48, 72, 96 hours and days *in vitro* 7 and 14 (DIV7 and DIV14)). By western blotting we found that both Cdkl5 and shootin1 levels are comparatively lower at 18 hrs hours after plating and get concomitantly induced between 40-72 hours and are significantly expressed

till 14 days (DIV14) of culturing (**Fig 2 *A***).

To assess the localization of Cdkl5 and shootin1 in cultured neurons, we performed immunofluorescence experiments with cultured E16 mouse hippocampal neurons at 18 and 24 hrs after plating. Consistent with role of shootin1 in axonal specification we found it localized in the distal tip of minor neurites at both time points. Interestingly, Cdkl5, besides being present in the soma and the nucleus, was also found in the growth cone of neurites where it partially localizes with shootin1 (**Fig 2 *B***). Altogether, the physical association of Cdkl5 and shootin1 and their co-localization in the growth cone of minor neurites is in line with a possible role of both proteins in regulating axon outgrowth.

We further investigated the expression pattern of shootin1 and compared it with that of Cdkl5 in the developing cortex through *in situ* hybridization and immunohistochemistry.

The *in situ* hybridization assay demonstrated that both *Cdkl5* and *shootin1* mRNAs are present at detectable levels in E13 and E14 mouse embryonic cortical post-mitotic neurons, both in the proliferating zone (ventricular zone; VZ) and sub-ventricular zone (SVZ), and in neurons residing in cortical plate (CP). Apparently, at E16, *shootin1* mRNA levels increase and significant levels of *Cdkl5* and *shootin1* mRNAs were detected in the cortex at E18, demonstrating the presence of *shootin1* in the developing mouse brain together with *Cdkl5* (**Fig 3**).

Immunohistochemistry experiments allowed visualizing shootin1 protein levels at different embryonic stages. In accordance with the *in situ* hybridization experiments, very low but detectable shootin1 signals were observed at E14 whereas significant levels were detected at E16 and E18. Moreover, we detected an overlapping signal of shootin1 and Tag1 (a glycoprotein expressed in the growing cortico-thalamic axonal connections) at E16. Gradually, at E18, the overlapping signals become prominent in fibres invading the internal capsule (IC) or the corpus callosum that is supposed to be cortico-thalamic or cortico-cortical connections, therefore, confirming the presence of shootin1 in cortical glutamatergic axons.

Cdkl5 regulates shootin1 phosphorylation

An early report suggested shootin1 to be a phosphoprotein but no data revealed the involved kinase or the functional consequences of this phosphorylation event [119]. However, recently, Toriyama and colleagues demonstrated that Pak1 (p21-activated kinase 1) phosphorylates shootin1 on at least two sites via activation of Cdc42 and Rac1 by netrin-1; interestingly,

these phosphorylation events seem to promote clutch engagement and formation of traction forces at the axonal growth cones, leading to axon outgrowth [117].

Thus, considering the kinase activity of Cdkl5 and its interaction with shootin1 identified through the yeast two-hybrid screening and confirmed by immunoprecipitation, we speculated that Cdkl5 might work upstream shootin1 modulating its activity in developing neurons in a phosphorylation dependent manner.

To analyze whether Cdkl5 is involved in phosphorylating shootin1, we first performed two-dimensional (2D) SDS-polyacrylamide gel electrophoresis (SDS-PAGE) to detect the phosphorylation of shootin1 in cultured primary cortical neurons grown for 7 days *in vitro*. Seven distinct spots of shootin1 with different isoelectric points could be observed suggesting that shootin1 is indeed phosphorylated in cortical neurons. The intensity of the two most acidic spots was reduced when the extract was treated with lambda phosphatase (**Fig 4 *A***) confirming that these two distinct spots correspond to phospho-isoforms of shootin1. The disappearance of the phospho-ERK signals in the lambda phosphatase treated extracts assures the efficient phosphatase activity.

We further investigated the role of Cdkl5 in imposing the post-translational mark on shootin1. We therefore used primary cortical neurons silenced for Cdkl5 expression through infection with lentiviral particles expressing a shRNA against Cdkl5. As control, a shRNA against LacZ was used. By western blotting the efficient silencing of Cdkl5 7 days after plating and infection was confirmed (**Fig 4 *B***). The infected neurons were distinguished by GFP that is concomitantly expressed by the virus. In this case, the three distinct GFP spots were used as an internal standard for aligning the spots corresponding to shootin1. Interestingly, we noticed a reduction in signal intensity of the two most acidic spots corresponding to the two phospho-isoforms of shootin1. By normalizing the signal intensity of the distinct shootin1 isoforms to that of all the spots, we confirmed that the intensity of spots 6 and 7 was significantly reduced while spot 4 remained constant (**Fig 4 C, *D***).

Altogether, these experiments allowed us to propose that Cdkl5 works upstream shootin1, directly or indirectly affecting its phosphorylation.

Cdkl5 and shootin1 levels influence neuronal polarization

As described, it has been demonstrated previously that shootin1 regulates neuronal polarization through its accumulation in the distal tip of the axon to be. Since our results

indicate that Cdkl5 acts upstream shootin1, we found it challenging to analyze the role of Cdkl5 in axon formation.

For this purpose, we prepared primary hippocampal neurons from E16 mouse embryos and infected the cells at the day of plating with lentiviral particles containing shRNA for silencing Cdkl5 and shootin1. Two shRNAs for each protein were used, designated as shCDKL5#1, shCDKL5#2, shShootin1#1 and shShootin1#2 and as negative control, shLacZ was used. These constructs and sites of annealing are schematically illustrated in **figure 5** ***A*** and ***B***. As shown in **figure 5** ***C***, the shRNAs against shootin1 were found to efficiently silence exogenously expressed shootin1 in HeLa cells.

By western blotting we confirmed the efficient silencing of Cdkl5 and shootin1 in lysates of hippocampal neurons cultured for 96 hours after plating and infection (**Fig 6** ***A***). The infected neurons were easily distinguished through the concomitant expression of GFP. Morphological analysis of GFP-positive neurons demonstrated that a large amount of Cdkl5 deficient neurons displayed several long processes whereas others appeared stunted (**Fig 6** ***B***). On the other hand shootin1 deficient neurons appeared severely stunted devoid of any long process and bearing several small neurites. The immunostaining with the axonal specific marker Tau-1 and the somatodendritic marker MAP2 was then performed to analyze how the loss of CDKL5 or shootin1 influenced axon specification. Tau-1 typically shows a proximal to distal increase in intensity while MAP2 segregates into the minor neurites shortly after axogenesis in developing cortical and hippocampal neurons. Three categories of neurons could thus be classified based on their Tau-1 and MAP2 staining. Neurons showing only one long axon and several small dendrites were considered as polarized whereas others contained multiple axons or no axon as illustrated in **figure 7**. Considering this, we observed that the vast majority of control neurons expressing shLacZ were showing one long axon and several neurites (polarized) (means ±SEM:90.32±0.63). Neurons devoid of Cdkl5 were significantly impaired in axon formation. Approximately 40% of the neurons silenced with shCDKL5#1 were not properly polarized; however, the situation was rather complex since 30% of the neurons bore multiple axons and the remaining 10% did not grow any axon. On the other hand, and as expected, a significant number of neurons silenced for shootin1 were devoid of axons (40%) whereas 56% appeared as polarized, and 3% had grown multiple axons (**Fig 8** ***A***). Similar data were obtained with shCDKL5#2 and shShootin1#2 demonstrating that they were not due to off target effects. Interestingly, neurons silenced with shCDKL5#2, which silences Cdkl5 expression less efficiently, were less prone to generate multiple axons, suggesting that the level of the kinase is important to exhibit its effects on neuronal morphology.

Since Cdkl5 was previously found to regulate neurite outgrowth [83], we analyzed the length of axons and dendrites in neurons devoid of either Cdkl5 or shootin1 at 96 hours after plating. Shootin1 depleted neurons exhibited a marked reduction in the total length of axons and neurites in accordance with published data [114]. Conversely, neurons devoid of Cdkl5 did not show any significant alteration either in the total axon or neurite length (**Fig 8 *B***). However, when the same analysis was performed exclusively with Cdkl5 depleted neurons that appeared as correctly polarized, we found a significant reduction in the total length of both axons and neurites in comparison with polarized control neurons (**Fig 8 *C***). Notably, total dendrite length was not significantly changed in any of the samples. Presently, we cannot explain the discrepancy of our results and those of Chen [83]. However, since murine hippocampi and rat cortices have been used for the two studies, it may be difficult to directly compare the results. Moreover, the timing of the experiments is different: whereas Chen et al. analyzed neuronal morphology at DIV3 (from rat E18 embryos) our analyses were performed at DIV4 (from mouse E16 embryos), when a defect in neuronal polarization may be more prominent.

In the above experiments we observed that shootin1 levels as detected by western blotting seemed reduced in neurons silenced for Cdkl5. As seen in **figure 9 *A***, at both 72 and 96 hours after plating and lentiviral infection with the shRNAs against Cdkl5 shootin1 levels appeared significantly reduced. Further quantification of the expression level of shootin1 and Cdkl5, using the house keeping protein Tuj-1 for normalization, allowed us to conclude that shootin1 levels are significantly decreased upon silencing of Cdkl5 (**Fig 9 *B***).

We next proceeded analyzing how increased CDKL5 or shootin1 levels influence neuronal polarization. To this purpose, we nucleofected hippocampal neurons, prepared from E17 mouse embryos, a time point in which neurons were found to be more resistant to the treatment, with different vectors. Three expression vectors pCAGGS-shootin1-IRES-GFP, pCAGGS-Cdkl5-IRES-GFP and pCAGGS-Cdkl5-A40V-IRES-GFP, were used to overexpress shootin1, wild-type Cdkl5 and a disease causing Cdkl5 derivative (Cdkl5-A40V) that has significantly reduced catalytic activity (our unpublished data) in neurons (**Fig 10**). These vectors express GFP from an internal ribosome entry site (IRES). Neurons were nucleofected at DIV0 just before plating and were analyzed at DIV7 when significant overexpression of Cdkl5 and shootin1 could be determined by western blot analysis (**Fig 11 *A***). The majority of GFP positive control neurons (means ±SEM: 94.07±1.07) were correctly polarized and displayed only a single long Tau-1 positive axon and several dendrites. In contrast, Cdkl5 overexpressing neurons were significantly altered, bearing several Tau-1

positive long processes (means ±SEM:40.54±3.43%; n=129; **Fig 11 *B, C***). In addition, neurons expressing the disease causing derivative, CDKL5-A40V, were characterized by the presence of multiple axons; however, the effect was not as strong as that caused by expression of wild-type CDKL5, suggesting that the catalytic activity plays a role in regulating axon formation (means ± SEM:27.6±7.5% n=123; **Fig 11 *C***). Consistent with the previous results observed by Toriyama and colleagues, neurons overexpressing shootin1 displayed multiple axons as well (means ±SEM:48.71±2.54%; n=123). These experiments thus demonstrate that excess of either shootin1 or CDKL5 disturb neuronal polarization in a similar way.
Altogether, our data suggest that neuronal polarization and axon specification require proper levels of both CDKL5 and shootin1.

Shootin1 regulates neuronal migration *in vivo*

The neo-cortex controls nearly all aspects of brain activities, including perception, language, and decision-making. It contains an immense number of neurons produced through extensive progenitor cell divisions in the lateral ventricle of the cerebral cortex. These neurons are spatially organized into six horizontal layers, called cortical layers, where newly born neurons migrate in an inside out manner through the sub-ventricular zone, the intermediate zone and form the outer cortical layer while later born neurons reside elsewhere in the cortex forming different cortical layers. The formation of this laminar structure requires the exquisite control of neuronal migration from their birthplace to their final destination.
Studies suggested that CDKL5 effects neuronal migration in rat and mouse brains [83,97], whereas the role of shootin1 for neuronal migration was unknown. To explore the role of shootin1 in neuronal migration, we performed *in utero* electroporation (IUE) experiments. This technique is an alternative tool to genetically engineer animals and the overexpression and/or knockdown of target genes can easily be achieved by introducing expression vectors into the proliferating zone (ventricular zone; VZ) of the mouse cerebral cortex at certain embryonic stages. The concomitant expression of GFP/RFP allows tracking the genetically modified neurons for migration defects at later stages of development as illustrated in **figure 12**.
GFP-expressing shShootin1#1 and #2 or shLacZ expressing pLentiLox3.7 vectors were thus injected into the lateral ventricle of E13 embryonic mouse brains and subsequently electroporated into the neuronal progenitors of the ventricular zone. After allowing embryos

to grow *in vivo* for four days (E17), the GFP signal was used to follow migration of transfected neurons (**Fig 13 *A, B***). The distribution of GFP positive cells in the neocortex was calculated by its subdivision into five distinct areas (**Fig 14 *A***): outer cortical layer (OCL), middle cortical layer (MCL), inner cortical layer (ICL), intermediate zone/sub-ventricular zone (IZ/SVZ), and ventricular zone (VZ). GFP positive cells were counted in each area and normalized against the total number of GFP positive cells from all areas. In control embryos expressing shLacZ, we observed almost 50% of GFP positive cells in the outer cortical layer. Conversely, the majority of shShootin1#1 expressing GFP positive cells (roughly 40%) resided in the intermediate zone/sub-ventricular zone (IZ/SVZ) and less than 20% reached the outer cortical layer (OCL) (**Fig 14 *B***). Shootin1 thus appears to be required for correct neuronal migration in the developing neocortex in accordance with recently published results [117]. Similar results were obtained with shShootin1#2 (data not shown) indicating the specificity of the phenotype. The shCDKL5-transfected embryos displayed a migration defect similar to that of previous reports [83,97] (**Fig 15 *A, B***).

To analyze whether the migration defect caused by the absence of shootin1 persists at later time points of brain development we allowed E13 electroporated embryos to develop till P0 or P8. Our analysis at P0 showed that a significant number of neurons (roughly 25%) was in IZ/SVZ (**Fig 16 *A, B* and 17**). Furthermore, at P8 the majority of neurons were still in the intermediate zone/sub-ventricular zone (IZ/SVZ) (statistic analysis was not done at this stage due to lack of controls embryos) compared to control embryos expressing LacZ (**Fig 16 *C, D***); altogether this suggests that the loss of shootin1 may cause long-term effects in neuronal migration during brain development.

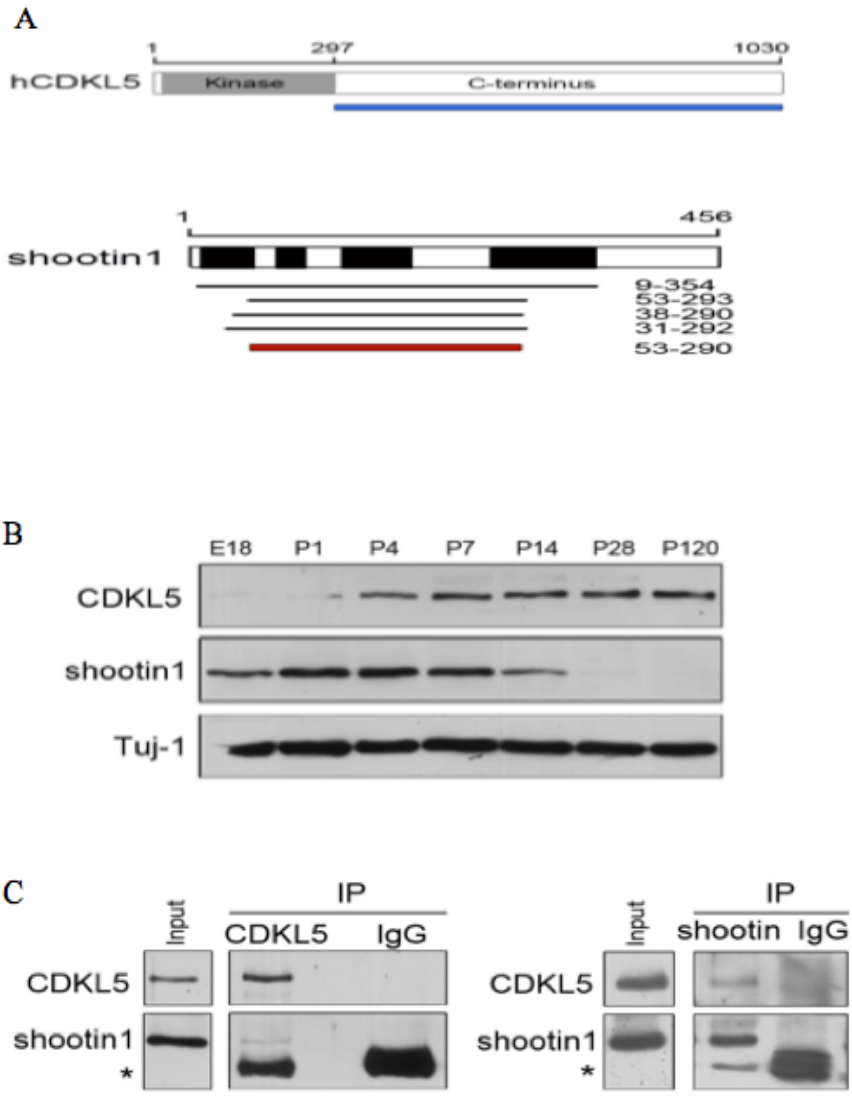

FIGURE 1. **Shootin1 associates with CDKL5 *in vivo*. *A*.** A yeast-two hybrid screening identified shootin1 as a CDKL5 interacting protein. The upper diagram depicts hCDKL5 and, in blue, the region spanning amino acids 299-1030 that was used as bait. The diagram below indicates shootin1 with its coiled coil domains in black. The black bars below show the human clones identified in the screening. The red bar represents the minimum CDKL5 interacting region. ***B*.** Immunoblot analysis showing Cdkl5 and shootin1 levels in whole cell lysates from mouse brains at various developmental stages. Tuj-1 was used as loading control. ***C*.** Co-immunoprecipitation experiments where P7 brain lysates were immunoprecipated with anti-CDKL5 (left) or anti-shootin1 (right) antibodies. IgG's were used as negative control. Inputs correspond to 5% of the total cell lysates of mouse brain. Asterisks (*) indicate the immunoglobulin heavy chains in the immunocomplexes.

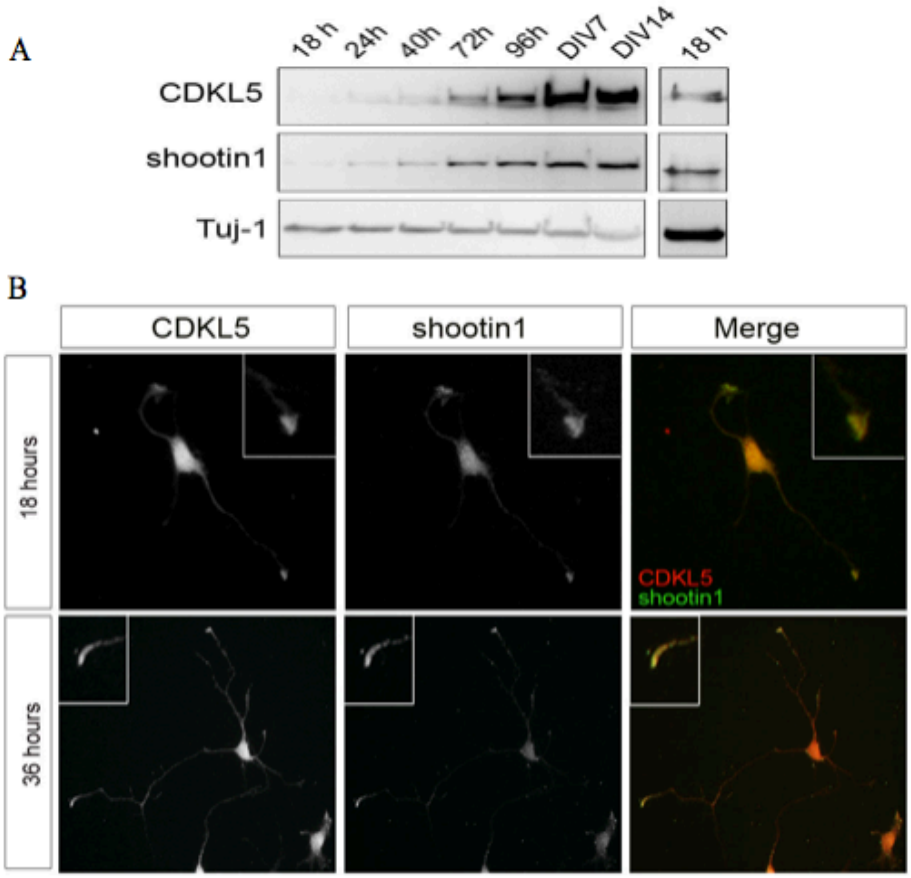

FIGURE 2. Shootin1 localizes with Cdkl5 in growth cones. ***A.*** Western blot analysis showing Cdkl5 and shootin1 levels in cultured murine hippocampal neurons at the indicated stages. Tuj-1 was used as loading control. A longer exposure of the 18 h time point is shown to the right. ***B.*** Immunofluorescence experiment showing Cdkl5 and shootin1 localization in hippocampal neurons cultured for 18 and 36 hours *in vitro*. Neurons were double stained with anti-shootin1 (green) and anti-CDKL5 (red). The small inserts show a magnification of the growth cones.

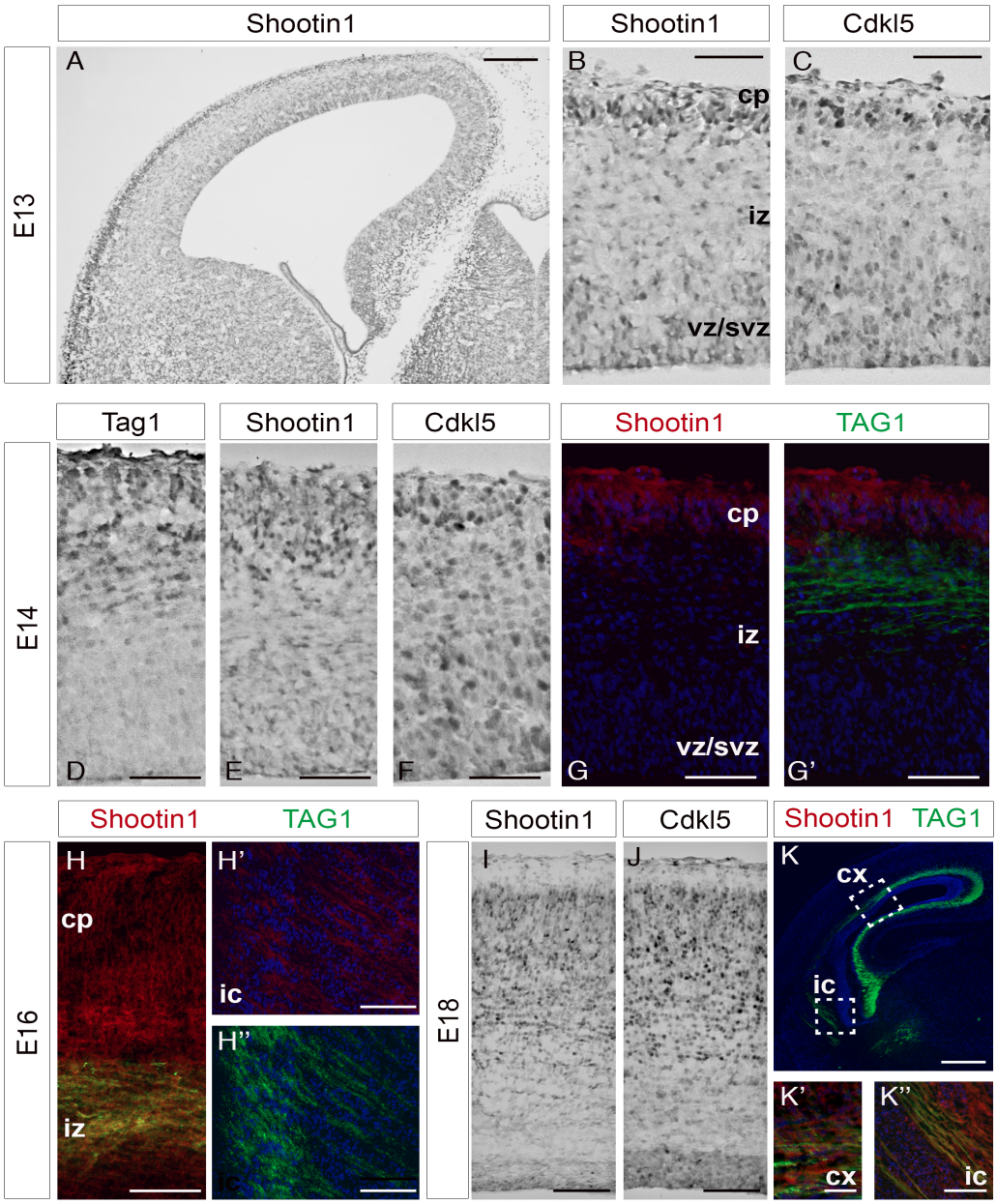

FIGURE 3. Expression pattern of Shootin1 and Cdkl5 in the developing mouse brain. *Shootin1* is expressed in the cortex, as early as E13, in the cortical plate (CP) and its levels increase ongoing with development (***A, B, E***); *Cdkl5* (***C, F***) and *Tag1* (***D***) follow the same pattern. Low but detectable levels of *shootin1* and *Cdkl5* mRNAs are present in cells migrating out of the ventricular and sub-ventricular zone (VZ-SVZ) towards their final destination in the cortical plate (***B, C***). At E14, shootin1 protein can be detected in the CP (***G, G'***). Starting from E16, shootin1 protein levels are detected not only in cell bodies, but also in fibers both in the cortex in the intermediate zone (IZ) and in the internal capsule (IC); in both the cases shootin1 (red) and TAG1 (green) staining overlap (***H, H', H'', K, K', K''***). At E18

shootin1 and *Cdkl5* are strongly expressed throughout the whole thickness of the cortex (***I, J***). Scale bars: 50 mm: ***B, C, D, E, F, G, G'***; 100 mm: ***H, H', H'', I, J, K', K''***; 500 mm.

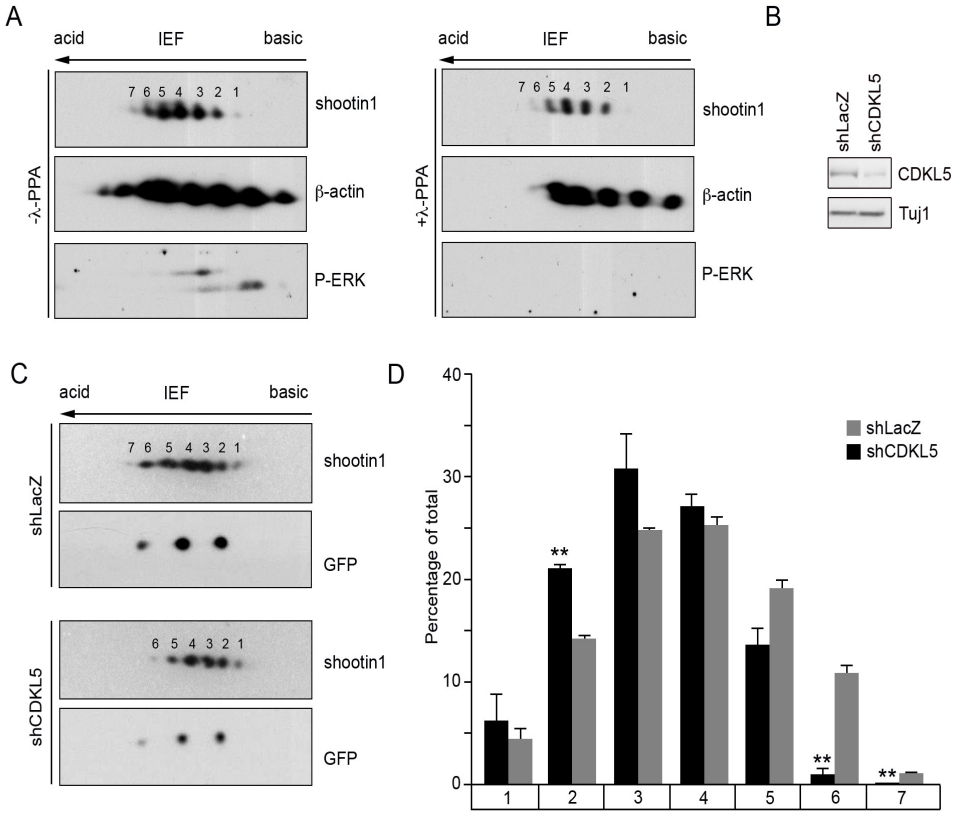

FIGURE 4. Cdkl5 mediates shootin1 phosphorylation in primary cortical neurons. ***A***. Total cell extracts of DIV7 cortical neurons were treated with or without lambda protein phosphatase and analyzed by two-dimensional gel electrophoresis and immunoblotting with antibodies against shootin1, beta-actin and, as control for the phosphatase treatment, phospho-ERK1/2. ***B***. Primary murine cortical neurons were infected with shLacZ or shCdkl5 expressing viral particles at DIV0 and Cdkl5 silencing verified by western blotting on total cell lysates using Tuj1 as loading control. ***C***. Total cell lysates from DIV7 cortical neurons in (*B*) were subjected to two-dimensional gel electrophoresis. Shootin1 and GFP were detected by immunoblotting. The three GFP isoforms were used as internal standard for alignment. ***D***. Graphic illustration showing the results of densitometric scanning quantification of spots 1-7 of shootin1 in shLacZ or shCdkl5 expressing neurons ±SE (**p<0.01; n=2). The intensity of the single spots was normalized to that of all seven spots.

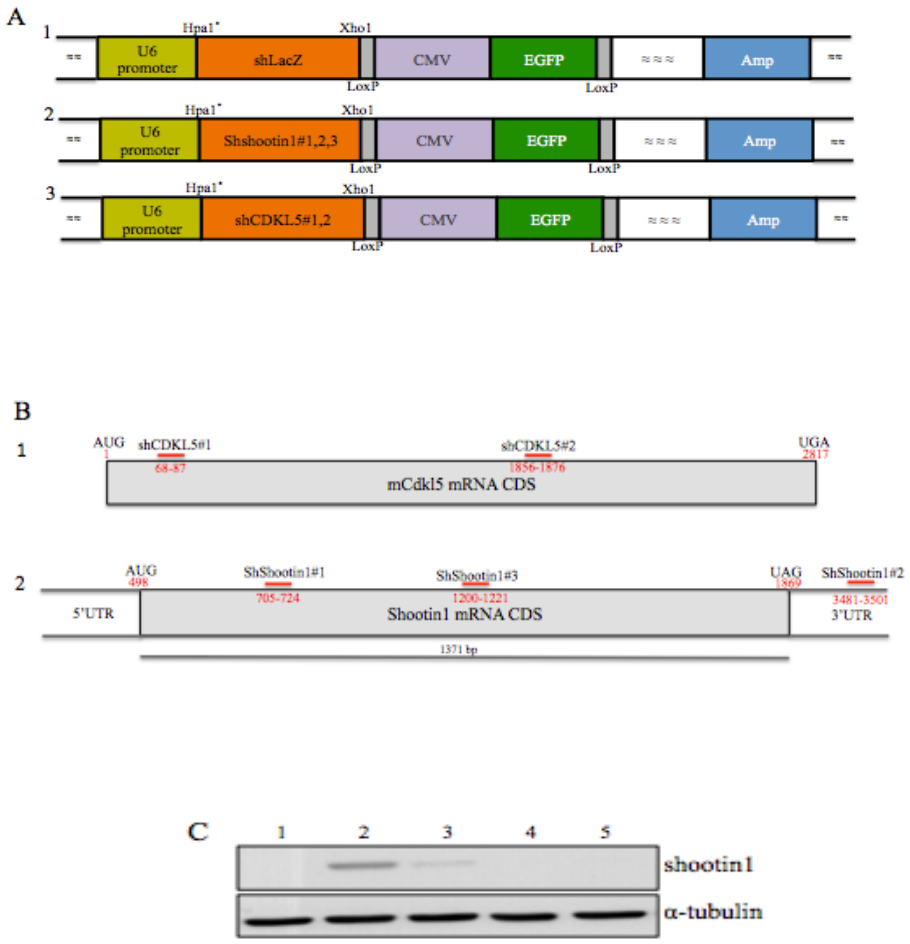

Figure 5. Graphic illustration of short hairpin RNAs expression vectors, their sites of annealing and western blot; ***A***. 1. pLentiLox3.7-shLacZ, 2. pLentiLox3.7-shCDKL5#1, #2, 3. pLentiLox3.7-shshootin1#1, #2, #3. Short hairpins against Cdkl5 and shootin1 were inserted into HpaI-XhoI sites of pLentiLox3.7 where Hpa1* denotes the loss of its restriction site after cloning. GFP expression is under control of CMV regulatory sequences. ***B.*** 1. shCDKL5#1 and #2 anneal at nucleotides 68-87 and 1856-1876 of the Cdkl5 ORF, respectively. 2. shShootin1#1 and #3 anneal at nucleotides 705-724 and 1200-1221 of shootin1 ORF, respectively, while shShootin#2 anneals at 3481-3501 of the 3'UTR. ***C.*** Western blot analysis showing the shRNA mediated silencing of exogenously expressed shootin1 in Hela cells. The cells were transfected with: 1. pCAG-IRES-GFP; 2. pCAG-Shootin1-IRES-GFP; 3. pCAG-Shootin1-IRES-GFP+pLentiLox3.7-ShShootin1#3; 4. pCAG-Shootin1-IRES-GFP+ pLentiLox3.7-ShShootin1#2; 5. pCAG-Shootin1-IRES-GFP+pLentiLox3.7- ShShootin1#1. Tubulin was used as a loading control. shShootin#1 and shShootin1#2 were used for further experiments due to their higher silencing efficiency.

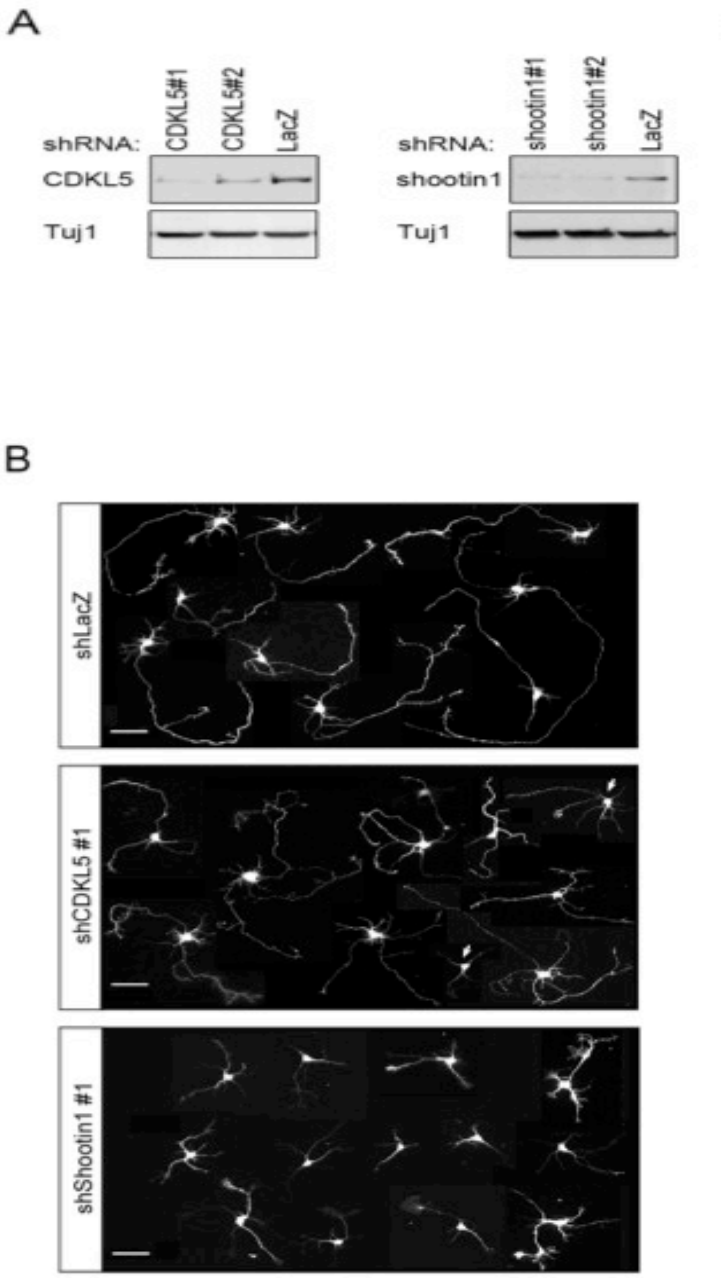

FIGURE 6. Cdkl5 and shootin1 knock-down cause aberrant neuronal polarization. *A*. Western blot showing Cdkl5 and shootin1 levels in primary hippocampal neurons infected with shRNAs against Cdkl5, shootin1, or, as control, LacZ. Neurons were infected at DIV0 and cell lysates prepared after 96 hours. Tuj1 was used as loading control. ***B***. Representative images of neurons 96 hours after plating and infection with viral particles expressing GFP together with shRNAs against LacZ, Cdkl5, or shootin1. The image corresponds to the GFP signals. Scale bar, 25 μm. Arrows indicate stunted neurons devoid of Cdkl5.

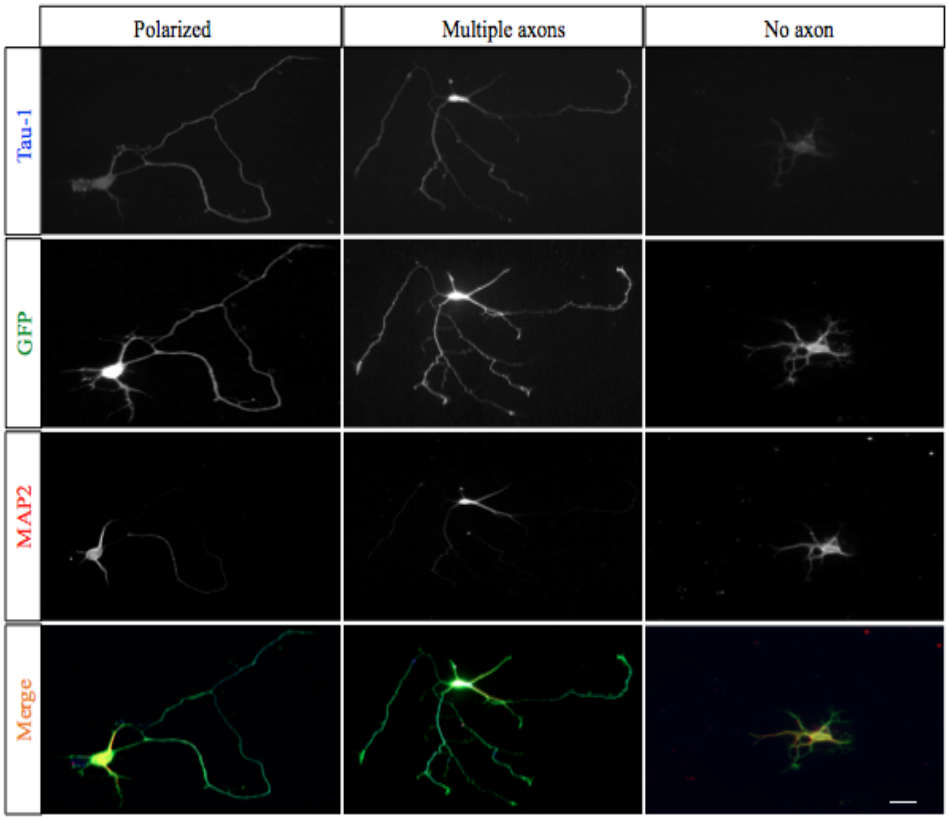

Figure 7. Representative images showing typical Tau1 and MAP2 staining of polarized neurons and those with multiple or no axons. Correctly polarized neurons bear only one long Tau-1 positive axon and several MAP2 positive dendrites. Non polarized neurons can be classified as having multiple axons or no axons. Tau1 staining is in blue, MAP2 in red and GFP in green. The merge shows the overlap of the three different stainings. Scale bar, 25µm.

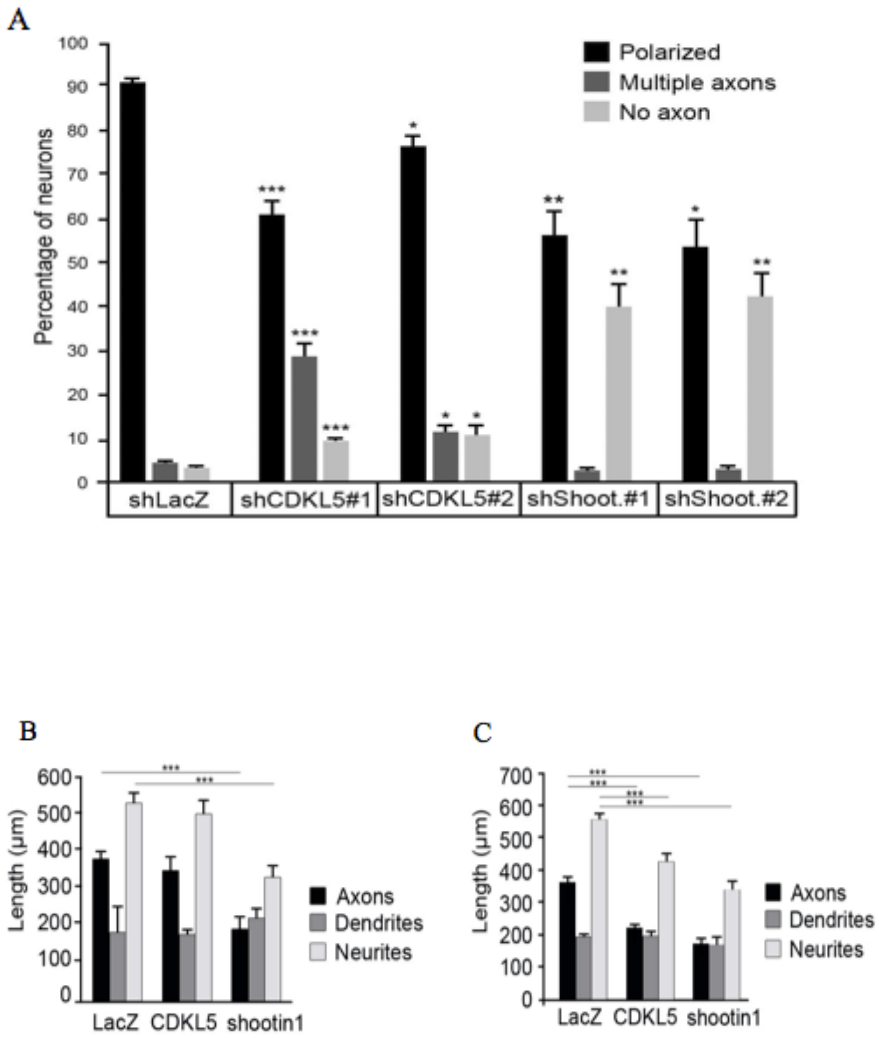

FIGURE 8. Analysis of polarization defects in neurons devoid of Cdkl5 or shootin1. ***A***. Graph showing the polarization of neurons expressing shRNAs against LacZ, Cdkl5 or Shootin1. Polarized neurons (with one axon) are indicated with black bars, those with numerous axons with dark grey bars and neurons with no axon with light grey bars. Data are expressed as ±SE (***p<0.001; n=3, a total of 725 neurons were examined). ***B***. Quantification of neurite length of the entire population of GFP-positive neurons at DIV4. The length of axons and dendrites were measured in neurons expressing shRNAs against LacZ, Cdkl5, or shootin1 (a total of 117 neurons were analyzed). ***C***. Quantification of neurite length of GFP-positive neurons bearing one axon (a total of 74 neurons were analyzed). Data in B and C present neurite length as means ±SE, ***p<0.001.

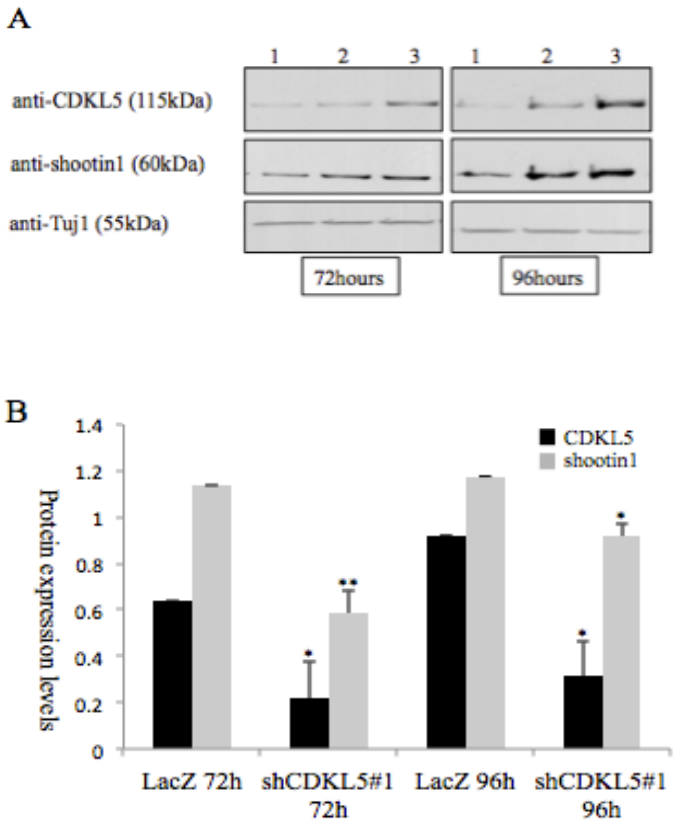

FIGURE 9. Shootin1 levels are reduced in neurons devoid of Cdkl5. ***A.*** Western blot analysis showing reduced shootin1 protein levels at the indicated time points in Cdkl5 silenced neurons. Tuj1 was used as loading control. 1; shCDKL5#1, 2; shCDKL5#2, 3; shLacZ. ***B.*** Graphic representation showing Cdkl5 and shootin1 protein levels in neurons expressing shCDKL5#1 or shLacZ. Cdkl5 and shootin1 levels were normalized with Tuj1. **p<0.01, *p<0.05, n=3.

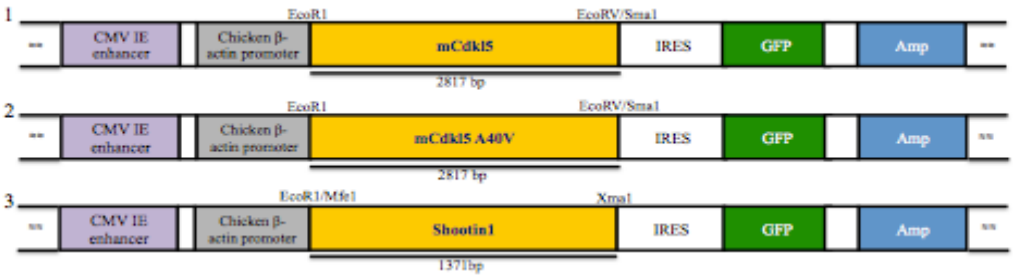

FIGURE 10. Graphic illustration of expression vectors. 1. pCAGGS-mCdkl5-IRES-GFP; 2. pCAGGS-mCdkl5A40V-IRES-GFP; 3. pCAGGS-Shootin1-IRES-GFP. The Cdkl5, Cdkl5A40V and shootin1 cDNAs were cloned into pCAGGS-IRES-GFP.

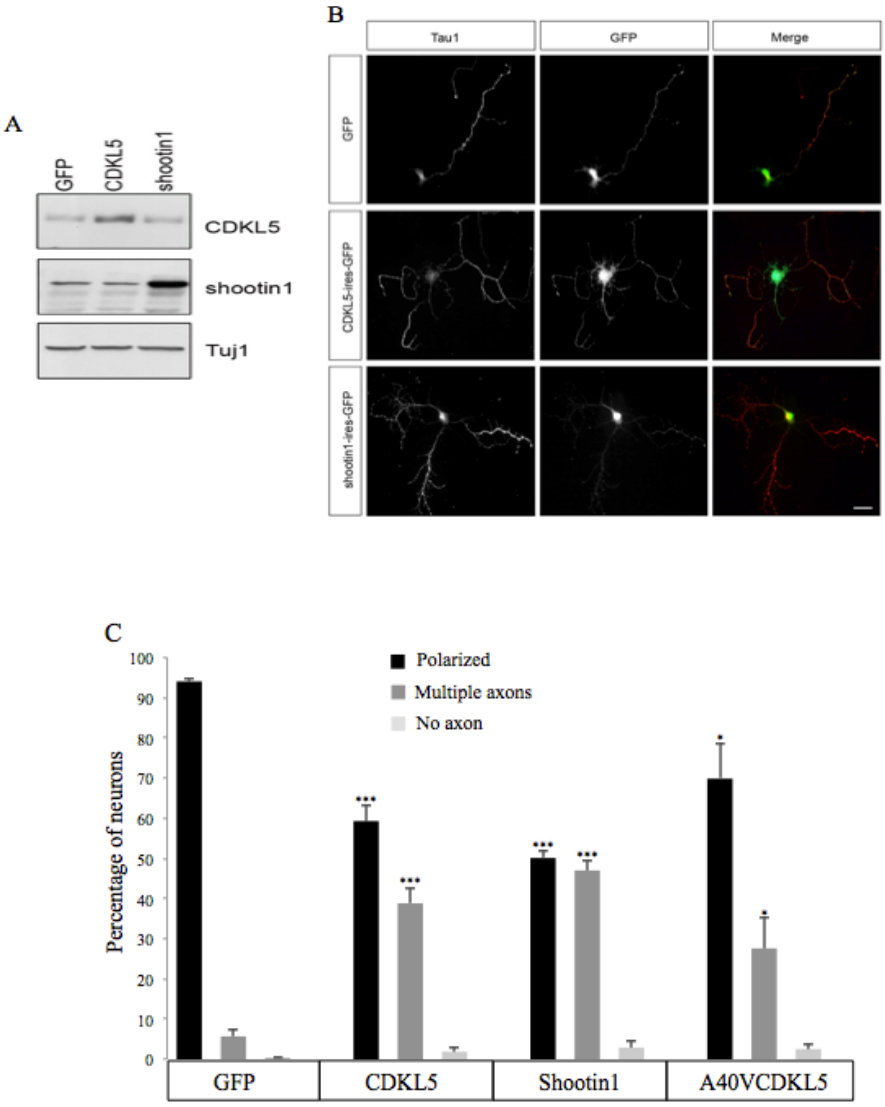

FIGURE 11. Increased Cdkl5 levels affect axon specification in primary hippocampal neurons. ***A.*** Western blot analysis of primary hippocampal neurons nucleofected before plating with vectors expressing GFP alone or together with Cdkl5 or shootin1. Cell lysates were prepared at DIV7 and analyzed for Cdkl5 and shootin1 expression using Tuj1 as loading control. ***B***. Representative images of hippocampal neurons expressing GFP together with exogenous Cdkl5 or shootin1. Nucleofected hippocampal neurons were analyzed at DIV7 by staining with anti-Tau1 (red) and anti-GFP (green) antibodies. Scale bar, 25 µm. ***C.*** Quantitative analysis of neuronal polarity in overexpressing neurons. Axon specification was analyzed by determining the number of polarized neurons with a single axon (black bars), neurons with multiple axons (dark grey bars), and neurons with no axon (light grey bars). Data are expressed as mean of four independent experiments ± SE; ***p<0.001; a total of 461 neurons were analyzed.

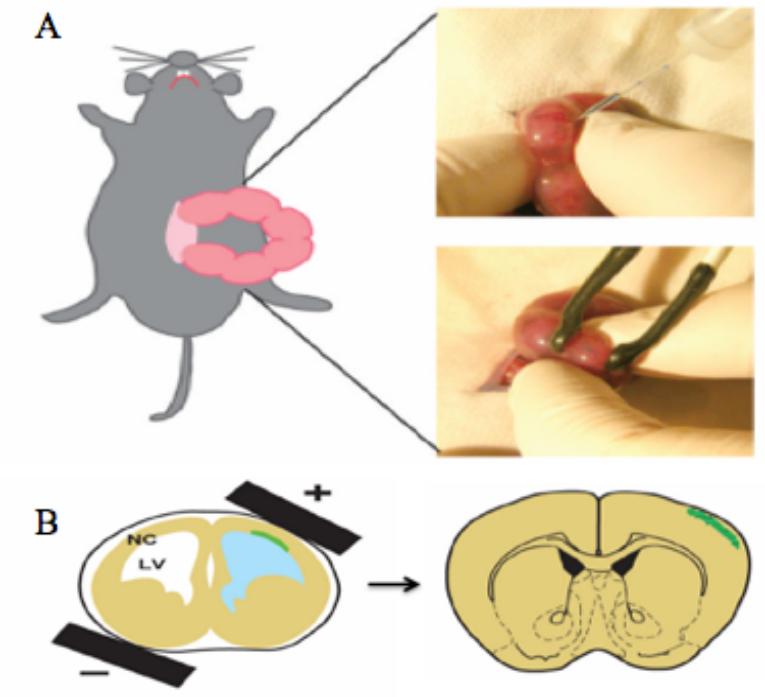

FIGURE 12. Illustration of *in utero* electroporation of injected DNA. ***A***. Injection of a DNA containing solution through a fine capillary needle into the lateral ventricle of exposed embryos is followed by gene delivery into the ventricular zone (VZ) via electroporation by holding the embryos with forceps-type electrodes. ***B***. The neuroepithelium is targeted by placing the positive electrode on the dorsal lateral side. GFP expressing electroporated cells are indicated in green. LV, lateral ventricle; NC, neocortex. Adapted from Taniguchi et al., 2012 [120].

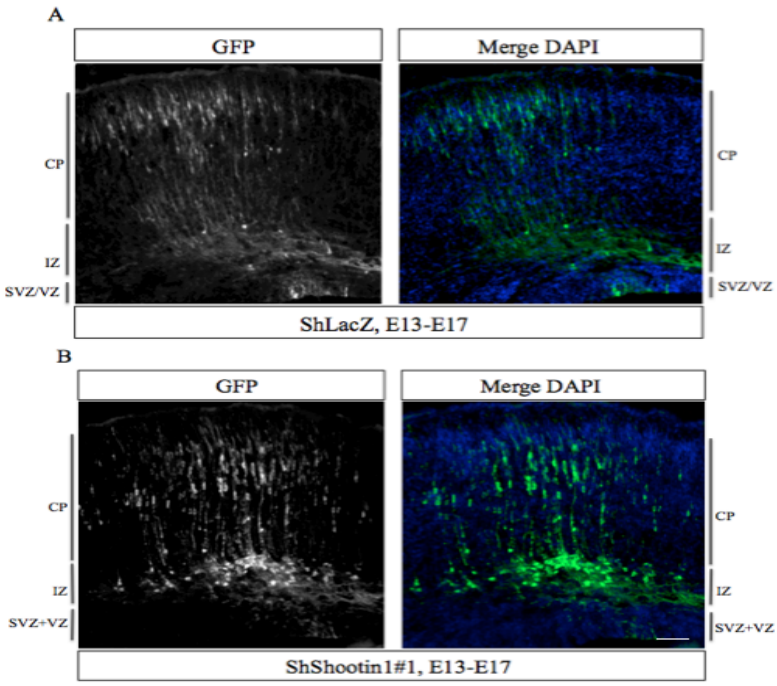

FIGURE 13. Loss of shootin1 causes neuronal migration defects. Representative images of coronal slices of E17 mouse brains expressing GFP together with shRNAs against either LacZ (***A***) or shootin1 (***B***) through *in utero* electroporation at E13. Staining with anti-GFP and DAPI was used to visualize transfected neurons and nuclei, respectively. CP, cortical plate; IZ, intermediate zone; SVZ, subventricular zone; VZ, ventricular zone. Scale bar, 25μm.

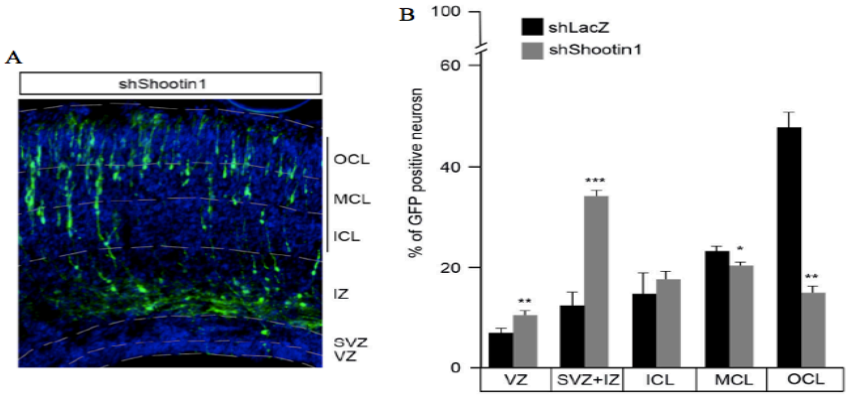

FIGURE 14. Neuronal migration deficits in the absence of shootin1. *A*. The dorsal telencephalon was divided into the five layers used for the quantification of migrating cells. ***B***. Quantification showing the percentage of transfected neurons in the distinct layers, i.e. OCL, outer cortical layer; MCL, middle cortical layer; ICL, inner cortical layer; IZ, SVZ, and VZ. *p<0.05, **p<0.01, ***p<0.001.

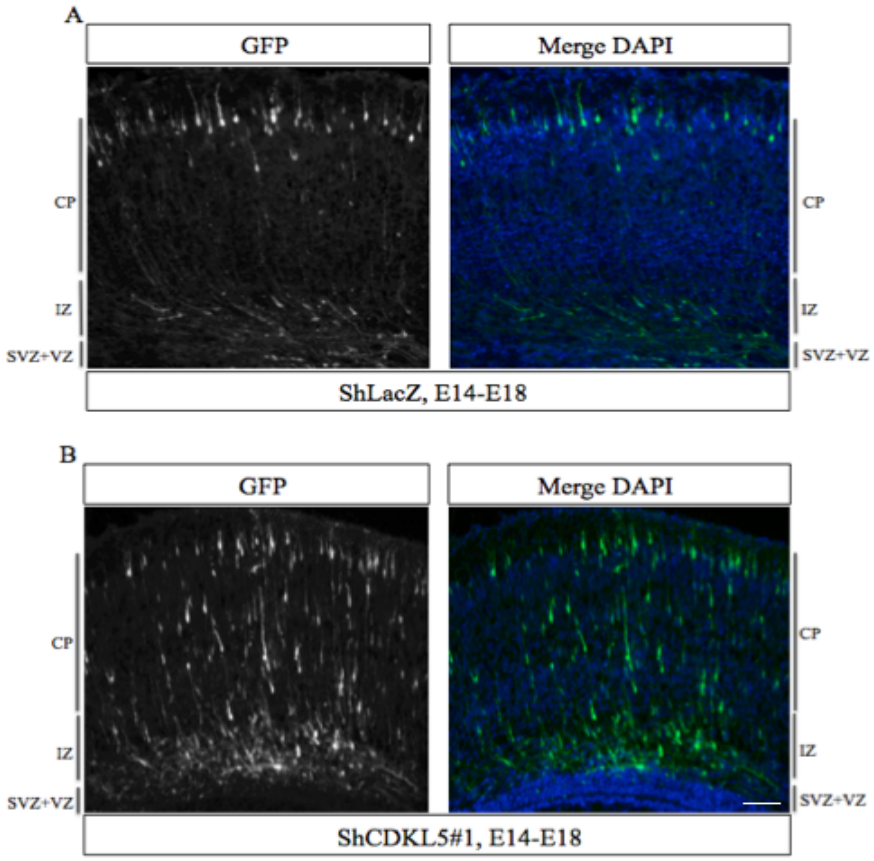

FIGURE 15. Cdkl5 regulates neuronal migration during brain development.

Immunohistochemistry of E18 mouse embryonic coronal slices, electroporated with ShLacZ (***A***) or ShCDKL5#1 (***B***) at E14. GFP expressed from the lentiviral vectors, was used to trace migrating transfected neurons. DAPI was used to visualize transfected/non-transfected neurons nuclei. Scale bar, 25μm.

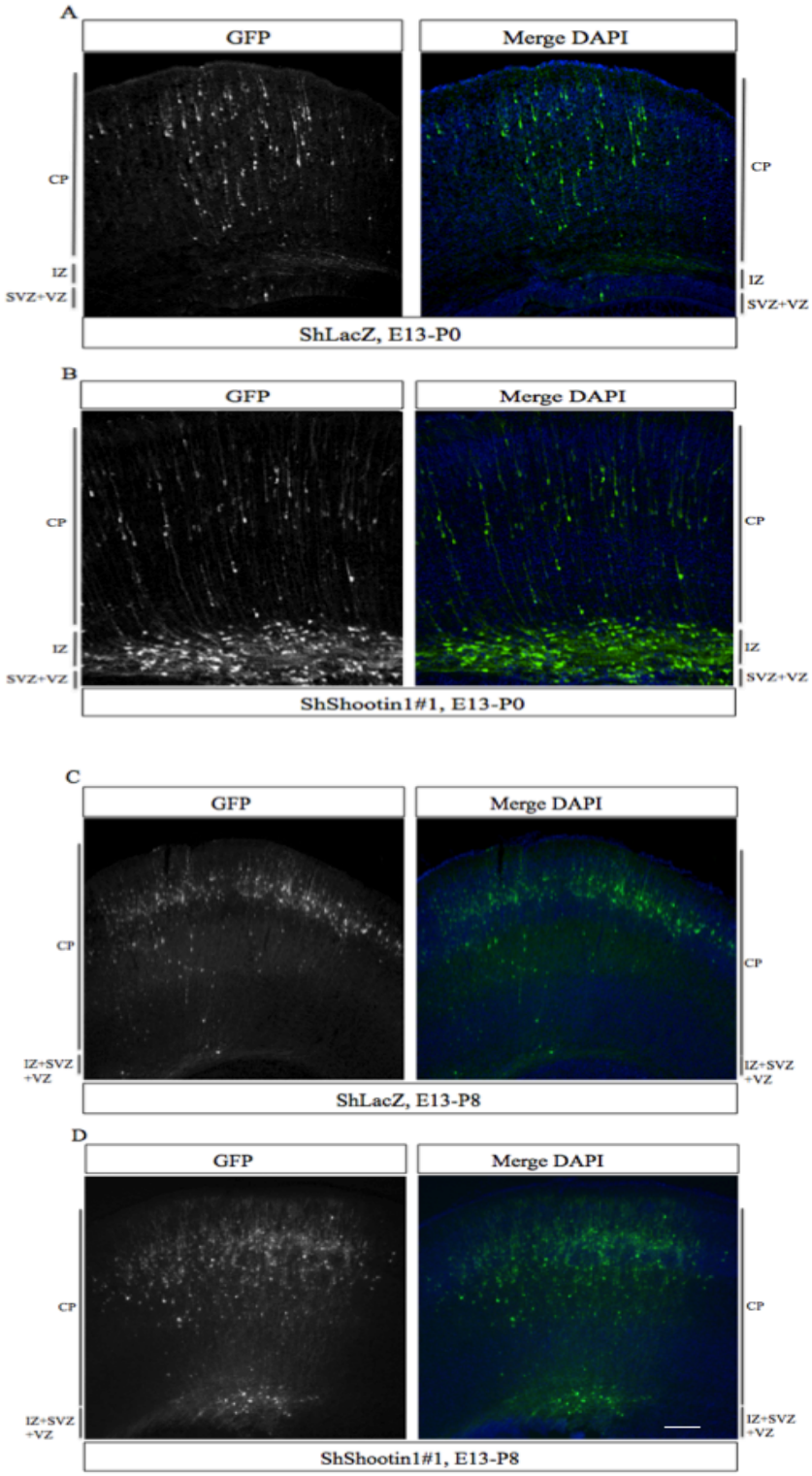

FIGURE 16. Long term-effect of shootin1 in neuronal migration of the developing cortex. Immunohistochemistry of P0 (***A***, ***B***) and P8 (***C***, ***D***) coronal mouse brain slices, electroporated at E13 with vectors expressing shRNAs against Shootin1 or LacZ. Scale bar, 25μm.

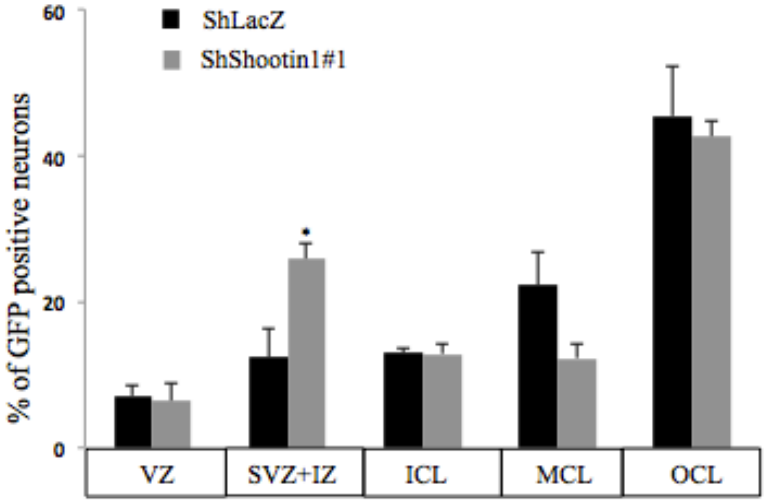

Figure 17. Graphic representation of neuronal migration deficits in the cerebral cortex at P0 under the influence of shootin1 depletion. Analysis showing percentage of neurons transfected at E13 in the distinct layers of the cerebral cortex at P0. *$p<0.05$, $n=3$.

DISCUSSION

Rett syndrome (RTT) is a post-natal neurodevelopmental disorder characterized by a period of normal development followed by the loss of intellectual functioning, fine and gross motor skills and communicative abilities, deceleration of head growth leading to microcephaly, and the development of stereotypic hand movements [2]. Girls with RTT often develop seizures ranging from easily controlled to intractable epilepsy, which decrease in severity after the teenage years and present less severe problems in adulthood [62]. RTT, which is considered to be one of the most common causes of complex disability in girls, is caused by mutations in the methyl-CpG-binding protein 2 gene (*MECP2*) in at least 95% of individuals fulfilling the criteria for classic RTT. Besides classical RTT, other atypical forms of the disease have been recognized in a small proportion of clinically well-defined Rett syndrome cases but with an apparent lack of *MECP2* mutations. In particular, three distinct variant forms of RTT, including the preserved speech variant [56], the congenital variant [57] and the early-onset seizure variant (ESV; [58]) have been well described. Mutations in the X-linked cyclin-dependent kinase-like 5 gene (*CDKL5*) have been identified in patients with the ESV of Rett syndrome and other neurological disorders that share the common features such as the appearance of often intractable seizures during the first months of life, infantile spasms, hypotonia, and severe intellectual disability [78]. The Neul criteria [5] for atypical RTT describe five specific items to differentiate the ESV from other variants. Although mutations in the *CDKL5* gene have been associated with the early-onset variant of RTT, the *CDKL5* disorder has recently started being considered a separate disorder rather than another RTT variant [78]. The reason for this is principally the lack of a regression period, which is a strict requirement for the RTT diagnosis and, moreover, that various dysmorphic features including large deep-set eyes, strabismus, high forehead, full lips, wide mouth and widely spaced teeth, have been described in individuals with CDKL5 mutations. However, the partial clinical overlap observed in patients with *CDKL5* and *MECP2* mutations, such as the presence of stereotypic hand movements, typical for Rett syndrome, suggest that some common molecular pathways are disrupted in these two groups of patients. A possible explanation might be that CDKL5 is involved in phosphorylating MeCP2 even if *in vivo* evidence still needs to be found [45].

The involvement of *CDKL5* in the etiology of the Hanefeld variant and related disorders urges a detailed characterization of the role of this protein in neuronal activities. Although rather little is still known about the functions of CDKL5, the neurological dysfunctions underlying the etiology of *CDKL5* associated disorders have recently started being elucidated [82]. The

development of the central nervous system (CNS) starts early in embryogenesis where distinct pattern of gene expression governs various neuronal subtypes. A range of molecular signalling cascades guide these neurons to maintain their morphology to form complete neuronal circuits and disruption of such regulatory pathways increases the susceptibility to various psychiatric and neurodevelopmental disorders. The striking organization of the neocortex into distinct layers contributes to increasing functional complexity of the mammalian brain and deficits in cortical development, resulting from defects in cell proliferation in the germinal zone, aberrant neuronal migration or connectivity and differentiation frequently cause epilepsy. Moreover, the cytoskeleton drives the process of neuronal polarization and morphology, important for the transmission of signals from one neuron to another. Given that the hippocampus and cerebral cortex are considered to be the most epileptogenic regions of the brain [121] it is interesting to note that these are the two brain areas expressing highest amounts of CDKL5 [89]. Moreover, the expression profile of CDKL5 suggests that it plays a role during the early steps of post-natal differentiation and this might, at least in part, fit with the precocious symptoms of CDKL5 related pathologies. Accordingly, it is intriguing to speculate that seizures, representing one of the characteristic phenotypes of patients with mutations in CDKL5, might originate from these deficits.

A delay in the migration of neuronal precursors devoid of CDKL5 through the developing cortex has already been reported [83, 97], reinforcing the idea that defective CDKL5 activity might affect early steps of differentiation by altering molecular processes that not only impact cytoskeletal modifications but eventually result in a delayed refinement of cortical architecture. Moreover, recent observations on the role of CDKL5 proved that it regulates neuronal morphology [83,97]. However, the recently developed *Cdkl5* knock-out mouse model does not display any gross alterations in brain structure, even though a detailed analysis of neuronal morphology has not yet been reported [106].

In neurons, CDKL5 is present both in the cytosolic and nuclear compartments [89] where it interacts with specific proteins to maintain neuronal morphology and functions. Considering the fact that CDKL5 interacts with DNMT1 [98], MeCP2 [45], the SR family splicing factor (SC35) [45] in the nucleus and with Rac1 [83], PSD95 [100] and NGL-1 [97] outside the nucleus, especially at synapses, it seems likely that the protein plays important roles ranging from regulating gene expression to the formation of spines. Given that the molecular mechanisms by which CDKL5 exerts such functions are far from being understood, we aimed at identifying novel CDKL5 interactors that might help shedding light on its role in neuronal functions. In a yeast two hybrid screening we identified shootin1 as a novel interactor of

CDKL5. As described, shootin1 is a brain specific intracellular protein acting as a determinant of axon formation during the process of neuronal polarization [114]. The expression of shootin1 gets upregulated during the period of axon formation and elongation, and, in particular, its asymmetric accumulation in the tip of the neurite that will become an axon is required for proper axon specification. Indeed, genetic manipulations disturbing this asymmetric distribution of shootin1 impairs neuronal polarization.

The interaction between CDKL5 and shootin1 thus led us to hypothesize a role of CDKL5 in this particular process of neuronal differentiation. By analyzing in details the functional interplay between shootin1 and CDKL5 we found evidence that CDKL5 is involved in regulating neuronal polarization, possibly through its interaction with shootin1. First of all, we observed low levels of CDKL5 in unpolarized hippocampal neurons and a strong induction in the transition from stage 2 to stage 3 where it localizes together with shootin1 in the distal tip of neurites or outgrowing axons. Moreover, we find that the two proteins associate *in vivo* in early post-natal brains and that correct CDKL5 levels are required for proper axon formation. Indeed, the majority of hippocampal neurons over-expressing CDKL5 generate a surplus of axons whereas a significant number of neurons devoid of it were not correctly polarized. A disease causing mutation of CDKL5, CDKL5-A40V, which has reduced catalytic activity (our unpublished data), was less efficient in generating the multiple axon phenotype, indicating that the kinase activity is required for CDKL5 to influence axon formation. Altogether, these observations indicate that correct neuronal polarization requires balanced levels of functional CDKL5.

Proper levels of shootin1 are a prerequisite for neuronal polarization [114] and, as described, it has been suggested to act as a linker that couples actin filament flow to the substrate, allowing the formation of the traction forces at axonal growth cones [117]. Shootin1 has previously been described as a phosphoprotein; in fact, shootin1 phosphorylation, which is induced by the activation of both Pak1 and cdc42/Rac1, is required for its association with the actin retrograde flow. Interestingly, we found that shootin1 phosphorylation is reduced in neurons silenced for CDKL5 reinforcing the idea that the two proteins work in a common molecular pathway. Whether CDKL5 directly or indirectly phosphorylates shootin1 remains to be revealed as well as the specific residues of shootin1 whose modification depends on CDKL5. *In vitro* phosphorylation experiments in which recombinant shootin1 was incubated with immunopurified CDKL5 did not reveal any significant phosphorylation of shootin1 (data not shown). Moreover, given the lack of available consensus sites for CDKL5, the mapping of its putative targets within shootin1 proves difficult. Serines 101 and 249 within shootin1 were

found as Pak1 targets and their phosphorylation is required for shootin1 to interact with the F-actin retrograde flow [117]. Future experiments will reveal whether the phosphorylation of these two serine residues depends on CDKL5. In addition, it is interesting to note that Rac1 appears to be common to the pathways of both CDKL5 and shootin1. As mentioned, shootin1 phosphorylation is induced by cdc42/Rac1 dependent Pak1 activation and CDKL5 has been reported to regulate neuronal morphology acting upstream Rac1 [83,117]. It will be therefore be interesting in the future to analyze whether CDKL5 exerts its regulatory functions on shootin1 in a Rac1 dependent manner.

Intriguingly, the expression level of shootin1 was significantly reduced in hippocampal neuronal cultures silenced for CDKL5. Whether this is caused by a transcriptional or post-transcriptional effect still remains unclear. It is interesting to note that the selective action of the ubiquitin-proteasome system (UPS) has been suggested to be involved in axon/dendrite differentiation [122,123]. The phosphorylation of some proteins has been found to render them less susceptible for E3 ligase dependent degradation. For example, Akt, a key regulatory protein in the PI3-kinase/Akt signaling pathways, is present in phosphorylated and unphosphorylated forms in axon and dendrites respectively. The dendritic unphosphorylated Akt is more susceptible to UPS-dependent degradation than axonal phospho-Akt and the selective degradation of unphosphorylated Akt thus represents a means to maintain the asymmetric distribution of Akt/phospho-Akt in polarized neurons [123]. Likewise, phosphorylation of LKB1 enhances its stability by the formation of LKB1/STRAD complex thereby reducing its susceptibility of ubiquitinylation. In an analogous situation, it could be speculated that phosphorylation of shootin1 might regulate its stability. By treating neurons silenced or not for Cdkl5 with the proteasome inhibitor Mg132 we addressed this point but did not yet obtain conclusive results. Alternatively, the activity or substrate specificity of specific E3 ligases may be regulated by their post-translational modification [124]. In the yeast two-hybrid screening, UBE4A (U-box-type ubiquitin ligase) and KLHL7 (a protein of the BTB-Kelch family that is implicated in ubiquitinylation through Cullin E3 ligases; [125]) that are both involved in ubiquitin mediated protein degradation were found as CDKL5 interactors. Therefore, it could also be speculated that CDKL5 controls the activity of factors involved in regulating shootin1 turnover.

Even if the main body of our experiments is in line with a role of CDKL5 in neuronal polarization through its association with shootin1, the picture is complicated by the fact that silencing of CDKL5 generates a mixed phenotype including both neurons devoid of axons and neurons with numerous axons. On the other hand, CDKL5 is very likely to activate

different downstream pathways through its diverse interaction partners and may thus target different factors involved in regulating axon specification and outgrowth. A kinome profiling of brain extracts from *Cdkl5*-null mice revealed that several signalling pathways are deregulated in its absence. Interestingly, the three pathways that were mostly influenced were those including AMPK kinase, PKA, and Akt that are all involved in neuronal polarization [106]. Moreover, as mentioned, CDKL5 works upstream of Rac1 [83] and it is well established that Rac1 influences various aspects of neuronal morphogenesis through different upstream regulators and downstream effectors. Axon initiation is mediated by Rac1 in a pathway involving DOCK7 and stathmin whereas this small Rho GTPase appears to have a dual role in regulating axon outgrowth: its inhibitory activity requires a pathway including PAK, LIMK, and cofilin whereas growth promotion is PAK independent [126]. It is possible that the silencing of CDKL5 has different efficiency and/or timing in different neurons thus influencing its down-stream effectors in distinct time windows with opposing outcomes.

As previously stated, along with shootin1, several other proteins were found to interact with CDKL5 in the yeast two-hybrid screening. These proteins attained lower biological scores than shootin1 but the importance of these CDKL5 interactors in CNS development cannot be ruled out. Among the interactors were: (1) Formin-like 2 (FMNL2), which is predominantly expressed in brain and known as a putative regulator of Rho-GTPases. It serves as a novel elongation factor of actin filaments and promotes actin polymerization at the tips of lamellipodia [127]. Interestingly, micro-deletions including *FMNL2* have been found associated with mental retardation [128]; (2) Glucocorticoid receptor DNA binding factor 1 (GRLF1), also termed as p190A (a member of RhoGAP protein family) is prominently expressed in the developing and adult brain. Protein kinase C stimulation or integrin activation leads to outgrowth processing and neuronal development by rapid translocation of p190A to lamellipodial regions [129,130]. Mice devoid of p190A show several defects in neuronal development indicating the role of this protein in axonal outgrowth and/or guidance [131]; (3) Dystonin (DST) is one of the larger members of spectrin superfamily of cytoskeletal interacting proteins. Neuronal dystonin isoforms interact with actin and microtubule networks, protein complexes, membrane bound organelles and cellular membranes. Mutations in DST cause an aggregation of axonal neurofilament and disorganization of axonal microtubule in sensory neurons in a neurodegenerative disorder, dystonia musculorum [132,133]; (4) Heavy chain of kinesin-1 (KIF5A), a neuronal microtubule motor protein, which plays an important role in outgrowth processing and axonal transport of mitochondria. The absence of KIF5A affects motor neurons more severely than

sensory neurons [134]. Mutations in this gene cause autosomal dominant hereditary spastic paraplegia 10 (SPG10), a group of genetically heterogeneous neurodegenerative disorders characterized by distal axonopathy that affects the longest axons in the cortico-spinal tract [135]; (5) Adenomatous polyposis coli (APC), a tumor suppressor gene, which is highly expressed in developing brain [136] and is mainly associated with the plus ends of microtubule that maintains the cell polarity [137]. Interestingly, APC is localized at growth cones of hippocampal axons and disruption of this protein interferes with axon specification [138,139].

Since neuronal morphology is established in a manner depending on an interplay of balanced positive and negative signals regulating different signaling cascades that range from maintaining cytoskeleton structures to correct localization of polarizing molecules, it is worth speculating that altered CDKL5 levels might cause a deregulation of one or more of the above mentioned proteins and thus interfere with neuronal polarization at different levels.

Normal cognitive function relies on the proper coordination of multiple steps of neuronal development and the correct neuronal migration throughout gestation and post-natal stages. During development, newly born post-mitotic neurons in the ventricular zone (VZ, mainly glutamatergic pyramidal neurons) migrate radially in an “inside out” fashion to their final positions in the developing cortex whereas GABAergic interneurons migrate tangentially from medial ganglionic eminence (MGE) to the cortex and reside there. Several studies have suggested that mutations in cytoskeletal regulators, extracellular matrix molecules, or post-translational modifiers tend to affect both radial and tangential migration [140]. Disruption in the early steps of neuronal development, including neuronal migration, can result in severe cognitive deficits and epilepsy. For example, mutations in the human doublecortin gene (*DCX*) cause defects in cortical neuronal migration and patients with *DCX* mutations have lissencephaly and infantile spasms [141]. In addition, defects in axonal growth are likely associated with abnormal connectivity and may be associated with seizure pathogenesis as seen in lissencephaly. Thus, the causative genes have a role in both stages of development, closely relating the molecular pathways regulating neuronal migration and axon outgrowth. The observed impairments in neuronal–migration in neocortices depleted for shootin1 resemble the situation regarding CDKL5 [83] and suggest the importance of shootin1 in the developing nervous system. Though our IUE experiments show that the majority of silenced neurons still reside in the intermediate zone at post-natal stage P8, we are not yet in a position to say whether this effect is persistent throughout the development or it is just a delay in

migration as have been described for CDKL5. Further experiments in which migration of silenced neurons is analyzed at later post-natal stages are required to determine the long-term effect of shootin1 in neuronal development as well as in neuronal migration. Although so far no studies have described mutations in the *SHOOTIN1* gene in humans, our findings suggest the possibility of its involvement in neurodevelopmental disorders and further studies are strongly recommended to validate the involvement of *SHOOTIN1* in neurological disorders.

Altogether, our data indicate a hitherto uncharacterized role of CDKL5 in the early phases of neuronal differentiation that may explain in part the clinical features associated with mutations in this gene. Finally, both the association of shootin1 with a molecular pathway belonging to CDKL5 and the defects in neuronal migration caused by its deficiency might make this gene an interesting candidate gene to analyze in patients with neurological disorders.

BIBLIOGRAPHY

1. **Rett A**. 1966. [On a unusual brain atrophy syndrome in hyperammonemia in childhood]. *Wien Med Wochenschr* 116:723-6

2. **Hagberg B**, Aicardi J, Dias K, Ramos O. 1983. A progressive syndrome of autism, dementia, ataxia, and loss of purposeful hand use in girls: Rett's syndrome: report of 35 cases. *Ann Neurol* 14:471-9

3. **Amir RE**, Van den Veyver IB, Wan M, Tran CQ, Francke U, Zoghbi HY. 1999. Rett syndrome is caused by mutations in X-linked MECP2, encoding methyl-CpG-binding protein 2. *Nat Genet* 23:185-8

4. **Chahrour M**, Zoghbi HY. 2007. The story of Rett syndrome: from clinic to neurobiology. *Neuron* 56:422-37

5. **Neul JL**, Kaufmann WE, Glaze DG, Christodoulou J, Clarke AJ, et al. 2010. Rett syndrome: revised diagnostic criteria and nomenclature. *Ann Neurol* 68:944-50

6. **Steffenburg U**, Hagberg G, Hagberg B. 2001. Epilepsy in a representative series of Rett syndrome. *Acta Paediatr* 90:34-9

7. **Huppke P**, Kohler K, Brockmann K, Stettner GM, Gartner J. 2007. Treatment of epilepsy in Rett syndrome. *Eur J Paediatr Neurol* 11:10-6

8. **Nissenkorn A**, Gak E, Vecsler M, Reznik H, Menascu S, Ben Zeev B. 2010. Epilepsy in Rett syndrome---the experience of a National Rett Center. *Epilepsia* 51:1252-8

9. **Pintaudi M**, Calevo MG, Vignoli A, Parodi E, Aiello F, et al. 2010. Epilepsy in Rett syndrome: clinical and genetic features. *Epilepsy Behav* 19:296-300

10. **Krajnc N**, Zupancic N, Orazem J. 2011. Epilepsy treatment in Rett syndrome. *J Child Neurol* 26:1429-33

11. **Hendrich B**, Bird A. 1998. Identification and characterization of a family of mammalian methyl-CpG binding proteins. *Mol Cell Biol* 18:6538-47

12. **Lewis JD**, Meehan RR, Henzel WJ, Maurer-Fogy I, Jeppesen P, et al. 1992. Purification, sequence, and cellular localization of a novel chromosomal protein that binds to methylated DNA. *Cell* 69:905-14

13. **Neul JL**, Fang P, Barrish J, Lane J, Caeg EB, et al. 2008. Specific mutations in methyl-CpG-binding protein 2 confer different severity in Rett syndrome. *Neurology* 70:1313-21

14. **D'Esposito M**, Quaderi NA, Ciccodicola A, Bruni P, Esposito T, et al. 1996. Isolation, physical mapping, and northern analysis of the X-linked human gene encoding methyl CpG-binding protein, MECP2. *Mamm Genome* 7:533-5

15. **Sirianni N**, Naidu S, Pereira J, Pillotto RF, Hoffman EP. 1998. Rett syndrome: confirmation of X-linked dominant inheritance, and localization of the gene to Xq28. *Am J Hum Genet* 63:1552-8

16. **Zachariah RM**, Rastegar M. 2012. Linking epigenetics to human disease and Rett syndrome: the emerging novel and challenging concepts in MeCP2 research. *Neural Plast* 2012:415825

17. **Nan X**, Campoy FJ, Bird A. 1997. MeCP2 is a transcriptional repressor with abundant binding sites in genomic chromatin. *Cell* 88:471-81

18. **Nan X**, Ng HH, Johnson CA, Laherty CD, Turner BM, et al. 1998. Transcriptional repression by the methyl-CpG-binding protein MeCP2 involves a histone deacetylase complex. *Nature* 393:386-9

19. **Jones PL**, Veenstra GJ, Wade PA, Vermaak D, Kass SU, et al. 1998. Methylated DNA and MeCP2 recruit histone deacetylase to repress transcription. *Nat Genet* 19:187-91

20. **Baker SA**, Chen L, Wilkins AD, Yu P, Lichtarge O, Zoghbi HY. 2013. An AT-hook domain in MeCP2 determines the clinical course of Rett syndrome and related disorders. *Cell* 152:984-96

21. **Chandler SP**, Guschin D, Landsberger N, Wolffe AP. 1999. The methyl-CpG binding transcriptional repressor MeCP2 stably associates with nucleosomal DNA. *Biochemistry* 38:7008-18

22. **Buschdorf JP**, Stratling WH. 2004. A WW domain binding region in methyl-CpG-binding protein MeCP2: impact on Rett syndrome. *J Mol Med (Berl)* 82:135-43

23. **Xu X**, Pozzo-Miller L. 2013. A novel DNA-binding feature of MeCP2 contributes to Rett syndrome. *Front Cell Neurosci* 7:64

24. **Matijevic T**, Knezevic J, Slavica M, Pavelic J. 2009. Rett syndrome: from the gene to the disease. *Eur Neurol* 61:3-10

25. **Chahrour M**, Jung SY, Shaw C, Zhou X, Wong ST, et al. 2008. MeCP2, a key contributor to neurological disease, activates and represses transcription. *Science* 320:1224-9

26. **Skene PJ**, Illingworth RS, Webb S, Kerr AR, James KD, et al. 2010. Neuronal MeCP2 is expressed at near histone-octamer levels and globally alters the chromatin state. *Mol Cell* 37:457-68

27. **Cohen S**, Gabel HW, Hemberg M, Hutchinson AN, Sadacca LA, et al. 2011. Genome-wide activity-dependent MeCP2 phosphorylation regulates nervous system development and function. *Neuron* 72:72-85

28. **LaSalle JM**, Goldstine J, Balmer D, Greco CM. 2001. Quantitative localization of heterogeneous methyl-CpG-binding protein 2 (MeCP2) expression phenotypes in normal and Rett syndrome brain by laser scanning cytometry. *Hum Mol Genet* 10:1729-40

29. **Shahbazian MD**, Antalffy B, Armstrong DL, Zoghbi HY. 2002. Insight into Rett syndrome: MeCP2 levels display tissue- and cell-specific differences and correlate with neuronal maturation. *Hum Mol Genet* 11:115-24

30. **Braunschweig D**, Simcox T, Samaco RC, LaSalle JM. 2004. X-Chromosome inactivation ratios affect wild-type MeCP2 expression within mosaic Rett syndrome and Mecp2-/+ mouse brain. *Hum Mol Genet* 13:1275-86

31. **Armstrong DD**. 2002. Neuropathology of Rett syndrome. *Ment Retard Dev Disabil Res Rev* 8:72-6

32. **Chapleau CA**, Calfa GD, Lane MC, Albertson AJ, Larimore JL, et al. 2009. Dendritic spine pathologies in hippocampal pyramidal neurons from Rett syndrome brain and after expression of Rett-associated MECP2 mutations. *Neurobiol Dis* 35:219-33

33. **Palmer A**, Qayumi J, Ronnett G. 2008. MeCP2 mutation causes distinguishable phases of acute and chronic defects in synaptogenesis and maintenance, respectively. *Mol Cell Neurosci* 37:794-807

34. **Smrt RD**, Eaves-Egenes J, Barkho BZ, Santistevan NJ, Zhao C, et al. 2007. Mecp2 deficiency leads to delayed maturation and altered gene expression in hippocampal neurons. *Neurobiol Dis* 27:77-89

35. **Fukuda T**, Itoh M, Ichikawa T, Washiyama K, Goto Y. 2005. Delayed maturation of neuronal architecture and synaptogenesis in cerebral cortex of Mecp2-deficient mice. *J Neuropathol Exp Neurol* 64:537-44

36. **Dani VS**, Chang Q, Maffei A, Turrigiano GG, Jaenisch R, Nelson SB. 2005. Reduced cortical activity due to a shift in the balance between excitation and inhibition in a mouse model of Rett syndrome. *Proc Natl Acad Sci U S A* 102:12560-5

37. **Asaka Y**, Jugloff DG, Zhang L, Eubanks JH, Fitzsimonds RM. 2006. Hippocampal synaptic plasticity is impaired in the Mecp2-null mouse model of Rett syndrome. *Neurobiol Dis* 21:217-27

38. **Moretti P**, Levenson JM, Battaglia F, Atkinson R, Teague R, et al. 2006. Learning and memory and synaptic plasticity are impaired in a mouse model of Rett syndrome. *J Neurosci* 26:319-27

39. **Ballas N**, Lioy DT, Grunseich C, Mandel G. 2009. Non-cell autonomous influence of MeCP2-deficient glia on neuronal dendritic morphology. *Nat Neurosci* 12:311-7

40. **Maezawa I**, Swanberg S, Harvey D, LaSalle JM, Jin LW. 2009. Rett syndrome astrocytes are abnormal and spread MeCP2 deficiency through gap junctions. *J Neurosci* 29:5051-61

41. **Maezawa I**, Jin LW. 2010. Rett syndrome microglia damage dendrites and synapses by the elevated release of glutamate. *J Neurosci* 30:5346-56

42. **Tao J**, Hu K, Chang Q, Wu H, Sherman NE, et al. 2009. Phosphorylation of MeCP2 at Serine 80 regulates its chromatin association and neurological function. *Proc Natl Acad Sci U S A* 106:4882-7

43. **Zhou Z**, Hong EJ, Cohen S, Zhao WN, Ho HY, et al. 2006. Brain-specific phosphorylation of MeCP2 regulates activity-dependent Bdnf transcription, dendritic growth, and spine maturation. *Neuron* 52:255-69

44. **Ebert DH**, Gabel HW, Robinson ND, Kastan NR, Hu LS, et al. 2013. Activity-dependent phosphorylation of MeCP2 threonine 308 regulates interaction with NCoR. *Nature* 499:341-5

45. **Mari F**, Azimonti S, Bertani I, Bolognese F, Colombo E, et al. 2005. CDKL5 belongs to the same molecular pathway of MeCP2 and it is responsible for the early-onset seizure variant of Rett syndrome. *Hum Mol Genet* 14:1935-46

46. **Chen RZ**, Akbarian S, Tudor M, Jaenisch R. 2001. Deficiency of methyl-CpG binding protein-2 in CNS neurons results in a Rett-like phenotype in mice. *Nat Genet* 27:327-31

47. **Kishi N**, Macklis JD. 2004. MECP2 is progressively expressed in post-migratory neurons and is involved in neuronal maturation rather than cell fate decisions. *Mol Cell Neurosci* 27:306-21

48. **Guy J**, Hendrich B, Holmes M, Martin JE, Bird A. 2001. A mouse Mecp2-null mutation causes neurological symptoms that mimic Rett syndrome. *Nat Genet* 27:322-6

49. **Collins AL**, Levenson JM, Vilaythong AP, Richman R, Armstrong DL, et al. 2004. Mild overexpression of MeCP2 causes a progressive neurological disorder in mice. *Hum Mol Genet* 13:2679-89

50. **Luikenhuis S**, Giacometti E, Beard CF, Jaenisch R. 2004. Expression of MeCP2 in postmitotic neurons rescues Rett syndrome in mice. *Proc Natl Acad Sci U S A* 101:6033-8

51. **Van Esch H**. 2012. MECP2 Duplication Syndrome. *Mol Syndromol* 2:128-36

52. **Guy J**, Gan J, Selfridge J, Cobb S, Bird A. 2007. Reversal of neurological defects in a mouse model of Rett syndrome. *Science* 315:1143-7

53. **Giacometti E**, Luikenhuis S, Beard C, Jaenisch R. 2007. Partial rescue of MeCP2 deficiency by post-natal activation of MeCP2. *Proc Natl Acad Sci U S A* 104:1931-6

54. **McGraw CM**, Samaco RC, Zoghbi HY. 2011. Adult neural function requires MeCP2. *Science* 333:186

55. **Derecki NC**, Cronk JC, Lu Z, Xu E, Abbott SB, et al. 2012. Wild-type microglia arrest pathology in a mouse model of Rett syndrome. *Nature* 484:105-9

56. **Zappella M**. 1992. The Rett girls with preserved speech. *Brain Dev* 14:98-101

57. **Rolando S**. 1985. Rett syndrome: report of eight cases. *Brain Dev* 7:290-6

58. **Hanefeld F**. 1985. The clinical pattern of the Rett syndrome. *Brain Dev* 7:320-5

59. **Renieri A**, Mari F, Mencarelli MA, Scala E, Ariani F, et al. 2009. Diagnostic criteria for the Zappella variant of Rett syndrome (the preserved speech variant). *Brain Dev* 31:208-16

60. **Huppke P**, Laccone F, Kramer N, Engel W, Hanefeld F. 2000. Rett syndrome: analysis of MECP2 and clinical characterization of 31 patients. *Hum Mol Genet* 9:1369-75

61. **Archer HL**, Evans J, Edwards S, Colley J, Newbury-Ecob R, et al. 2006. CDKL5 mutations cause infantile spasms, early onset seizures, and severe mental retardation in female patients. *J Med Genet* 43:729-34

62. **Bahi-Buisson N**, Kaminska A, Boddaert N, Rio M, Afenjar A, et al. 2008a. The three stages of epilepsy in patients with CDKL5 mutations. *Epilepsia* 49:1027-37

63. **Ariani F**, Hayek G, Rondinella D, Artuso R, Mencarelli MA, et al. 2008. FOXG1 is responsible for the congenital variant of Rett syndrome. *Am J Hum Genet* 83:89-93

64. **Tao J**, Van Esch H, Hagedorn-Greiwe M, Hoffmann K, Moser B, et al. 2004. Mutations in the X-linked cyclin-dependent kinase-like 5 (CDKL5/STK9) gene are associated with severe neurodevelopmental retardation. *Am J Hum Genet* 75:1149-54

65. **Weaving LS**, Christodoulou J, Williamson SL, Friend KL, McKenzie OL, et al. 2004. Mutations of CDKL5 cause a severe neurodevelopmental disorder with infantile spasms and mental retardation. *Am J Hum Genet* 75:1079-93

66. **Scala E**, Ariani F, Mari F, Caselli R, Pescucci C, et al. 2005. CDKL5/STK9 is mutated in Rett syndrome variant with infantile spasms. *J Med Genet* 42:103-7

67. **Goutieres F**, Aicardi J. 1986. Atypical forms of Rett syndrome. *Am J Med Genet Suppl* 1:183-94

68. **Evans JC**, Archer HL, Colley JP, Ravn K, Nielsen JB, et al. 2005. Early onset seizures and Rett-like features associated with mutations in CDKL5. *Eur J Hum Genet* 13:1113-20

69. **Montini E**, Andolfi G, Caruso A, Buchner G, Walpole SM, et al. 1998. Identification and characterization of a novel serine-threonine kinase gene from the Xp22 region. *Genomics* 51:427-33

70. **Kalscheuer VM**, Tao J, Donnelly A, Hollway G, Schwinger E, et al. 2003. Disruption of the serine/threonine kinase 9 gene causes severe X-linked infantile spasms and mental retardation. *Am J Hum Genet* 72:1401-11

71. **Bahi-Buisson N**, Nectoux J, Rosas-Vargas H, Milh M, Boddaert N, et al. 2008b. Key clinical features to identify girls with CDKL5 mutations. *Brain* 131:2647-61

72. **Elia M**, Falco M, Ferri R, Spalletta A, Bottitta M, et al. 2008. CDKL5 mutations in boys with severe encephalopathy and early-onset intractable epilepsy. *Neurology* 71:997-9

73. **Nemos C**, Lambert L, Giuliano F, Doray B, Roubertie A, et al. 2009. Mutational spectrum of CDKL5 in early-onset encephalopathies: a study of a large collection of French patients and review of the literature. *Clin Genet* 76:357-71

74. **Mei D**, Marini C, Novara F, Bernardina BD, Granata T, et al. 2010. Xp22.3 genomic deletions involving the CDKL5 gene in girls with early onset epileptic encephalopathy. *Epilepsia* 51:647-54

75. **Melani F**, Mei D, Pisano T, Savasta S, Franzoni E, et al. 2011. CDKL5 gene-related epileptic encephalopathy: electroclinical findings in the first year of life. *Dev Med Child Neurol* 53:354-60

76. **Klein KM**, Yendle SC, Harvey AS, Antony JH, Wallace G, et al. 2011. A distinctive seizure type in patients with CDKL5 mutations: Hypermotor-tonic-spasms sequence. *Neurology* 76:1436-8

77. **Liang JS**, Shimojima K, Takayama R, Natsume J, Shichiji M, et al. 2011. CDKL5 alterations lead to early epileptic encephalopathy in both genders. *Epilepsia* 52:1835-42

78. **Fehr S**, Wilson M, Downs J, Williams S, Murgia A, et al. 2013. The CDKL5 disorder is an independent clinical entity associated with early-onset encephalopathy. *Eur J Hum Genet* 21:266-73

79. **Sartori S**, Di Rosa G, Polli R, Bettella E, Tricomi G, et al. 2009. A novel CDKL5 mutation in a 47,XXY boy with the early-onset seizure variant of Rett syndrome. *Am J Med Genet A* 149A:232-6

80. **Kankirawatana P**, Leonard H, Ellaway C, Scurlock J, Mansour A, et al. 2006. Early progressive encephalopathy in boys and MECP2 mutations. *Neurology* 67:164-6

81. **Williamson SL**, Giudici L, Kilstrup-Nielsen C, Gold W, Pelka GJ, et al. 2012. A novel transcript of cyclin-dependent kinase-like 5 (CDKL5) has an alternative C-terminus and is the predominant transcript in brain. *Hum Genet* 131:187-200

82. **Kilstrup-Nielsen C**, Rusconi L, La Montanara P, Ciceri D, Bergo A, et al. 2012. What we know and would like to know about CDKL5 and its involvement in epileptic encephalopathy. *Neural Plast* 2012:728267

83. **Chen Q**, Zhu YC, Yu J, Miao S, Zheng J, et al. 2010. CDKL5, a protein associated with rett syndrome, regulates neuronal morphogenesis via Rac1 signaling. *J Neurosci* 30:12777-86

84. **Fichou Y**, Nectoux J, Bahi-Buisson N, Chelly J, Bienvenu T. 2011. An isoform of the severe encephalopathy-related CDKL5 gene, including a novel exon with extremely high sequence conservation, is specifically expressed in brain. *J Hum Genet* 56:52-7

85. **Rademacher N**, Hambrock M, Fischer U, Moser B, Ceulemans B, et al. 2011. Identification of a novel CDKL5 exon and pathogenic mutations in patients with severe mental retardation, early-onset seizures and Rett-like features. *Neurogenetics* 12:165-7

86. **Bertani I**, Rusconi L, Bolognese F, Forlani G, Conca B, et al. 2006. Functional consequences of mutations in CDKL5, an X-linked gene involved in infantile spasms and mental retardation. *J Biol Chem* 281:32048-56

87. **Rosas-Vargas H**, Bahi-Buisson N, Philippe C, Nectoux J, Girard B, et al. 2008. Impairment of CDKL5 nuclear localisation as a cause for severe infantile encephalopathy. *J Med Genet* 45:172-8

88. **Lin C**, Franco B, Rosner MR. 2005. CDKL5/Stk9 kinase inactivation is associated with neuronal developmental disorders. *Hum Mol Genet* 14:3775-86

89. **Rusconi L**, Salvatoni L, Giudici L, Bertani I, Kilstrup-Nielsen C, et al. 2008. CDKL5 expression is modulated during neuronal development and its subcellular distribution is tightly regulated by the C-terminal tail. *J Biol Chem* 283:30101-11

90. **Tzschach A**, Chen W, Erdogan F, Hoeller A, Ropers HH, et al. 2008. Characterization of interstitial Xp duplications in two families by tiling path array CGH. *Am J Med Genet A* 146A:197-203

91. **Thorson L**, Bryke C, Rice G, Artzer A, Schilz C, et al. 2010. Clinical and molecular characterization of overlapping interstitial Xp21-p22 duplications in two unrelated individuals. *Am J Med Genet A* 152A:904-15

92. **Sismani C**, Anastasiadou V, Kousoulidou L, Parkel S, Koumbaris G, et al. 2011. 9 Mb familial duplication in chromosome band Xp22.2-22.13 associated with mental retardation, hypotonia and developmental delay, scoliosis, cardiovascular problems and mild dysmorphic facial features. *Eur J Med Genet* 54:e510-5

93. **Russo S**, Marchi M, Cogliati F, Bonati MT, Pintaudi M, et al. 2009. Novel mutations in the CDKL5 gene, predicted effects and associated phenotypes. *Neurogenetics* 10:241-50

94. **Carouge D**, Host L, Aunis D, Zwiller J, Anglard P. 2010. CDKL5 is a brain MeCP2 target gene regulated by DNA methylation. *Neurobiol Dis* 38:414-24

95. **Ricciardi S**, Kilstrup-Nielsen C, Bienvenu T, Jacquette A, Landsberger N, Broccoli V. 2009. CDKL5 influences RNA splicing activity by its association to the nuclear speckle molecular machinery. *Hum Mol Genet* 18:4590-602

96. **Rusconi L**, Kilstrup-Nielsen C, Landsberger N. 2011. Extrasynaptic N-methyl-D-aspartate (NMDA) receptor stimulation induces cytoplasmic translocation of the CDKL5 kinase and its proteasomal degradation. *J Biol Chem* 286:36550-8

97. **Ricciardi S**, Ungaro F, Hambrock M, Rademacher N, Stefanelli G, et al. 2012. CDKL5 ensures excitatory synapse stability by reinforcing NGL-1-PSD95 interaction in the postsynaptic compartment and is impaired in patient iPSC-derived neurons. *Nat Cell Biol* 14:911-23

98. **Kameshita I**, Sekiguchi M, Hamasaki D, Sugiyama Y, Hatano N, et al. 2008. Cyclin-dependent kinase-like 5 binds and phosphorylates DNA methyltransferase 1. *Biochem Biophys Res Commun* 377:1162-7

99. **Elias GM**, Nicoll RA. 2007. Synaptic trafficking of glutamate receptors by MAGUK scaffolding proteins. *Trends Cell Biol* 17:343-52

100. **Zhu YC**, Li D, Wang L, Lu B, Zheng J, et al. 2013. Palmitoylation-dependent CDKL5-PSD-95 interaction regulates synaptic targeting of CDKL5 and dendritic spine development. *Proc Natl Acad Sci U S A* 110:9118-23

101. **Yoshii A**, Murata Y, Kim J, Zhang C, Shokat KM, Constantine-Paton M. 2011. TrkB and protein kinase Mzeta regulate synaptic localization of PSD-95 in developing cortex. *J Neurosci* 31:11894-904

102. **El-Husseini Ael D**, Schnell E, Dakoji S, Sweeney N, Zhou Q, et al. 2002. Synaptic strength regulated by palmitate cycling on PSD-95. *Cell* 108:849-63

103. **Lin JC**, Ho WH, Gurney A, Rosenthal A. 2003. The netrin-G1 ligand NGL-1 promotes the outgrowth of thalamocortical axons. *Nat Neurosci* 6:1270-6

104. **Lapray D**, Popova IY, Kindler J, Jorquera I, Becq H, et al. 2010. Spontaneous epileptic manifestations in a DCX knockdown model of human double cortex. *Cereb Cortex* 20:2694-701

105. **Patrylo PR**, Browning RA, Cranick S. 2006. Reeler homozygous mice exhibit enhanced susceptibility to epileptiform activity. *Epilepsia* 47:257-66

106. **Wang IT**, Allen M, Goffin D, Zhu X, Fairless AH, et al. 2012. Loss of CDKL5 disrupts kinome profile and event-related potentials leading to autistic-like phenotypes in mice. *Proc Natl Acad Sci U S A* 109:21516-21

107. **McLin JP**, Steward O. 2006. Comparison of seizure phenotype and neurodegeneration induced by systemic kainic acid in inbred, outbred, and hybrid mouse strains. *Eur J Neurosci* 24:2191-202

108. **Tahirovic S**, Bradke F. 2009. Neuronal polarity. *Cold Spring Harb Perspect Biol* 1:a001644

109. **Dotti CG**, Sullivan CA, Banker GA. 1988. The establishment of polarity by hippocampal neurons in culture. *J Neurosci* 8:1454-68

110. **Arimura N**, Kaibuchi K. 2007. Neuronal polarity: from extracellular signals to intracellular mechanisms. *Nat Rev Neurosci* 8:194-205

111. **Andersen SS**, Bi GQ. 2000. Axon formation: a molecular model for the generation of neuronal polarity. *Bioessays* 22:172-9

112. **Goslin K**, Banker G. 1989. Experimental observations on the development of polarity by hippocampal neurons in culture. *J Cell Biol* 108:1507-16

113. **Kunda P**, Paglini G, Quiroga S, Kosik K, Caceres A. 2001. Evidence for the involvement of Tiam1 in axon formation. *J Neurosci* 21:2361-72

114. **Toriyama M**, Shimada T, Kim KB, Mitsuba M, Nomura E, et al. 2006. Shootin1: A protein involved in the organization of an asymmetric signal for neuronal polarization. *J Cell Biol* 175:147-57

115. **Sapir T**, Levy T, Sakakibara A, Rabinkov A, Miyata T, Reiner O. 2013. Shootin1 acts in concert with KIF20B to promote polarization of migrating neurons. *J Neurosci* 33:11932-48

116. **Arimura N**, Kaibuchi K. 2005. Key regulators in neuronal polarity. *Neuron* 48:881-4

117. **Toriyama M**, Kozawa S, Sakumura Y, Inagaki N. 2013. Conversion of a signal into forces for axon outgrowth through Pak1-mediated shootin1 phosphorylation. *Curr Biol* 23:529-34

118. **Formstecher E**, Aresta S, Collura V, Hamburger A, Meil A, et al. 2005. Protein interaction mapping: a Drosophila case study. *Genome Res* 15:376-84

119. **Shimada T**, Toriyama M, Uemura K, Kamiguchi H, Sugiura T, et al. 2008. Shootin1 interacts with actin retrograde flow and L1-CAM to promote axon outgrowth. *J Cell Biol* 181:817-29

120. **Taniguchi Y**, Young-Pearse T, Sawa A, Kamiya A. 2012. *In utero* electroporation as a tool for genetic manipulation *in vivo* to study psychiatric disorders: from genes to circuits and behaviors. *Neuroscientist* 18:169-79

121. **Pitkanen A**, Sutula TP. 2002. Is epilepsy a progressive disorder? Prospects for new therapeutic approaches in temporal-lobe epilepsy. *Lancet Neurol* 1:173-81

122. **Schwamborn JC**, Muller M, Becker AH, Puschel AW. 2007. Ubiquitination of the GTPase Rap1B by the ubiquitin ligase Smurf2 is required for the establishment of neuronal polarity. *EMBO J* 26:1410-22

123. **Yan D**, Guo L, Wang Y. 2006. Requirement of dendritic Akt degradation by the ubiquitin-proteasome system for neuronal polarity. *J Cell Biol* 174:415-24

124. **Cheng PL**, Lu H, Shelly M, Gao H, Poo MM. 2011. Phosphorylation of E3 ligase Smurf1 switches its substrate preference in support of axon development. *Neuron* 69:231-43

125. **Friedman JS**, Ray JW, Waseem N, Johnson K, Brooks MJ, et al. 2009. Mutations in a BTB-Kelch protein, KLHL7, cause autosomal-dominant retinitis pigmentosa. *Am J Hum Genet* 84:792-800

126. **Hall A**, Lalli G. 2010. Rho and Ras GTPases in axon growth, guidance, and branching. *Cold Spring Harb Perspect Biol* 2:a001818

127. **Block J**, Breitsprecher D, Kuhn S, Winterhoff M, Kage F, et al. 2012. FMNL2 drives actin-based protrusion and migration downstream of Cdc42. *Curr Biol* 22:1005-12

128. **Lybaek H**, Orstavik KH, Prescott T, Hovland R, Breilid H, et al. 2009. An 8.9 Mb 19p13 duplication associated with precocious puberty and a sporadic 3.9 Mb 2q23.3q24.1 deletion containing NR4A2 in mentally retarded members of a family with an intrachromosomal 19p-into-19q between-arm insertion. *Eur J Hum Genet* 17:904-10

129. **Brouns MR**, Matheson SF, Hu KQ, Delalle I, Caviness VS, et al. 2000. The adhesion signaling molecule p190 RhoGAP is required for morphogenetic processes in neural development. *Development* 127:4891-903

130. **Brouns MR**, Matheson SF, Settleman J. 2001. p190 RhoGAP is the principal Src substrate in brain and regulates axon outgrowth, guidance and fasciculation. *Nat Cell Biol* 3:361-7

131. **Tomar A**, Lim ST, Lim Y, Schlaepfer DD. 2009. A FAK-p120RasGAP-p190RhoGAP complex regulates polarity in migrating cells. *J Cell Sci* 122:1852-62

132. **Dalpe G**, Leclerc N, Vallee A, Messer A, Mathieu M, et al. 1998. Dystonin is essential for maintaining neuronal cytoskeleton organization. *Mol Cell Neurosci* 10:243-57

133. **De Repentigny Y**, Deschenes-Furry J, Jasmin BJ, Kothary R. 2003. Impaired fast axonal transport in neurons of the sciatic nerves from dystonia musculorum mice. *J Neurochem* 86:564-71

134. **Karle KN**, Mockel D, Reid E, Schols L. 2012. Axonal transport deficit in a KIF5A(-/-) mouse model. *Neurogenetics* 13:169-79

135. **Deluca GC**, Ebers GC, Esiri MM. 2004. The extent of axonal loss in the long tracts in hereditary spastic paraplegia. *Neuropathol Appl Neurobiol* 30:576-84

136. **Bhat RV**, Baraban JM, Johnson RC, Eipper BA, Mains RE. 1994. High levels of expression of the tumor suppressor gene APC during development of the rat central nervous system. *J Neurosci* 14:3059-71

137. **Barth AI**, Caro-Gonzalez HY, Nelson WJ. 2008. Role of adenomatous polyposis coli (APC) and microtubules in directional cell migration and neuronal polarization. *Semin Cell Dev Biol* 19:245-51

138. **Etienne-Manneville S**, Hall A. 2003. Cdc42 regulates GSK-3beta and adenomatous polyposis coli to control cell polarity. *Nature* 421:753-6

139. **Votin V**, Nelson WJ, Barth AI. 2005. Neurite outgrowth involves adenomatous polyposis coli protein and beta-catenin. *J Cell Sci* 118:5699-708

140. **Valiente M**, Marin O. 2010. Neuronal migration mechanisms in development and disease. *Curr Opin Neurobiol* 20:68-78

141. **Pilz DT**, Matsumoto N, Minnerath S, Mills P, Gleeson JG, et al. 1998. LIS1 and XLIS (DCX) mutations cause most classical lissencephaly, but different patterns of malformation. *Hum Mol Genet* 7:2029-37